AEDC-TR-69-47

Copy 9

BOUNDARY INTERFERENCE AT SUBSONIC SPEEDS IN WIND TUNNELS WITH VENTILATED WALLS

M. Pindzola and C. F. Lo

ARO, Inc.

May 1969

PROPULSION WIND TUNNEL FACILITY
ARNOLD ENGINEERING DEVELOPMENT CENTER
AIR FORCE SYSTEMS COMMAND
ARNOLD AIR FORCE STATION, TENNESSEE

NOTICES

When U. S. Government drawings specifications, or other data are used for any purpose other than a definitely related Government procurement operation, the Government thereby incurs no responsibility nor any obligation whatsoever, and the fact that the Government may have formulated, furnished, or in any way supplied the said drawings, specifications, or other data, is not to be regarded by implication or otherwise, or in any manner licensing the holder or any other person or corporation, or conveying any rights or permission to manufacture, use, or sell any patented invention that may in any way be related thereto.

Qualified users may obtain copies of this report from the Defense Documentation Center.

References to named commercial products in this report are not to be considered in any sense as an endorsement of the product by the United States Air Force or the Government.

BOUNDARY INTERFERENCE AT SUBSONIC SPEEDS IN WIND TUNNELS WITH VENTILATED WALLS

M. Pindzola and C. F. Lo

ARO, Inc.

FOREWORD

The work presented herein was sponsored by the Arnold Engineering Development Center (AEDC), Air Force Systems Command (AFSC), Arnold Air Force Station, Tennessee, under Program Element 63101F, Project A016.

The results of research presented were obtained by ARO, Inc. (a subsidiary of Svèrdrup & Parcel and Associates, Inc.), contract operator of AEDC, AFSC, under Contract F40600-69-C-0001. The work was done under ARO Project No. PD3914 from October 1968 to January 1969. The manuscript was submitted for publication on January 29, 1969.

This technical report has been reviewed and is approved.

David C. Reynolds
1st Lt, USAF
Research Division
Directorate of Plans
and Technology

Edward R. Feicht
Colonel, USAF
Director of Plans
and Technology

ABSTRACT

Equations and charts as obtained by theoretical analyses are presented for the evaluation of corrections which must be applied to test data as obtained from wind tunnels because of the presence of the test section boundaries. Results are presented for two-dimensional, circular, and rectangular tunnels with boundaries of the completely closed, completely open, slotted, or perforated variety. Interference factors accounting for the direct effects of model and wake blockage on the longitudinal velocity and of model lift on the upwash velocity are enumerated. In addition, consideration is given to the variation of the longitudinal and vertical velocity components along the tunnel axis leading to buoyancy and streamline-curvature corrections.

CONTENTS

APPENDIXES

NOMENCLATURE

A	Cross-sectional area of wing
A_m	Series coefficient constants, see Appendix II
A_n	Series coefficient in Eq. (5.16)
a	Width of slot
B_m	Series coefficient constants, see Appendix II
B_n	Series coefficient in Eq. (5.17)
b	Semiwidth of a rectangular tunnel
C	Cross-sectional area of tunnel test section
C_D	Drag coefficient
C_F	Force or moment coefficient
C_L	Lift coefficient
C_m	Pitching-moment coefficient
C_n	Series coefficient in Eq. (5.57)
C_p	Pressure coefficient, $\Delta p/q_\infty$
c	Wing chord
$\bar{c}$	Mean aerodynamic chord
D	Model drag
D_m	Series coefficient constants, see Appendix III
D_n	Series coefficient in Eq. (5.63)
d	Doublet strength (Eqs. (3.2) and (4.2))
E_m	Series coefficient constants, see Appendix III
E_n	Series coefficient in Eq. (5.63)
F	Geometric slot parameter (see Fig. 2.1)
G_m	Series coefficient constants, see Appendix III
h	Semiheight of a two-dimensional or rectangular tunnel
I_n	Portion of the integrand of various equations where n = A through R, see Appendix I
I_o, I_1	Modified Bessel functions of the first kind
K	Geometric slot parameter (Eq.(2.7))
K_o, K_1	Modified Bessel functions of the second kind
L	Model lift

ℓ	Slot spacing (see Fig. 2.1)
M	Mach number of the undisturbed stream
m	Source strength (Eqs. (3.23) and (4.18))
N	Number of slots
n	Coordinate in the direction of the outward normal to the wall
P	Slot parameter, $1/(1 + F)$
p	Pressure
Δp	Pressure difference across the wall
Q	Porosity parameter, $1/(1 + \beta/R)$
q	Variable of integration
q_∞	Dynamic pressure of the undisturbed stream
R	Porosity parameter (Eq. (2.9))
Re	Reynolds number
r_o	Radius of a circular tunnel
S	Reference area of the model
s	Semispan of wing
U	Velocity of the undisturbed stream
u	Perturbation velocity in the axial direction
V	Volume of the model
v	Velocity of the flow normal to the wall
w	Upwash velocity
x,y,z	Cartesian coordinates
x,r,θ	Cylindrical coordinates
α	Airfoil angle of attack
α_n	$[q^2 + (n\pi h/b)^2]^{1/2}$
β	$(1 - M^2)^{1/2}$
Γ	Circulation about the wing (Eqs. (3.45) and (4.36))
Δ	Prefix denoting change due to wall interference
δ	Lift-interference factor (Eqs. (3.51), (4.42), and (5.42))
δ_o	Value of δ at x = 0
δ_1	Gradient of δ at x = 0

ϵ	Blockage-interference factor, u/U
θ	Flow angle at the wall, v/U
λ_o, λ_1	Constants in Eqs. (6.10) and (6.11)
μ	$\cot^{-1}(\beta/R)$
ν	$\tan^{-1}(\beta/R)$
ρ	Density of the undisturbed stream
φ	Perturbation velocity potential
φ_i	Interference velocity potential
φ_m	Velocity potential of the model
Ω	Blockage-factor ratio, $\epsilon/\epsilon_{c(x=0)}$

SUBSCRIPTS

B	Effect of blockage
C	Corrected
c	Closed tunnel
g	Effect of velocity gradient (buoyancy)
h	Effect of horizontal walls
o	Open tunnel
p	Perforated tunnel
s	Slotted tunnel or solid blockage
t	Tail surface
v	Effect of vertical walls
w	Wake blockage

SECTION I
INTRODUCTION

Since the conception of the use of ventilated walls for transonic testing in the late 1940's, a large number of tunnels with walls of this type have been put into operation. Inasmuch as these facilities are equally suited for subsonic testing, the question arises as to how these tunnels compare with closed and open jet tunnels in the level of wall interference. A goodly number of papers have therefore appeared treating this question.

In this report, an attempt has been made to summarize and extend the theoretical studies of boundary interference obtained in ventilated walls when operating at subsonic speeds. In Section II, the general approach to the problem is outlined along with the development of a general boundary condition. The material in Sections III and IV is a consolidation of that presented in Refs. 1 and 2 using some of the parameters introduced in Ref. 3. The cases of solid blockage in a two-dimensional tunnel, solid blockage in a circular tunnel, and lift interference in a circular tunnel follow those of Ref. 1. The analyses for lift in a two-dimensional tunnel and wake blockage in both a two-dimensional and a circular tunnel follow the material presented in the Appendix of Ref. 2. The material on interference in a rectangular tunnel presented in Section V is a summary and extension of the work presented in Refs. 4 and 5. A brief review of the equations used to apply interference parameters is given in Section VI.

The consolidation of this material into a single volume in a consistent form and a uniform nomenclature assists in pointing out the similarity of the expressions obtained in the various types of tunnels. The figures in Appendix V also provide a complete recording of the interference parameters required to apply first-order corrections to test data. Since in many cases the interference obtained in ventilated wall tunnels is compared to that in either closed or open boundary tunnels, the magnitude of these interference parameters is included in the presentation. The closed tunnel parameters are denoted by the subscript c and the open jet parameters by the subscript o.

SECTION II
GENERAL ANALYSIS

The effects of the walls of a ventilated wind tunnel on the flow past a test model can be determined using the same basic approach as that used for a tunnel with either completely closed or completely open boundaries. The model is represented by various singularities; a doublet to represent the model solid blockage, a source to represent the model wake, and a vortex to represent the model lift. For tunnels of circular or rectangular shape with either solid or open boundaries, a system of images of the singularity is usually constructed to obtain the interference potential of the boundaries. In the case of a circular closed tunnel the image system is particularly simple. For a rectangular closed tunnel the image system gets more complicated but still manageable. For ventilated walls, however, a suitable image system is impractical to apply so that special analytical treatment is required to obtain the interference potential.

2.1 DIFFERENTIAL EQUATION FOR THE PERTURBATION POTENTIAL

The governing equation for the perturbation potential is based on the linearized equation for subsonic compressible flow given in cartesian coordinates by

$$\beta^2 \frac{\partial^2 \varphi}{\partial x^2} + \frac{\partial^2 \varphi}{\partial y^2} + \frac{\partial^2 \varphi}{\partial z^2} = 0 \tag{2.1}$$

or in the cylindrical coordinates $y = r \cos \theta$ and $z = r \sin \theta$ by

$$\beta^2 \frac{\partial^2 \varphi}{\partial x^2} + \frac{\partial^2 \varphi}{\partial r^2} + \frac{1}{r} \frac{\partial \varphi}{\partial r} + \frac{1}{r^2} \frac{\partial^2 \varphi}{\partial \theta^2} = 0 \tag{2.2}$$

where φ is the perturbation velocity potential of the flow in the tunnel.

The perturbation potential may be written as

$$\varphi = \varphi_m + \varphi_i \tag{2.3}$$

where φ_m is the potential of the flow about the model in free air and φ_i is the interference potential induced by the tunnel boundaries.

If φ_m is taken to be a known solution of Eq. (2.1) which approximates the true free-air potential at points far from the model, φ_i can be calculated from the fact that the sum $\varphi_m + \varphi_i$ satisfies a known boundary condition at the wall. Since the values of φ_m are used only at the wall, any inaccuracy in the value of φ_m near the model would not appreciably affect the calculation of φ_i.

The primary objective in this procedure is to estimate the change in stream conditions caused by the walls at the position of the model. It is assumed that the velocity components derived from φ_i are constants near the model which can be subtracted from the stream velocity to obtain the equivalent free-air stream velocity. Thus,

$$u = \frac{\partial \varphi_i}{\partial x}$$

gives the blockage corrections due to the model and its wake, and

$$w = \frac{\partial \varphi_i}{\partial z}$$

is the upwash correction.

The variations of these velocity components along the model axis in turn lead to the so-called buoyancy and streamline curvature corrections.

2.2 BOUNDARY CONDITIONS

In this section a single expression approximately representating the boundary conditions of solid, open, slotted, and perforated walls will be developed.

2.2.1 Solid Wall

Let x be the coordinate in the direction of the free stream and n the coordinate in a direction perpendicular to the x direction. Consider a wall which is perpendicular to the n direction (i.e., parallel to the free stream). If the wall is solid, the condition of no flow through the wall can be expressed as

$$\frac{\partial \varphi}{\partial n} = 0 \qquad (2.4)$$

2.2.2 Open Boundary

In the case of an open jet there is no pressure drop across the jet boundary so that there is zero perturbation pressure at the boundary. With a disturbance in the stream this boundary does not remain parallel to the free stream. However, for convenience, the condition of zero perturbation pressure is imposed at a surface parallel to the free stream and coinciding with the jet boundary far upstream of the disturbance. Also, for convenience, this surface can be called an open wall and the boundary condition can be expressed as

$$\frac{\partial \varpi}{\partial x} = 0 \tag{2.5}$$

2.2.3 Slotted Wall

An approximate boundary equation for a slotted wall has been derived by a number of authors (see for example Ref. 1). The pressure at the slots is assumed constant and equal to the free-stream pressure. The resulting uniform boundary condition is

$$\frac{\partial \varpi}{\partial x} + K \frac{\partial^2 \varpi}{\partial x \partial n} = 0 \tag{2.6}$$

where K is related to the slot geometry (see Fig. 2.1) by

$$K = \frac{\ell}{\pi} \ln \left[\csc \left(\frac{\pi a}{2\ell} \right) \right] \tag{2.7}$$

and a/ℓ is the open area ratio of the wall. A plot of $\ln [\csc(\pi a/2\ell)]$ versus a/ℓ is shown in Fig. 2.2. Slotted walls to which Eq. (2.6) is applicable will henceforth be referred to in this report as ideal slotted walls.

2.2.4 Perforated Wall

An average boundary condition for a perforated wall is derived in Ref. 6. The average velocity of the flow normal to the wall is assumed to be proportional to the pressure drop through the wall. This leads to the boundary equation

$$\frac{\partial \varpi}{\partial x} + \frac{1}{R} \frac{\partial \varpi}{\partial n} = 0 \tag{2.8}$$

where R is a porosity parameter defined as

$$R = \frac{\partial\varphi/\partial n}{\partial\varphi/\partial x} = \frac{2\ v/U}{\Delta p/q_\infty} = \frac{2\theta}{C_p} \qquad (2.9)$$

in which

v = velocity of the flow normal to the wall

U = velocity of the undisturbed stream

Δp = pressure difference across the wall

q_∞ = dynamic pressure of the undisturbed stream

and

$\theta = v/U$

$C_p = \Delta p/q_\infty$

The parameter R can be determined experimentally by measuring the mass flow and pressure drop through a sample of wall as discussed for example in Ref. 7.

2.2.5 General Boundary Condition

Solutions for the boundary interference based on Eqs. (2.6) and (2.8) can be obtained in one calculation by combining the two equations in the form

$$\frac{\partial\varphi}{\partial x} + K\frac{\partial^2\varphi}{\partial x\partial n} + \frac{1}{R}\frac{\partial\varphi}{\partial n} = 0 \qquad (2.10)$$

Thus, wall interference solutions based on Eq. (2.10) contain as special cases:

a. Closed wall, $K \to \infty$ or $1/R \to \infty$

b. Open wall, $K = 0$ and $1/R = 0$

c. Ideal slotted wall, $1/R = 0$

d. Perforated wall, $K = 0$

SECTION III
INTERFERENCE IN A TWO-DIMENSIONAL TUNNEL

The present section is concerned with the interference on two-dimensional models spanning a tunnel of height 2h as shown in Fig. 2.1a. The tunnel sidewalls are assumed to act merely as reflection planes contributing nothing to the flow about a model located midway between the horizontal walls.

Blockage interference arises from both the model and its wake, the two components being called solid and wake blockage respectively. It manifests itself as an increment $u = \epsilon_B U$ in the stream velocity. The total blockage factor ϵ_B is conveniently expressed as the sum of the solid-blockage factor ϵ_s and the wake-blockage factor ϵ_w, which are derived independently at zero model lift. Associated with both the solid- and wake-blockage increments are longitudinal velocity gradients, which impose a corresponding drag force on the model.

Lift interference arises from the lift produced by the model. The interference may be regarded as composed of two parts; an upwash velocity, w, and a streamline curvature associated with the variation in the wall-induced upwash along the model length.

3.1 SOLID BLOCKAGE

If the model is small and thin, the solid blockage may be represented by a two-dimensional doublet whose velocity potential in a free stream of subsonic Mach number, M, is

$$\varphi_m = \frac{d}{2\pi} \frac{x}{x^2 + \beta^2 z^2} \tag{3.1}$$

The origin of the coordinate system is at the centroid of the model. The doublet strength, d, is related to the cross-sectional area of the model, A, by the relationship

$$d = AU/\beta \tag{3.2}$$

In Ref. 1, the interference potential is obtained by a Fourier transform method using the approach outlined in Section II and is given by

$$\varphi_i = -\frac{d}{2\pi\beta h}\left\{\frac{\beta}{R}\int_o^\infty \frac{1}{I_A}\cosh\left(\frac{qz}{h}\right)\cos\left(\frac{qx}{\beta h}\right)dq + \frac{1}{2}\int_o^\infty \frac{I_B}{I_A}\cosh\left(\frac{qz}{h}\right)\sin\left(\frac{qx}{\beta h}\right)dq\right\} \quad (3.3)$$

where the various portions of the integrands denoted by I and a corresponding subscript are listed in Appendix I and a slot parameter, F (see Fig. 2.1) has been introduced.

The interference velocity, $\partial\varphi_i/\partial x$, is given by

$$u_s = \frac{d}{2\pi\beta^2 h^2}\left\{\frac{\beta}{R}\int_o^\infty \frac{1}{I_A}\cosh\left(\frac{qz}{h}\right)\sin\left(\frac{qx}{\beta h}\right)|q\,dq - \frac{1}{2}\int_o^\infty \frac{I_B}{I_A}\cosh\left(\frac{qz}{h}\right)\cos\left(\frac{qx}{\beta h}\right)q\,dq\right\} \quad (3.4)$$

The longitudinal velocity gradient is given by

$$\frac{\partial u_s}{\partial x} = \frac{d}{2\pi\beta^3 h^3}\left\{\frac{\beta}{R}\int_o^\infty \frac{1}{I_A}\cosh\left(\frac{qz}{h}\right)\cos\left(\frac{qx}{\beta h}\right)q^2\,dq + \frac{1}{2}\int_o^\infty \frac{I_B}{I_A}\cosh\left(\frac{qz}{h}\right)\sin\left(\frac{qx}{\beta h}\right)q^2\,dq\right\} \quad (3.5)$$

At $x = z = 0$, the equations for the interference velocity and the velocity gradient reduce to

$$u_s = -\frac{d}{4\pi\beta^2 h^2}\int_o^\infty \frac{I_B}{I_A}\,q\,dq \quad (3.6)$$

and

$$\frac{\partial u_s}{\partial x} = \frac{d}{2\pi\beta^3 h^3}\frac{\beta}{R}\int_o^\infty \frac{1}{I_A}\,q^2\,dq \quad (3.7)$$

3.1.1 Closed Tunnel

Letting $F \to \infty$ or $\beta/R \to \infty$ in Eq. (3.6) and using Eq. (3.2) gives

$$(\epsilon_s)_c = \frac{u_s}{U} = \frac{\pi}{24} \frac{A}{\beta^3 h^2} = 0.131 \frac{A}{\beta^3 h^2} \tag{3.8}$$

and from Eq. (3.7)

$$\left(\frac{\partial \epsilon_s}{\partial x} \right)_c = 0 \tag{3.9}$$

3.1.2 Open Jet

Letting $F = 0$ and $\beta/R = 0$ yields

$$(\epsilon_s)_o = -\frac{\pi}{48} \frac{A}{\beta^3 h^2} = -0.066 \frac{A}{\beta^3 h^2} \tag{3.10}$$

and

$$\left(\frac{\partial \epsilon_s}{\partial x} \right)_o = 0 \tag{3.11}$$

3.1.3 Slotted Wall Tunnel

To study the blockage effects in a ventilated wall tunnel, the parameter Ω is introduced as in Ref. 3 which is defined as the ratio of ϵ in a ventilated tunnel to its value ϵ_c at $x = 0$ in a similar tunnel with closed walls. Thus, using Eq. (3.8), the solid-blockage factor for a slotted tunnel is given by

$$(\Omega_s)_s = \frac{(\epsilon_s)_s}{(\epsilon_s)_{c\,(x=0)}} = \left(\frac{24\ \beta^3 h^2}{\pi\ A} \right) (\epsilon_s)_s \tag{3.12}$$

Equation (3.4) has been evaluated at various values of the slot parameter $P = 1/(1+F)$ to obtain the distribution of the solid-blockage ratio Ω along the x-axis of a slotted tunnel. The results are shown in Fig. 3.1.

Equation (3.6) for the interference velocity at x = z = 0 for the case of a slotted wall tunnel ($\beta/R = 0$) reduces to

$$(\Omega_S)_S = -\frac{6}{\pi^2}\int_0^\infty \frac{1 - (Fq)^2 + (1 - Fq)^2\, e^{-2q}}{(\cosh q + Fq \sinh q)^2}\, q\, dq \quad (3.13)$$

or as given in Ref. 1

$$(\Omega_S)_S = -\frac{24}{\pi^2}\int_0^\infty \frac{(1 - Fq)\, e^{-2q}}{(1 + Fq) + (1 - Fq)\, e^{-2q}}\, q\, dq \quad (3.14)$$

The variation of Ω_S at the model position (x = 0) versus the slot parameter P in a two-dimensional slotted tunnel is shown in Fig. 3.2. Zero solid blockage is achieved at P = 0.45 or F = 1.18.

Examination of the slot parameter indicates that for each value of the ratio (h/ℓ) there is a different value of the open-area ratio (a/ℓ) for zero blockage as shown in the following table:

$\frac{h}{\ell}$	1	2	3	4
$100\,\frac{a}{\ell}$	1.6	0.4×10^{-1}	0.9×10^{-3}	0.2×10^{-4}

As seen from Eq. (3.7), the longitudinal velocity gradient at the model position is zero in an ideal slotted wall tunnel. The solid-blockage factor varies symmetrically on either side of the position of the model as shown in Fig. 3.1. Hence there is no horizontal buoyancy force and no correction to be applied to the measured drag. See Eq. (3.20).

3.1.4 Perforated Wall Tunnel

The variation of the solid-blockage ratio along the x-axis of a perforated wall tunnel as obtained from Eq. (3.4) for various values of the porosity parameter $Q = 1/(1 + \beta/R)$ is shown in Fig. 3.3. The solid-blockage ratio at the model position for the perforated tunnel (F = 0), can be obtained from Eq. (3.6) and is given by

$$(\Omega_S)_P = -\frac{6}{\pi^2}\int_0^\infty \frac{1 - (\beta/R)^2 + \left[1 + (\beta/R)^2\right] e^{-2q}}{\cosh^2 q + (\beta/R)^2 \sinh^2 q}\, q\, dq \quad (3.15)$$

or as given in Ref. 1

$$(\Omega_s)_p = -\frac{12}{\pi^2}\int_0^\infty \frac{[\cosh q - (\beta/R)^2 \sinh q]\, e^{-q}}{\cosh^2 q + (\beta/R)^2 \sinh^2 q}\, q\, dq \quad (3.16)$$

This case was initially considered by Goodman (Ref. 6) and Kassner (Ref. 8). By employing a modified image method, Kassner obtained a simple expression for the solid-blockage ratio given by

$$(\Omega_s)_p = 1 - 6\left(\frac{\mu}{\pi}\right) + 6\left(\frac{\mu}{\pi}\right)^2 \quad (3.17)$$

where $\mu = \cot^{-1}(\beta/R)$. The variation of Ω_s versus the porosity parameter Q is shown in Fig. 3.4. Zero solid blockage occurs when $Q = 0.44$ or $\beta/R = 1.28$.

As indicated in Fig. 3.3, the boundaries of a perforated wall tunnel, unlike the ideal slotted wall tunnel, induce a velocity gradient in the region of the model because of the solid blockage of the model. At the model position, this gradient is obtained from Eq. (3.7) and is given by

$$\left(\frac{\partial \Omega_s}{\partial x}\right)_p = \frac{12}{\pi^2}\frac{\beta}{\beta h}\frac{\beta}{R}\int_0^\infty \frac{q^2}{\cosh^2 q + (\beta/R)^2 \sinh^2 q}\, dq \quad (3.18)$$

A plot of $\left[\frac{\partial \Omega_s}{\partial (x/2\beta h)}\right]_p$ is presented in Fig. 3.5 where it is seen that the gradient is a maximum at a value of Q at which the solid blockage is zero.

The pressure gradient associated with blockage is related to the velocity gradient by the equation

$$\frac{\partial p}{\partial x} = -\rho U^2 \frac{\partial \epsilon}{\partial x} \quad (3.19)$$

This pressure gradient imposes an unwanted drag force on the model which is given by

$$(\Delta C_D)_g = \frac{\partial p}{\partial x}\frac{A}{\frac{1}{2}\rho U^2 c} = -\frac{2A}{c}\frac{\partial \epsilon}{\partial x} \quad (3.20)$$

The interference drag imposed by the solid-blockage velocity gradient ε_s thus given by

$$(\Delta C_D)_{sg} = -\frac{2A}{c}\left(\frac{\partial \varepsilon_s}{\partial x}\right)_p = -\frac{\pi A^2}{2\beta^4 h^3 c}\left[\frac{\partial \Omega_s}{\partial (x/2\beta h)}\right]_p \tag{3.21}$$

where the value of the term in the brackets can be obtained from Fig. 3.5.

3.2 WAKE BLOCKAGE

The presence of the wake downstream of the model gives rise to two constraint effects when the tunnel walls are solid. One is an increment in the longitudinal stream velocity, the other is the horizontal buoyancy associated with the longitudinal velocity gradient at the model position. In the open-jet tunnel, the first effect (but not the second) is usually taken to be zero, because the boundaries of the jet can be displaced away from the tunnel axis in order to compensate for the low-velocity air in the model wake. There is then no need to increase the stream velocity in the flow outside the wake in order to maintain the same mass flow upstream and downstream of the model. Similar considerations would apply to the slotted tunnel.

The model wake is represented by a two-dimensional source, the potential of which is given by

$$\varphi_m = \frac{m}{2\pi\beta} \ln (x^2 + \beta^2 z^2)^{\frac{1}{2}} \tag{3.22}$$

The source strength m is related to the drag of a model by the formula

$$m = \frac{D}{\rho U} = \frac{1}{2} U C_D c \tag{3.23}$$

In Ref. 2 the interference potential is given as

$$\varphi_i = \frac{m}{2\pi\beta}\left\{\int_o^\infty \frac{I_C}{I_A} \cosh\left(\frac{qz}{h}\right) \cos\left(\frac{qx}{\beta h}\right) \frac{dq}{q} - \frac{\beta}{R}\int_o^\infty \frac{I_D}{I_A} \cosh\left(\frac{qz}{h}\right) \sin\left(\frac{qx}{\beta h}\right) \frac{dq}{q}\right\} \tag{3.24}$$

The interference velocity is obtained as

$$u_w = -\frac{m}{2\pi\beta^2 h}\left\{\int_o^\infty \frac{I_C}{I_A}\cosh\left(\frac{qz}{h}\right)\sin\left(\frac{qx}{\beta h}\right)dq + \frac{\beta}{R}\int_o^\infty \frac{I_D}{I_A}\cosh\left(\frac{qz}{h}\right)\cos\left(\frac{qx}{\beta h}\right)dq\right\} \quad (3.25)$$

The longitudinal velocity gradient is

$$\frac{\partial u_w}{\partial x} = -\frac{m}{2\pi\beta^3 h^2}\left\{\int_o^\infty \frac{I_C}{I_A}\cosh\left(\frac{qz}{h}\right)\cos\left(\frac{qx}{\beta h}\right)q\,dq - \frac{\beta}{R}\int_o^\infty \frac{I_D}{I_A}\cosh\left(\frac{qz}{h}\right)\sin\left(\frac{qx}{\beta h}\right)q\,dq\right\} \quad (3.26)$$

At $x = z = 0$ the interference velocity and the velocity gradient reduce to

$$u_w = \frac{-m}{2\pi\beta^2 h}\frac{\beta}{R}\int_o^\infty \frac{I_D}{I_A}dq \quad (3.27)$$

and

$$\frac{\partial u_w}{\partial x} = -\frac{m}{2\pi\beta^3 h^2}\int_o^\infty \frac{I_C}{I_A}q\,dq \quad (3.28)$$

or in terms of $I_B = 2\,I_C$ as

$$\frac{\partial u_w}{\partial x} = -\frac{m}{4\pi\beta^3 h^2}\int_o^\infty \frac{I_B}{I_A}q\,dq \quad (3.29)$$

The integral in Eq. (3.29) is identical to that in Eq. (3.6) thus providing a direct correspondence between the solid-blockage correction and the correction due to the wake velocity gradient.

3.2.1 Closed Tunnel

For the closed tunnel, the interference velocity at the position of the model, x = z = 0, is given by Eq. (3.27) as zero. Far upstream, however, the interference velocity is equal to $-m/4\beta^2 h$. Thus the flow at the model has an interference velocity relative to the flow far upstream given by

$$(\epsilon_w)_c = \frac{u_w}{U} = \frac{C_D c}{8\beta^2 h} \tag{3.30}$$

The velocity gradient at the model due to the wake is from Eq. (3.29) given by

$$\left(\frac{\partial \epsilon_w}{\partial x}\right)_c = \frac{\pi C_D c}{48\beta^3 h^2} \tag{3.31}$$

3.2.2 Open Jet

For the open tunnel, the interference velocity, is zero both at the model and far upstream. Therefore

$$(\epsilon_w)_o = 0 \tag{3.32}$$

The velocity gradient at the model is

$$\left(\frac{\partial \epsilon_w}{\partial x}\right)_o = -\frac{\pi C_D c}{96\beta^3 h^2} \tag{3.33}$$

3.2.3 Slotted Wall Tunnel

For an ideal slotted wall tunnel, $\beta/R = 0$, the interference velocity, $\epsilon_w U$, as obtained from Eq. (3.25) is zero both at the model and far upstream.

The velocity gradient at the model position is obtained from Eq. (3.29) for $\beta/R = 0$ and is given by

$$\left(\frac{\partial \epsilon_w}{\partial x}\right)_s = -\frac{C_D c}{4\pi\beta^3 h^2} \int_o^\infty \frac{(1 - Fq)e^{-q}}{\cosh q + Fq \sinh q}\, q\, dq \tag{3.34}$$

or in an equivalent form

$$\left(\frac{\partial \epsilon_w}{\partial x}\right)_s = -\frac{C_D c}{8\pi\beta^3 h^2} \int_o^\infty \frac{1 - (Fq)^2 + (1 - Fq)^2 e^{-2q}}{(\cosh q + Fq \sinh q)^2}\, q\, dq \qquad (3.35)$$

The integral in Eq. (3.35) is the same as that in Eq. (3.13). The wake-blockage gradient can therefore be identified with the solid-blockage factor. By combining Eqs. (3.13) and (3.35)

$$\left(\frac{\partial \epsilon_w}{\partial x}\right)_s = \frac{\pi}{48} \frac{C_D c}{\beta^3 h^2} (\Omega_s)_s = \left(\frac{\partial \epsilon_w}{\partial x}\right)_c (\Omega_s)_s \qquad (3.36)$$

which becomes zero when $(\Omega_s)_s$ vanishes. Hence, in an ideal slotted tunnel, the wake-blockage gradient or buoyancy correction is eliminated if zero solid-blockage conditions are present. If this is not the case, the correction to the measured drag as obtained from Eqs. (3.20) and (3.36) is

$$(\Delta C_D)_{wg} = -\frac{2A}{c} \left(\frac{\partial \epsilon_w}{\partial x}\right)_c (\Omega_s)_s = -C_D (\epsilon_s)_c (\Omega_s)_s \qquad (3.37)$$

where $(\partial \epsilon_w/\partial x)_c$ is given by Eq. (3.31) and the value of $(\Omega_s)_s$ can be obtained from Fig. 3.2.

3.2.4 Perforated Wall Tunnel

For a perforated wall tunnel, F = 0, the interference velocity at the position of the model from Eq. (3.27) becomes

$$(\epsilon_w)_p = -\frac{C_D c}{4\pi\beta^2 h} \frac{\beta}{R} \int_o^\infty \frac{dq}{\cosh^2 q + (\beta/R)^2 \sinh^2 q} \qquad (3.38)$$

or

$$(\epsilon_w)_p = -\frac{C_D c}{4\pi\beta^2 h} \tan^{-1} \frac{\beta}{R} \qquad (3.39)$$

In terms of the parameter Ω_w, Eq. (3.39) may be written

$$(\Omega_w)_p = \frac{(\epsilon_w)_p}{(\epsilon_w)_{c(x=0)}} = -\frac{2}{\pi} \tan^{-1} \frac{\beta}{R} = -\frac{2\nu}{\pi} \qquad (3.40)$$

The variation of $(\Omega_w)_p$ with Q is shown in Fig. 3.4. At zero solid blockage, $(\Omega_w)_p$ is about -0.58; for $Q < 0.44$, the wake blockage would tend to counter the solid blockage.

The velocity gradient at the model position from Eq. (3.29) with F = 0 is given by

$$\left(\frac{\partial \epsilon_w}{\partial x}\right)_p = -\frac{C_D c}{4\pi\beta^3 h^2} \int_0^\infty \frac{[\cosh q - (\beta/R)^2 \sinh q]\, e^{-q}}{\cosh^2 q + (\beta/R)^2 \sinh^2 q}\, q\, dq \qquad (3.41)$$

The integrand in Eq. (3.41) is the same as that in Eq. (3.16) and the gradient due to the wake blockage will therefore be zero for the same value of Q as that for which the solid blockage is zero. In general, the velocity gradient and the corresponding drag correction are given by

$$\left(\frac{\partial \epsilon_w}{\partial x}\right)_p = \frac{\pi}{48} \frac{C_D c}{\beta^3 h^2} (\Omega_s)_p = \left(\frac{\partial \epsilon_w}{\partial x}\right)_c (\Omega_s)_p \qquad (3.42)$$

and

$$(\Delta C_D)_{wg} = - C_D (\epsilon_s)_c (\Omega_s)_p \qquad (3.43)$$

where the value of $(\Omega_s)_p$ can be obtained from Fig. 3.4.

3.3 LIFT INTERFERENCE

The upwash correction for a two-dimensional wing is calculated using a single bound vortex to represent the model. The potential of the vortex in free air is given by

$$\varphi_m = -\frac{\Gamma}{2\pi} \tan^{-1} \frac{\beta z}{x} \qquad (3.44)$$

The circulation, Γ, about the wing is related to the model lift per unit width by the relationship

$$L = \rho U \Gamma = \frac{1}{2} \rho U^2 C_L c \qquad (3.45)$$

In Ref. 2 the interference potential for this case has been determined as

$$\omega_i = -\frac{\Gamma}{2\pi}\left\{\frac{\beta}{R}\int_o^\infty \frac{I_E}{I_F}\sinh\left(\frac{qz}{h}\right)\cos\left(\frac{qx}{\beta h}\right)\frac{dq}{q} + \int_o^\infty \frac{I_G}{I_F}\sinh\left(\frac{qz}{h}\right)\sin\left(\frac{qx}{\beta h}\right)\frac{dq}{q}\right\} \quad (3.46)$$

From Eq. (3.46), the interference velocity in the free-stream direction is seen to be zero.

The upwash velocity is

$$w = \frac{\partial \omega_i}{\partial z} = -\frac{\Gamma}{2\pi h}\left\{\frac{\beta}{R}\int_o^\infty \frac{I_E}{I_F}\cosh\left(\frac{qz}{h}\right)\cos\left(\frac{qx}{\beta h}\right)dq + \int_o^\infty \frac{I_G}{I_F}\cosh\left(\frac{qz}{h}\right)\sin\left(\frac{qx}{\beta h}\right)dq\right\} \quad (3.47)$$

The streamwise gradient of the upwash velocity or the streamline curvature is obtained by differentiating Eq. (3.47) with respect to the free-stream direction, x, and is given by

$$\frac{\partial w}{\partial x} = \frac{\Gamma}{2\pi\beta h^2}\left\{\frac{\beta}{R}\int_o^\infty \frac{I_E}{I_F}\cosh\left(\frac{qz}{h}\right)\sin\left(\frac{qx}{\beta h}\right)q\,dq - \int_o^\infty \frac{I_G}{I_F}\cosh\left(\frac{qz}{h}\right)\cos\left(\frac{qx}{\beta h}\right)q\,dq\right\} \quad (3.48)$$

At x = z = 0, the upwash velocity and the velocity gradient reduce to

$$w = -\frac{\Gamma}{2\pi h}\frac{\beta}{R}\int_o^\infty \frac{I_E}{I_F}\,dq \quad (3.49)$$

and

$$\frac{\partial w}{\partial x} = -\frac{\Gamma}{2\pi\beta h^2}\int_o^\infty \frac{I_G}{I_F}\,q\,dq \quad (3.50)$$

For a small model, the lift interference in a two-dimensional tunnel is expressed by the following parameters. The distribution of the upwash velocity, δ, along the tunnel axis is expressed as

$$\delta = \delta(x) = \frac{2h}{cC_L} \frac{w}{U} \tag{3.51}$$

where w is obtained from Eq. (3.47). The upwash interference at the model position (x = z = 0) is defined as

$$\delta_o = \frac{2h}{cC_L} \frac{w}{U} \tag{3.52}$$

where w is given by Eq. (3.49). The final parameter which denotes the streamline curvature at the model position is given by

$$\delta_1 = \frac{\partial \delta}{\partial (x/2\beta h)} = \frac{4\ \beta h^2}{cC_L} \left(\frac{1}{U} \frac{\partial w}{\partial x} \right) \tag{3.53}$$

where ∂w/∂x is obtained from Eq. (3.50).

3.3.1 Closed Tunnel

In a closed tunnel the upwash both at the model and far upstream is zero giving

$$\delta_o = 0 \tag{3.54}$$

The curvature of the flow at the model from Eq. (3.50) in the closed tunnel is

$$\left(\frac{1}{U} \frac{\partial w}{\partial x} \right)_c = \frac{\pi\ C_L c}{96\ \beta h^2} \tag{3.55}$$

or in terms of the interference factor δ_1

$$\delta_1 = \frac{\pi}{24} = 0.1309 \tag{3.56}$$

3.3.2 Open Jet

For an open jet, the upwash is zero at the position of the model but far upstream the upwash becomes $\Gamma/4h$. Thus relative to conditions far upstream, the upwash at the model is given by

$$\left(\frac{w}{U}\right)_o = -\frac{C_L c}{8h} \tag{3.57}$$

or

$$\delta_o = -\frac{1}{4} \tag{3.58}$$

The curvature at $x = z = 0$ is given as

$$\left(\frac{1}{U}\frac{\partial w}{\partial x}\right)_o = -\frac{\pi C_L c}{48\beta h^2} \tag{3.59}$$

or

$$\delta_1 = -\frac{\pi}{12} = -0.2618 \tag{3.60}$$

3.3.3 Slotted Wall Tunnel

For a slotted wall tunnel ($\beta/R = 0$), Eq. (3.47) reduces to

$$w = -\frac{\Gamma}{2\pi h}\int_o^\infty \frac{(1 - Fq)\, e^{-q} \cosh(qz/h) \sin(qx/\beta h)}{\sinh q + Fq \cosh q}\, dq \tag{3.61}$$

Equation (3.61) has been evaluated at various values of the slot parameter P to obtain the distribution of the upwash velocity in terms of the interference factor δ along the x-axis of the tunnel. At $x = z = 0$, Eq. (3.61) yields zero upwash. However, far upstream an upwash equal to $\Gamma/4h(1+F)$ is obtained. The results obtained for δ in the vicinity of the model are therefore plotted in Fig. 3.6 relative to the upwash that exists far upstream. The relative value of the upwash at the model position in terms of the interference factor can be expressed as

$$\delta_o = -\frac{1}{4(1+F)} = -\frac{P}{4} \tag{3.62}$$

The streamline curvature at x = z = 0 from Eq. (3.60) becomes

$$\left(\frac{1}{U}\frac{\partial w}{\partial x}\right)_s = -\frac{\Gamma}{2\pi\beta h^2 U}\int_o^\infty \frac{(1 - Fq)\, q\, e^{-q}}{\sinh q + Fq \cosh q}\, dq \tag{3.63}$$

or in terms of the interference factor

$$\delta_1 = -\frac{1}{\pi}\int_o^\infty \frac{(1 - Fq)\, q\, e^{-q}}{\sinh q + Fq \cosh q}\, dq \tag{3.64}$$

Values of the interference factors δ_o and δ_1 are presented in Fig. 3.7 in terms of the slot parameter P. Zero streamline curvature occurs when P = 0.39 or F = 1.59. The values of δ_o and δ_1 at P = 0.45 where the solid blockage is zero are -0.11 and -0.02, respectively.

3.3.4 Perforated Wall Tunnel

In the case of a perforated wall tunnel (F = 0) Eq. (3.47) reduces to

$$w = -\frac{\Gamma}{2\pi h}\left\{\frac{\beta}{R}\int_o^\infty \frac{\cosh(qz/h)\cos(qx/\beta h)}{\sinh^2 q + (\beta/R)^2\cosh^2 q}\, dq + \int_o^\infty \frac{\left[\sinh q - (\beta/R)^2\cosh q\right]e^{-q}}{\sinh^2 q + (\beta/R)^2\cosh^2 q}\cosh\left(\frac{qz}{h}\right)\sin\left(\frac{qx}{\beta h}\right)dq\right\} \tag{3.65}$$

The results of an evaluation of the upwash velocity in terms of δ for various values of the porosity parameter Q are shown in Fig. 3.8. In this case, the upwash far upstream is zero so that the total upwash is that obtained directly from Eq. (3.65). At x = z = 0 the interference factor is given by

$$\delta_o = -\frac{1}{2\pi}\cot^{-1}\frac{\beta}{R} = -\frac{\mu}{2\pi} \tag{3.66}$$

The curvature of the flow at x = z = 0 from Eq. (3.60) is

$$\left(\frac{1}{U}\frac{\partial w}{\partial x}\right)_p = -\frac{\Gamma}{2\pi\beta h^2 U}\int_o^\infty \frac{\left[\sinh q - (\beta/R)^2\cosh q\right]e^{-q}}{\sinh^2 q + (\beta/R)^2\cosh^2 q}\, q\, dq \tag{3.67}$$

Brescia (Ref. 9) used a different analytical approach to obtain the interference factor in a form similar to Eq. (3.17) as

$$\delta_1 = -\frac{\pi}{12}\left[1 - 6\left(\frac{\nu}{\pi}\right) + 6\left(\frac{\nu}{\pi}\right)^2\right] \tag{3.68}$$

where $\nu = \tan^{-1}(\beta/R)$. The streamline curvature will thus be zero at a value of $\beta/R = 0.78$ which is the reciprocal of the value at which the solid blockage is zero. Values of the interference factors are presented in Fig. 3.9. For a tunnel designed for zero solid blockage ($Q = 0.44$), the lift interference is 0.42 of that in an open tunnel and the streamline curvature is 0.46 of that in a closed tunnel.

SECTION IV
INTERFERENCE IN A CIRCULAR TUNNEL

In a manner similar to the two-dimensional tunnel, the model blockage, model wake, and lift of the wing will be represented by simple singularities. A three-dimensional doublet will be used to represent the model blockage, a three-dimensional source to represent the wake, and a horseshoe vortex to represent the wing lift. In all cases the singularity is placed at the center of the tunnel and the x-axis is taken positive downstream along the centerline of the tunnel as shown in Fig. 2.1b.

4.1 SOLID BLOCKAGE

The potential for a three-dimensional doublet at the origin in cylindrical coordinates is expressed by

$$\varphi_m = \frac{d}{4\pi}\,\frac{x}{(x^2 + \beta^2 r^2)^{3/2}} \tag{4.1}$$

The strength of the doublet, d, is related to the model size by the relationship

$$d = UV \tag{4.2}$$

where V is the volume of the model..

Fourier integral expressions may again be used to deduce the perturbation velocity and hence the solid-blockage factor. In Ref. 1, the solution is given as

$$\varphi_i = -\frac{d}{2\pi^2\beta^2 r_o^2}\left\{\frac{\beta}{R}\int_o^\infty \frac{I_H}{I_M} I_o\left(\frac{qr}{r_o}\right)\cos\left(\frac{qx}{\beta r_o}\right) q\, dq + \int_o^\infty \frac{I_K}{I_M} I_o\left(\frac{qr}{r_o}\right)\sin\left(\frac{qx}{\beta r_o}\right) q\, dq\right\} \tag{4.3}$$

where r_o is the radius of the tunnel test section.

The interference velocity (noting that $I_H = 1/q$) is given by

$$u_s = \frac{d}{2\pi^2\beta^3 r_o^3}\left\{\frac{\beta}{R}\int_o^\infty \frac{1}{I_M} I_o\left(\frac{qr}{r_o}\right)\sin\left(\frac{qx}{\beta r_o}\right) q\, dq - \int_o^\infty \frac{I_K}{I_M} I_o\left(\frac{qr}{r_o}\right)\cos\left(\frac{qx}{\beta r_o}\right) q^2\, dq\right\} \tag{4.4}$$

The longitudinal velocity gradient becomes

$$\frac{\partial u_s}{\partial x} = \frac{d}{2\pi^2\beta^4 r_o^4}\left\{\frac{\beta}{R}\int_o^\infty \frac{1}{I_M} I_o\left(\frac{qr}{r_o}\right)\cos\left(\frac{qx}{\beta r_o}\right) q^2\, dq + \int_o^\infty \frac{I_K}{I_M} I_o\left(\frac{qr}{r_o}\right)\sin\left(\frac{qx}{\beta r_o}\right) q^3\, dq\right\} \tag{4.5}$$

At $x = r = 0$, the equations for the interference velocity and the velocity gradient reduce to

$$u_s = -\frac{d}{2\pi^2\beta^3 r_o^3}\int_o^\infty \frac{I_K}{I_M} q^2\, dq \tag{4.6}$$

and

$$\frac{\partial w_s}{\partial x} = \frac{d}{2\pi^2 \beta^4 r_o^4} \frac{\beta}{R} \int_o^\infty \frac{1}{l_M} q^2 \, dq \tag{4.7}$$

4.1.1 Closed Tunnel

For a closed wall tunnel with $F \to \infty$ or $\beta/R \to \infty$, Eq. (4.6) yields

$$(\epsilon_s)_c = \frac{1.2 \, V}{\pi^2 \beta^3 r_o^3} = 0.121 \frac{V}{\beta^3 r_o^3} \tag{4.8}$$

and from Eq. (4.7)

$$\left(\frac{\partial \epsilon_s}{\partial x}\right)_c = 0 \tag{4.9}$$

4.1.2 Open Jet

For an open jet with both $F = 0$ and $\beta/R = 0$, Eq. (4.6) gives

$$(\epsilon_s)_o = -\frac{0.324 \, V}{\pi^2 \beta^3 r_o^3} = -0.033 \frac{V}{\beta^3 r_o^3} \tag{4.10}$$

and from Eq. (4.7)

$$\left(\frac{\partial \epsilon_s}{\partial x}\right)_o = 0 \tag{4.11}$$

4.1.3 Slotted Wall Tunnel

For an ideal slotted wall tunnel Eq. (4.6) reduces to

$$(\epsilon_s)_s = - \frac{V}{2\pi^2 \beta^3 r_o^3} \int_o^\infty \frac{K_o(q) - qF\, K_1(q)}{I_o(q) + qF\, I_1(q)}\, q^2\, dq \qquad (4.12)$$

In terms of the blockage-factor ratio

$$(\Omega_s)_s = - \frac{1}{2.4} \int_o^\infty \frac{K_o(q) - qF\, K_1(q)}{I_o(q) + qF\, I_1(q)}\, q^2\, dq \qquad (4.13)$$

The variation of $(\Omega_s)_s$ with the slot geometry parameter, P, is shown in Fig. 4.1 for the ideal slotted tunnel. Zero blockage in the ideal slotted tunnel occurs when the abscissa P = 0.64, i.e., when F = 0.57. The variation of the open-area ratio with the number of slots to give zero blockage in an ideal tunnel is illustrated in the following table.

N	2	4	6	8	12
$100\left(\frac{a}{\ell}\right)$	38.3	20.7	11.6	6.5	2.1

The longitudinal pressure gradient along the model due to solid blockage is zero for slotted walls.

4.1.4 Perforated Wall Tunnel

The solid-blockage interference in a perforated tunnel is obtained from Eqs. (4.6) and (4.7). At the model position, the blockage-factor ratio becomes

$$(\Omega_s)_p = - \frac{1}{2.4} \int_o^\infty \frac{K_o(q)\, I_o(q) - (\theta/R)^2\, K_1(q)\, I_1(q)}{\left[I_o(q)\right]^2 + \left[(\theta/R)\, I_1(q)\right]^2}\, q^2\, dq \qquad (4.14)$$

The variation of $(\Omega_s)_p$ with β/R is shown in Fig. 4.2. Zero solid blockage occurs for $Q = 0.45$ or $\beta/R = 1.22$.

The velocity gradient at the model position is given by

$$\left(\frac{\partial \Omega_s}{\partial x}\right)_p = \frac{1}{2.4\,\beta r_o}\,\frac{\beta}{R}\int_o^\infty \frac{q^2}{\left[I_o(q)\right]^2 + \left[(\beta/R)\,I_1(q)\right]^2}\,dq \tag{4.15}$$

and is shown plotted versus Q in Fig. 4.3.

From an analysis similar to that leading to Eq. (3.21), the interference drag imposed on the model by this velocity gradient is

$$(\Delta C_D)_{sg} = -\frac{2V}{S}\left(\frac{\partial \epsilon_s}{\partial x}\right)_p = -\frac{1.2V^2}{\pi^2\beta^4 r_o^4 S}\left[\frac{\partial \Omega_s}{\partial (x/2\beta r_o)}\right]_p \tag{4.16}$$

where the value of the term in the brackets can be obtained from Fig. 4.3.

4.2 WAKE BLOCKAGE

The wake-blockage effects of a small three-dimensional model in a circular tunnel are discussed in Ref. 2, where the wake is represented by a three-dimensional point source. The potential of the source in unrestricted flow is given by

$$\varphi_m = -\frac{m}{4\pi\,(x^2 + \beta^2 r^2)^{\frac{1}{2}}} \tag{4.17}$$

The strength of the source is related to the model drag by the expression

$$m = \frac{D}{\rho U} = \frac{1}{2}\,U\,C_D S. \tag{4.18}$$

The interference potential is given in Ref. 2 as

$$\varphi_i = \frac{m}{2\pi^2 \beta r_o} \left\{ \int_o^\infty \frac{I_K}{I_M} I_o \left(\frac{qr}{r_o} \right) \cos\left(\frac{qx}{\beta r_o} \right) dq \right.$$

$$\left. - \frac{\beta}{R} \int_o^\infty \frac{I_H}{I_M} I_o\left(\frac{qr}{r_o} \right) \sin \left(\frac{qx}{\beta r_o} \right) dq \right\} \qquad (4.19)$$

The axial interference velocity, again noting that $I_H = 1/q$, is

$$u_w = \frac{-m}{2\pi^2 \beta^2 r_o^2} \left\{ \int_o^\infty \frac{I_K}{I_M} I_o\left(\frac{qr}{r_o} \right) \sin \left(\frac{qx}{\beta r_o} \right) q \, dq \right.$$

$$\left. + \frac{\beta}{R} \int_o^\infty \frac{1}{I_M} I_o \left(\frac{qr}{r_o} \right) \cos \left(\frac{qx}{\beta r_o} \right) dq \right\} \qquad (4.20)$$

The velocity gradient in the axial direction is

$$\frac{\partial u_w}{\partial x} = \frac{-m}{2\pi^2 \beta^3 r_o^3} \left\{ \int_o^\infty \frac{I_K}{I_M} I_o \left(\frac{qr}{r_o} \right) \cos\left(\frac{qx}{\beta r_o} \right) q^2 \, dq \right.$$

$$\left. - \frac{\beta}{R} \int_o^\infty \frac{1}{I_M} I_o\left(\frac{qr}{r_o} \right) \sin\left(\frac{qx}{\beta r_o} \right) q \, dq \right\} \qquad (4.21)$$

At the position of the source, x = r = 0, the velocity and velocity gradient become, respectively

$$u_w = \frac{-m}{2\pi^2\beta^2 r_o^2} \frac{\beta}{R} \int_o^\infty \frac{dq}{I_M} \tag{4.22}$$

and

$$\frac{\partial u_w}{\partial x} = \frac{-m}{2\pi^2\beta^3 r_o^3} \int_o^\infty \frac{I_K}{I_M} q^2\, dq \tag{4.23}$$

The integral in Eq. (4.23) is the same as that in Eq. (4.6) for the solid-blockage interference velocity. Thus if the velocity interference at the model due to solid blockage is zero , the velocity gradient at the model due to wake blockage is also zero.

4.2.1 Closed Tunnel

In a closed tunnel Eq. (4.22) gives zero interference velocity at the position of the source. However, at a position far upstream Eq. (4.20) gives an interference velocity of $-m/2\pi\beta^2 r_o^2$. Thus the interference velocity at the model relative to the free stream is given as

$$(\epsilon_w)_c = \frac{C_D S}{4\pi\beta^2 r_o^2} \tag{4.24}$$

The velocity gradient at the model due to the wake is from Eq. (4.23) given by

$$\left(\frac{\partial \epsilon_w}{\partial x}\right)_c = \frac{0.6\, C_D S}{\pi^2\beta^3 r_o^3} \tag{4.25}$$

4.2.2 Open Jet

In an open jet, the interference velocity is zero at both the source and far upstream giving

$$(\varepsilon_w)_o = 0 \tag{4.26}$$

The velocity gradient at the model is

$$\left(\frac{\partial \varepsilon_w}{\partial x}\right)_o = \frac{-\ 0.16\ C_D S}{\pi^2 \beta^3 r_o^3} \tag{4.27}$$

4.2.3 Slotted Wall Tunnel

In an ideal slotted tunnel, as in an open jet, the interference velocity from Eqs. (4.20) and (4.22) is found to be zero both far upstream and at the model position.

The velocity gradient due to wake blockage is given by

$$\left(\frac{\partial \varepsilon_w}{\partial x}\right)_s = -\frac{C_D S}{4\pi^2 \beta^3 r_o^3} \int_o^\infty \frac{K_o(q) - qF\ K_1(q)}{I_o(q) + qF\ I_1(q)}\ q^2\, dq \tag{4.28}$$

The integral in Eq. (4.28) is identical to that in Eq. (4.13). An expression for the velocity gradient due to wake blockage can therefore be obtained by combining Eqs. (4.13) and (4.28) which gives

$$\left(\frac{\partial \varepsilon_w}{\partial x}\right)_s = \frac{0.6\ C_D S}{\pi^2 \beta^3 r_o^3}\ (\Omega_s)_s = \left(\frac{\partial \varepsilon_w}{\partial x}\right)_c\ (\Omega_s)_s \tag{4.29}$$

From Eq. (4.29), it follows that when the solid-blockage factor is zero, then the velocity gradient at the model due to the wake will also be zero. When zero solid blockage is not obtained, the buoyancy correction to the measured drag is given by

$$(\Delta C_D)_{wg} = - C_D(\epsilon_s)_c \ (\Omega_s)_s \tag{4.30}$$

where $(\epsilon_s)_c$ is given by Eq. (4.8) and the value of $(\Omega_s)_s$ can be obtained from Fig. 4.1.

4.2.4 Perforated Wall Tunnel

For a perforated wall tunnel, the wake-blockage ratio at the model position is obtained from Eq. (4.22) as

$$(\Omega_w)_p = - \frac{1}{\pi} \frac{\beta}{R} \int_0^\infty \frac{dq}{\left[I_o(q)\right]^2 + \left[(\beta/R)\ I_1(q)\right]^2} \tag{4.31}$$

A curve of $(\Omega_w)_p$ versus Q is shown in Fig. 4.2; $(\Omega_w)_p$ only vanishes for an open-jet tunnel (Q = 1), and no perforated wall geometry will remove the wake-blockage effect. For a tunnel designed to have zero solid blockage, $(\Omega_w)_p = - 0.44$.

From Eq. (4.23), the velocity gradient at the model position is given by

$$\left(\frac{\partial \epsilon_w}{\partial x}\right)_p = - \frac{C_D S}{4\pi^2 \beta^3 r_o^3} \int_0^\infty \frac{K_o(q)\ I_o(q) - (\beta/R)^2\ K_1(q)\ I_1(q)}{\left[I_o(q)\right]^2 + \left[(\beta/R)\ I_1(q)\right]^2} q^2\, dq \tag{4.32}$$

Since the integral in Eq. (4.32) is the same as in Eq. (4.14), the velocity gradient due to wake blockage can be related to the solid blockage by combining Eqs. (4.14) and (4.32) and obtaining

$$\left(\frac{\partial \epsilon_w}{\partial x}\right)_p = \frac{0.6\ C_D S}{\pi^2 \beta^3 r_o^3} \ (\Omega_s)_p = \left(\frac{\partial \epsilon_w}{\partial x}\right)_c \ (\Omega_s)_p \tag{4.33}$$

as in the slotted wall case. For zero solid blockage, the gradient is equal to zero. For other values of $(\Omega_s)_p$, the bouyancy correction to the measured drag is given by

$$(\Delta C_D)_{wg} = - C_D(\epsilon_s)_c \ (\Omega_s)_p \tag{4.34}$$

where the value of $(\Omega_s)_p$ can be obtained from Fig. 4.2.

4.3 LIFT INTERFERENCE

The upwash corrections for a three-dimensional wing are calculated using a horseshoe vortex to represent the wing. The potential of the wing with the circulation Γ at the origin is given by

$$\varphi_m = \frac{\Gamma s}{2\pi}\left[1 + \frac{x}{(x^2 + \beta^2 r^2)^{\frac{1}{2}}}\right]\frac{\sin\theta}{r} \tag{4.35}$$

These equations represent the potential of a horseshoe vortex having infinitesimal span. The fact that the actual span is finite introduces higher-order terms which are negligible at distances large compared to the size of the model. The value Γs is related to the lift of the model by the equation

$$L = 2\rho U\Gamma s = C_L \rho U^2 S/2 \tag{4.36}$$

In Ref. 1, the interference potential is given as

$$\varphi_i = \frac{\Gamma s}{2\pi r_o}\left\{\frac{r\sin\theta}{r_o} - \frac{\beta}{R}\frac{2}{\pi}\int_o^\infty \frac{I_H}{I_N} I_1\left(\frac{qr}{r_o}\right)\sin\theta\cos\left(\frac{qx}{\beta r_o}\right) q^2\,dq - \frac{2}{\pi}\int_o^\infty \frac{I_Q}{I_N} I_1\left(\frac{qr}{r_o}\right)\sin\theta\sin\left(\frac{qx}{\beta r_o}\right) dq\right\} \tag{4.37}$$

The upwash velocity at r = 0 (noting that $I_H = 1/q$) is obtained as

$$w = \frac{\Gamma s}{2\pi r_o^2}\left\{1 - \frac{\beta}{R}\frac{1}{\pi}\int_o^\infty \frac{1}{I_N}\cos\left(\frac{qx}{\beta r_o}\right) q^2\,dq - \frac{1}{\pi}\int_o^\infty \frac{I_Q}{I_N}\sin\left(\frac{qx}{\beta r_o}\right) q\,dq\right\} \tag{4.38}$$

The streamline curvature at r = 0 is given by

$$\frac{\partial w}{\partial x} = \frac{\Gamma s}{2\pi\beta\, r_o^3}\left\{\frac{\beta}{R}\frac{1}{\pi}\int_o^\infty \frac{1}{I_N}\sin\left(\frac{qx}{\beta r_o}\right) q^3\,dq - \frac{1}{\pi}\int_o^\infty \frac{I_Q}{I_N}\cos\left(\frac{qx}{\beta r_o}\right) q^2\,dq\right\} \tag{4.39}$$

At x = 0 Eqs. (4.38) and (4.39) reduce to

$$w = \frac{\Gamma s}{2\pi r_o^2}\left\{1 - \frac{\beta}{R}\frac{1}{\pi}\int_o^\infty \frac{1}{I_N} q^2\,dq\right\} \tag{4.40}$$

and

$$\frac{\partial w}{\partial x} = -\frac{\Gamma s}{2\pi^2\beta\, r_o^3}\int_o^\infty \frac{I_Q}{I_N} q^2\,dq \tag{4.41}$$

For a small model, the lift interference in a circular tunnel is usually expressed by the factors

$$\delta = \frac{C}{SC_L}\frac{w}{U} \tag{4.42}$$

and

$$\delta_1 = \frac{2\beta r_o C}{S C_L} \left(\frac{1}{U} \frac{\partial w}{\partial x} \right) \tag{4.43}$$

4.3.1 Closed Tunnel

For a closed tunnel Eq. (4.40) yields

$$\delta_o = \frac{1}{8} \tag{4.44}$$

The curvature from Eq. (4.41) is

$$\delta_1 = \frac{1}{4} \tag{4.45}$$

4.3.2 Open Jet

For an open jet, the lift interference factor is

$$\delta_o = -\frac{1}{8} \tag{4.46}$$

and the curvature is

$$\delta_1 = -\frac{1}{5} \tag{4.47}$$

4.3.3 Slotted Wall Tunnel

The distribution of the lift-interference factor along the axis of a circular slotted tunnel as obtained from Eq. (4.38) with $\beta/R = 0$ is shown in Fig. 4.4. Starting with Eq. (4.40), a limiting process is required to obtain the equation for the upwash velocity at the model position which is given as

$$w = \frac{\Gamma s}{2\pi r_o^2} \left[\frac{F - 1}{F + 1} \right] \tag{4.48}$$

or alternately in terms of the interference factor as

$$\delta_o = \frac{1}{8}\left[\frac{F - 1}{F + 1}\right] \tag{4.49}$$

which is plotted as a straight line versus P in Fig. 4.5.

The condition for zero upwash interference corresponds to the value P = 0.5, compared with a value of 0.64 to eliminate solid-blockage effects. It is apparent therefore that it is not possible to eliminate both upwash and blockage interference simultaneously in a circular slotted tunnel. At P = 0.5, the relationship between the total number of slots and the open area ratio is as follows:

N	2	4	6	8	12
$100\left(\frac{a}{\ell}\right)$	24.0	8.6	3.2	1.2	0.16

If the tunnel is designed for the zero-blockage condition δ_o is then -0.034, which is of the opposite sign to the correction in a solid-wall tunnel and about 27 percent of its magnitude.

The streamline curvature from Eq. (4.41) is obtained as

$$\delta_1 = -\frac{1}{4\pi}\int_o^\infty \frac{(1 - F)K_1(q) - qFK_o(q)}{(1 - F)I_1(q) + qFI_o(q)}\, q^2\, dq \tag{4.50}$$

A plot of this factor is shown in Fig. 4.5.

4.3.4 Perforated Wall Tunnel

The lift-interference factor along the axis of a circular perforated tunnel as obtained from Eq. (4.38) with F = 0 is shown in Fig. 4.6. The upwash velocity at the model position is obtained from Eq. (4.40) and is given by

$$w = \frac{\Gamma s}{2\pi r_o^2}\left[1 - \frac{\beta}{\pi R}\int_o^\infty \frac{1}{I_p}\, q^2\, dq\right] \tag{4.51}$$

The corresponding interference factor is given by

$$\delta_o = \frac{1}{8}\left[1 - \frac{8}{\pi R}\int_o^\infty \frac{1}{I_p}\, q^2\, dq\right] \tag{4.52}$$

The flow curvature at the origin is obtained from Eq. (4.41) and is given by

$$\delta_1 = -\frac{1}{4\pi}\int_o^\infty \frac{I_R}{I_p}\, q^2\, dq \tag{4.53}$$

The variations of the interference factor δ_o and the flow-curvature factor δ_1 with the porosity parameter, Q, is shown in Fig. 4.7. Zero lift interference at the model position occurs when Q = 0.46 as compared to a value of 0.45 for zero-blockage interference. At zero-blockage conditions, the streamline curvature at the model position is 0.59 of its value in a closed tunnel.

SECTION V
INTERFERENCE IN A RECTANGULAR TUNNEL

The material presented in this section extends the work presented in Refs. 4 and 5 to cover all of the cases of wall interference considered in the two previous sections for two-dimensional and circular tunnels. Prior studies of rectangular tunnels with ventilated walls were somewhat limited. In Ref. 10, Theodorsen considered the lift interference in a rectangular tunnel with one set of parallel walls completely open with the opposing set closed. Davis and Moore (Ref. 11) later considered both the solid blockage and lift interference for the case with solid vertical walls and slotted horizontal walls. The work of Davis and Moore on solid blockage was extended by Acum (Ref. 12) to include a wider range of tunnel height-to-width ratios and on lift interferences by Holder (Refs. 13 and 14) to include wings of finite span in both slotted and porous tunnels with solid vertical walls.

The following results are obtained in a manner similar to that for the circular tunnel. The singularities again are placed at the center of the tunnel and the coordinate system as shown in Fig. 2.1c.

5.1 SOLID BLOCKAGE

The potential for the three-dimensional doublet used to obtain solid-blockage correction factors is expressed in Eq. (4.1). A method using Fourier transforms and the point-matching technique is used to obtain the perturbation potential which is expressed by

$$\varphi_i = \frac{d}{2\pi^2 \beta^2 b^2} \left\{ \int_0^\infty \sum_{0,2,4}^{\infty} B_m(q)\ I_m\left(\frac{qr}{b}\right) \cos m\theta \cos\left(\frac{qx}{\beta b}\right) q\ dq + \int_0^\infty \sum_{0,2,4}^{\infty} A_m(q)\ I_m\left(\frac{qr}{b}\right) \cos m\theta \sin\left(\frac{qx}{\beta b}\right) q\ dq \right\} \tag{5.1}$$

where the equations used to determine $B_m(q)$ and $A_m(q)$ are listed in Appendix II.

The interference velocity is given by

$$u_s = \frac{-d}{2\pi^2 \beta^3 b^3} \left\{ \int_0^\infty \sum_{0,2,4}^{\infty} B_m(q)\ I_m\left(\frac{qr}{b}\right) \cos m\theta \sin\left(\frac{qx}{\beta b}\right) q^2\ dq - \int_0^\infty \sum_{0,2,4}^{\infty} A_m(q)\ I_m\left(\frac{qr}{b}\right) \cos m\theta \cos\left(\frac{qx}{\beta b}\right) q^2\ dq \right\} \tag{5.2}$$

The longitudinal velocity gradient becomes

$$\frac{\partial u_s}{\partial x} = \frac{-d}{2\pi^2 \beta^4 b^4} \left\{ \int_0^\infty \sum_{0,2,4}^{\infty} B_m(q)\ I_m\left(\frac{qr}{b}\right) \cos m\theta \cos\left(\frac{qx}{\beta b}\right) q^3\ dq + \int_0^\infty \sum_{0,2,4}^{\infty} A_m(q)\ I_m\left(\frac{qr}{b}\right) \cos m\theta \sin\left(\frac{qx}{\beta b}\right) q^3\ dq \right\} \tag{5.3}$$

At $x = r = 0$, the equations for the interference velocity and the velocity gradient reduce to

$$u_s = \frac{d}{2\pi^2 \beta^3 b^3} \int_0^\infty A_0(q)\ q^2\, dq \tag{5.4}$$

and

$$\frac{\partial u_s}{\partial x} = - \frac{d}{2\pi^2 \beta^4 b^4} \int_o^\infty B_o(q)\ q^3\, dq \tag{5.5}$$

5.1.1 Closed Tunnel

For a closed wall tunnel with $F \to \infty$ or $\delta/R \to \infty$, Eq. (5.4) yields

$$(\epsilon_s)_c = \frac{u_s}{U} = \frac{V}{2\pi^2 \beta^3 b^3} \int_o^\infty A_{o_c}(q)\ q^2\, dq \tag{5.6}$$

This parameter can also be expressed in an equivalent form (Ref. 3) as

$$(\epsilon_s)_c = \frac{V}{\beta^3 b^3} \left\{ \frac{1}{32\pi} \left(\frac{b}{h} \right)^{3/2} \sum_{-\infty}^{\infty} \sum \left(\frac{bh}{m^2 b^2 + n^2 h^2} \right)^{3/2} \right\} \tag{5.7}$$

where $\sum_{-\infty}^{\infty} \sum$ denotes that (m,n) takes on all possible integral pairs except (0,0). Values of the expression in the brackets are plotted in Fig. 5.1 for a range of tunnel height-to-width ratios.

Since $B_o = 0$ for a closed tunnel, Eq. (5.5) indicates that at the model position

$$\left(\frac{\partial \epsilon_s}{\partial x} \right)_c = 0 \tag{5.8}$$

5.1.2 Open Jet

For an open jet with both $F = 0$ and $\delta/R = 0$, Eq. (5.4) reduces to

$$(\epsilon_s)_o = \frac{V}{2\pi^2 \beta^3 b^3} \int_o^\infty A_{o_o}(q)\ q^2\, dq \tag{5.9}$$

An equivalent expression as obtained from Ref. 3 is

$$(\varepsilon_s)_o = \frac{V}{\beta^3 b^3} \left\{ \frac{1}{32\pi} \left(\frac{b}{h} \right)^{3/2} \sum_{-\infty}^{\infty} \sum (-1)^{m+n} \left(\frac{bh}{m^2 b^2 + n^2 h^2} \right)^{3/2} \right\} \quad (5.10)$$

where $\sum_{-\infty}^{\infty} \sum$ denotes that (m,n) takes on all possible integral pairs except (0,0). Values of the expression in the brackets are shown in Fig. 5.1.

With $B_o = 0$ in an open jet, Eq. (5.5) gives

$$\left(\frac{\partial \varepsilon_s}{\partial x} \right)_o = 0 \quad (5.11)$$

5.1.3 Slotted Wall Tunnel

For an ideal slotted wall tunnel, Eq. (5.4) reduces to

$$(\varepsilon_s)_s = \frac{V}{2\pi^2 \beta^3 b^3} \int_o^{\infty} A_{o_s}(q)\, q^2\, dq \quad (5.12)$$

where A_{o_s} is determined as shown in Appendix II.

The variation of Ω_s with the slot parameter P where the slot parameter of the horizontal walls, P_h, is equal to that of the vertical walls, P_v, is shown in Fig. 5.2 for tunnels of various height-to-width ratios.

The blockage ratio, Ω_s, has also been evaluated for various constant values of the slot parameter on the vertical walls over the complete range of the slot parameter on the horizontal walls. These results are shown in Figs. 5.3 for rectangular tunnels with height-to-width ratios of 1.0, 0.8, and 0.5.

The combinations of the vertical and horizontal wall slot parameters which give zero solid-blockage interference in a slotted tunnel are shown in Fig. 5.4 for tunnels of various height-to-width ratios. This figure shows that a change in the slot parameter of the vertical walls has a decreasing effect on the blockage interference as the tunnel height-to-width ratio is decreased.

Davis and Moore (Ref. 11) have obtained the blockage factor for the special case of a rectangular tunnel with solid vertical walls and slotted horizontal walls. The equation obtained as simplified by Acum in Ref. 12 is given by

$$(\epsilon_s)_s = \frac{V}{\beta^3 b^3}\left\{\frac{1}{16\pi}\sum_{n=1}^{\infty}\frac{1}{n^3} + \frac{b^2}{4\pi h^2}\int_0^{\infty}\frac{qe^{-q}(Fq-1)}{\cosh q + Fq \sinh q}\,dq + \sum_{n=1}^{\infty}\frac{b^3}{2\pi h^2}\int_{q_o}^{\infty}\frac{(q^2-q_o^2)^{\frac{1}{2}}e^{-q}(Fq-1)}{\cosh q + Fq \sinh q}\,dq\right\} \tag{5.13}$$

Results for this special case of a rectangular tunnel are shown in Fig. 5.5.

As in the case of a circular tunnel, the longitudinal pressure gradient of the model due to solid blockage is zero for slotted walls.

5.1.4 Perforated Wall Tunnel

The solid-blockage interference factors in a perforated tunnel are obtained from Eqs. (5.4) and (5.5). The blockage factor at the model position is given by

$$(\epsilon_s)_p = \frac{V}{2\pi^2\beta^3 b^3}\int_0^{\infty} A_{o_p}(q)\, q^2\, dq \tag{5.14}$$

and the velocity gradient at the model position by

$$\left(\frac{\partial \epsilon_s}{\partial x}\right)_p = \frac{V}{2\pi^2\beta^4 b^4}\int_0^{\infty} B_{o_p}(q)\, q^3\, dq \tag{5.15}$$

where the manner in which A_{o_p} and B_{o_p} are determined is shown in Appendix II. Values of $(\epsilon_s)_p$ and $\left(\frac{\partial \epsilon_s}{\partial x}\right)_p$ as given by Eqs. (5.14) and (5.15) for a rectangular tunnel with all walls perforated are being evaluated and will be presented in a separate report.

For the special case of a rectangular tunnel with solid vertical walls and perforated horizontal walls, the blockage interference can be derived by the image method in conjunction with Fourier transforms and is given by

$$(\epsilon_s)_p = \frac{V}{4\pi\beta^3 b^3}\left\{\frac{1}{4}\sum_{1}^{\infty}\frac{1}{n^3} + \frac{b^2}{h^2}\sum_{0}^{\infty} j\int_0^{\infty} A_n(q)\,dq\right\} \qquad (5.16)$$

where $j = \begin{cases} 1 & n = 0 \\ 2 & n \neq 0 \end{cases}$

$$A_n(q) = \frac{(q^4\cosh\alpha_n + q^2\alpha_n^2\sinh\alpha_n)\,e^{-\alpha_n}}{\alpha_n\left\{\left[(\beta/R)\,\alpha_n\sinh\alpha_n\right]^2 + \left[q\cosh\alpha_n\right]^2\right\}}$$

$$\alpha_n = \left[q^2 + (n\pi h/b)^2\right]^{\frac{1}{2}}$$

Values of the solid-blockage factor, $(\Omega_s)_p$, for this special case of a rectangular tunnel are shown in Fig. 5.6.

The longitudinal velocity gradient due to solid blockage at the model position is given by

$$\left(\frac{\partial\epsilon_s}{\partial x}\right)_p = \frac{V}{4\pi\beta^4 b^4}\,\frac{b^2}{h^2}\sum_{0}^{\infty} j\int_0^{\infty} B_n(q)\,dq \qquad (5.17)$$

where $B_n(q) = q^2\,e^{-\alpha_n}\left\{\frac{1}{\cosh\alpha_n} + \frac{\sinh\alpha_n\left[q^2 - (\beta/R)^2\alpha_n^2\tanh\alpha_n\right]}{(\beta/R)^2\alpha_n^2\sinh^2\alpha_n + q^2\cosh^2\alpha_n}\right\}$

The value of the interference drag imposed on the model by the longitudinal velocity gradient is given by

$$(\Delta C_D)_{sg} = -\frac{2V}{S}\left(\frac{\partial\epsilon_s}{\partial x}\right)_p = -\frac{V(\epsilon_s)_c}{\beta hS}\left[\frac{\partial\Omega_s}{\partial(x/2\beta h)}\right]_p \qquad (5.18)$$

The values of the term in the brackets are shown in Fig. 5.7 for tunnels of various height-to-width ratios for the special case of a rectangular tunnel with solid vertical walls and perforated horizontal walls. The corresponding values of $(\epsilon_s)_c$ in Eq. (5.18) can be obtained from Fig. 5.1.

5.2 WAKE BLOCKAGE

The wake-blockage effects of a small three-dimensional model in a rectangular tunnel are presented here for the first time as obtained by using Fourier integrals and the point-matching technique. The wake is represented by a three-dimensional point source. The potential of the source in unrestricted flow is given in Eq. (4.17).

The interference potential obtained is given by the expression:

$$\varphi_i = \frac{m}{2\pi^2 \beta b} \left\{ \int_0^\infty \sum_{0,2,4}^{\infty} A_m(q)\ I_m\left(\frac{qr}{b}\right) \cos m\theta\ \cos\left(\frac{qx}{\beta b}\right) dq \right.$$

$$\left. - \int_0^\infty \sum_{0,2,4}^{\infty} B_m(q)\ I_m\left(\frac{qr}{b}\right) \cos m\theta\ \sin\left(\frac{qx}{\beta b}\right) dq \right\} \qquad (5.19)$$

The axial interference velocity is obtained as

$$u_w = \frac{-m}{2\pi^2 \beta^2 b^2} \left\{ \int_0^\infty \sum_{0,2,4}^{\infty} A_m(q)\ I_m\left(\frac{qr}{b}\right) \cos m\theta\ \sin\left(\frac{qx}{\beta b}\right) q\, dq \right.$$

$$\left. + \int_0^\infty \sum_{0,2,4}^{\infty} B_m(q)\ I_m\left(\frac{qr}{b}\right) \cos m\theta\ \cos\left(\frac{qx}{\beta b}\right) q\, dq \right\} \qquad (5.20)$$

where the equations used to determine $A_m(q)$ and $B_m(q)$ are outlined in Appendix II.

The velocity gradient in the axial direction is given by:

$$\frac{\partial u_w}{\partial x} = \frac{-m}{2\pi^2 \beta^3 b^3} \left\{ \int_0^\infty \sum_{0,2,4}^{\infty} A_m(q)\ I_m\left(\frac{qr}{b}\right) \cos m\theta\ \cos\left(\frac{qx}{\beta b}\right) q^2\, dq \right.$$

$$\left. - \int_0^\infty \sum_{0,2,4}^{\infty} B_m(q)\ I_m\left(\frac{qr}{b}\right) \cos m\theta\ \sin\left(\frac{qx}{\beta b}\right) q^2\, dq \right\} \qquad (5.21)$$

At the position of the source, x = r = 0, the velocity and velocity gradient become, respectively

$$u_w = \frac{-m}{2\pi^2 \beta^2 b^2} \int_0^\infty B_o(q)\, q\, dq \qquad (5.22)$$

and

$$\frac{\partial u_w}{\partial x} = \frac{-m}{2\pi^2 \beta^3 b^3} \int_0^\infty A_o(q)\, q^2\, dq \qquad (5.23)$$

The integral in Eq. (5.23) is the same as that in Eq. (5.4) for the solid-blockage interference velocity. Thus if the velocity interference at the model due to solid blockage is zero, the velocity gradient at the model due to wake blockage is also zero.

5.2.1 Closed Tunnel

In a closed tunnel Eq. (5.22) gives zero interference velocity at the position of the source. However, at a position far upstream Eq. (5.20) gives an interference velocity of $-m/8\beta^2 bh$. Thus the interference velocity at the model relative to the free stream is given as

$$(\varepsilon_w)_c = \frac{C_D S}{4\beta^2 C} \qquad (5.24)$$

The velocity gradient at the model due to the wake is from Eq. (5.23) given by

$$\left(\frac{\partial \varepsilon_w}{\partial x}\right)_c = -\frac{C_D S}{4\pi^2 \beta^3 b^3} \int_0^\infty A_{o_c}(q)\, q^2\, dq \qquad (5.25)$$

Since the integral in Eq. (5.25) is identical to that in Eq. (5.6), the velocity gradient can be written as

$$\left(\frac{\partial \epsilon_w}{\partial x}\right)_c = -\frac{C_D S}{2V} (\epsilon_s)_c \tag{5.26}$$

where $(\epsilon_s)_c$ is given by Eq. (5.7) and is shown plotted in Fig. 5.1.

5.2.2 Open Jet

In an open jet, the interference velocity is zero at both the source and far upstream giving

$$(\epsilon_w)_o = 0 \tag{5.27}$$

The velocity gradient at the model is

$$\left(\frac{\partial \epsilon_w}{\partial x}\right)_o = -\frac{C_D S}{4\pi^2 \beta^3 b^3} \int_o^\infty A_{o_o}(q)\, q^2\, dq \tag{5.28}$$

Since the integral in Eq. (5.28) is identical to that in Eq. (5.9), the velocity gradient can be written as

$$\left(\frac{\partial \epsilon_w}{\partial x}\right)_o = -\frac{C_D S}{2V} (\epsilon_s)_o \tag{5.29}$$

where $(\epsilon_s)_o$ is given by Eq. (5.10) and is shown in Fig. 5.1.

5.2.3 Slotted Wall Tunnel

In an ideal slotted tunnel, as in an open jet, the interference velocity from Eqs. (5.20) and (5.22) is found to be zero both far upstream and at the model position.

The velocity gradient due to wake blockage is given by

$$\left(\frac{\partial \epsilon_w}{\partial x}\right)_s = -\frac{C_D S}{4\pi^2 \beta^3 b^3} \int_o^\infty A_{o_s}(q)\, q^2\, dq \tag{5.30}$$

The integral in Eq. (5.30) is identical to that in Eq. (5.12). An expression for the velocity gradient due to wake blockage can therefore be obtained by combining Eqs. (5.12) and (5.30) which gives

$$\left(\frac{\partial \epsilon_w}{\partial x}\right)_s = -\frac{C_D S}{2V} (\epsilon_s)_c (\Omega_s)_s = -\left(\frac{\partial \epsilon_w}{\partial x}\right)_c (\Omega_s)_s \qquad (5.31)$$

From Eq. (5.31), it follows that when the solid-blockage factor is zero, then the velocity gradient at the model due to the wake will also be zero. When zero solid blockage is not obtained, the buoyancy correction to the measured drag is given by

$$(\Delta C_D)_{wg} = -C_D (\epsilon_s)_c (\Omega_s)_s \qquad (5.32)$$

closed $\Omega_s = 1$
open $\Omega_s = .5$

where $(\epsilon_s)_c$ is given by Eq. (5.7). The value of $(\Omega_s)_s$ can be obtained from Fig. 5.2 for a tunnel with identical slots on the vertical and horizontal walls, $P_v = P_h$, and from Fig. 5.5 for a tunnel with solid vertical walls ($P_v = 0$) and slotted horizontal walls.

5.2.4 Perforated Wall Tunnel

For a perforated wall tunnel, the wake-blockage ratio at the model position is obtained from Eq. (5.22) as

$$(\Omega_w)_p = -\frac{4}{\pi^2} \frac{h}{b} \int_0^\infty B_{o_p}(q)\, q\, dq \qquad (5.33)$$

From Eq. (5.28), the velocity gradient at the model position is given by

$$\left(\frac{\partial \epsilon_w}{\partial x}\right)_p = -\frac{C_D S}{4\pi^2 \beta^3 b^3} \int_0^\infty A_{o_p}(q)\, q^2\, dq \qquad (5.34)$$

Since the integral in Eq. (5.34) is the same as in Eq. (5.14), the velocity gradient due to wake blockage can be related to the solid blockage by combining Eqs. (5.14) and (5.34) and obtaining

$$\left(\frac{\partial \epsilon_w}{\partial x}\right)_p = -\frac{C_D S}{2V} (\epsilon_s)_c (\Omega_s)_p = -\left(\frac{\partial \epsilon_w}{\partial x}\right)_c (\Omega_s)_p \tag{5.35}$$

as in the slotted wall case. For zero solid blockage, the gradient is equal to zero. For other values of $(\Omega_s)_p$, the buoyancy correction to the measured drag is given by

$$(\Delta C_D)_{wg} = -C_D (\epsilon_s)_c (\Omega_s)_p \tag{5.36}$$

where $(\epsilon_s)_c$ is given by Eq. (5.7). The value of $(\Omega_s)_p$ can be obtained from Fig. 5.6 for a tunnel with solid vertical walls ($Q_v = 0$) and perforated horizontal walls.

5.3 LIFT INTERFERENCE

The upwash corrections for a three-dimensional wing are calculated using a horseshoe vortex to represent the wing as in the case of a circular tunnel, see Eq. (4.35). The interference potential obtained by using Fourier transforms and the point-matching technique is given by

$$\varphi_i = \frac{\Gamma s}{2\pi b}\left\{\sum_{1,3,5}^{\infty} D_m r^m \sin \hat{m}\theta + \frac{\beta}{\pi}\int_0^{\infty}\sum_{1,3,5}^{\infty} G_m(q)\, I_m\left(\frac{qr}{b}\right)\sin m\theta \cos\left(\frac{qx}{\beta b}\right) dq + \frac{\beta}{\pi}\int_0^{\infty}\sum_{1,3,5}^{\infty} E_m(q)\, I_m\left(\frac{qr}{b}\right)\sin m\theta \sin\left(\frac{qx}{\beta b}\right) dq\right\} \tag{5.37}$$

where the series coefficients D_m, $G_m(q)$, and $E_m(q)$ are determined by the procedure outlined in Appendix III.

The upwash velocity at r = 0 is given as

$$w = \frac{\Gamma s}{2\pi b}\left\{D_1 + \frac{\beta}{2\pi b}\int_o^\infty G_1(q)\cos\left(\frac{qx}{\beta b}\right) q\,dq + \frac{\beta}{2\pi b}\int_o^\infty E_1(q)\sin\left(\frac{qx}{\beta b}\right) q\,dq\right\} \tag{5.38}$$

The streamline curvature at r = 0 is given by

$$\frac{\partial w}{\partial x} = \frac{\Gamma s}{4\pi^2 b^3}\left\{-\int_o^\infty G_1(q)\sin\left(\frac{qx}{\beta b}\right) q^2\,dq + \int_o^\infty E_1(q)\cos\left(\frac{qx}{\beta b}\right) q^2\,dq\right\} \tag{5.39}$$

At x = 0 Eqs. (5.38) and (5.39) reduce to

$$w = \frac{\Gamma s}{2\pi b}\left\{D_1 + \frac{\beta}{2\pi b}\int_o^\infty G_1(q)\,q\,dq\right\} \tag{5.40}$$

and

$$\frac{\partial w}{\partial x} = \frac{\Gamma s}{4\pi^2 b^3}\int_o^\infty E_1(q)\,q^2\,dq \tag{5.41}$$

In a rectangular tunnel as in a circular tunnel, the lift-interference factor is expressed as

$$\delta = \frac{C}{SC_L}\,\frac{w}{U} \tag{5.42}$$

The factor associated with streamline curvature is given by

$$\delta_1 = \frac{2\beta hC}{SC_L}\left(\frac{1}{U}\,\frac{\partial w}{\partial x}\right) \tag{5.43}$$

5.3.1 Closed Tunnel

For a closed tunnel Eq. (5.40) using Eq. (5.42) yields

$$\delta_o = \frac{h}{2\pi} D_{1_c} \tag{5.44}$$

An equivalent expression is given in Ref. 3 as

$$\delta_o = \frac{bh}{8\pi} \sum_{-\infty}^{\infty}\sum (-1)^n \frac{m^2b^2 - n^2h^2}{(m^2b^2 + n^2h^2)^2} \tag{5.45}$$

where $\sum_{-\infty}^{\infty}\sum$ denotes that (m,n) takes on all possible integral pairs except (0,0).

In Ref. 10, Theodorsen obtains an expression for the lift-interference factor as a single series given by

$$\delta_o = \frac{\pi}{48}\frac{b}{h} + \frac{\pi}{4}\frac{b}{h} \sum_{1}^{\infty} \frac{\cosh \pi m\, b/h}{\sinh^2 \pi m\, b/h} \tag{5.46}$$

The streamline curvature is obtained from Eq. (5.41) as

$$\delta_1 = \frac{h^2}{2\pi^2 b^2} \int_0^{\infty} E_{1_c}(q)\, q^2\, dq \tag{5.47}$$

or as given in Ref. 3 as

$$\delta_1 = \frac{bh^2}{8\pi} \sum_{-\infty}^{\infty}\sum (-1)^n \frac{m^2b^2 - 2n^2h^2}{(m^2b^2 + n^2h^2)^{5/2}} \tag{5.48}$$

5.3.2 Open Jet

For an open jet, the lift-interference factor is

$$\delta_o = \frac{h}{2\pi} D_{1_o} \tag{5.49}$$

From Ref. 3 the equivalent expression is given as

$$\delta_o = \frac{bh}{8\pi} \sum_{-\infty}^{\infty}\sum (-1)^m \frac{m^2 b^2 - n^2 h^2}{(m^2 b^2 + n^2 h^2)^2} \tag{5.50}$$

or as given in Ref. 10

$$\delta_o = -\frac{\pi}{24}\frac{b}{h} + \frac{\pi}{4}\frac{b}{h} \sum_{1}^{\infty} \frac{(-1)^m}{\sinh^2 \pi m\, b/h} \tag{5.51}$$

The streamline curvature from Eq. (5.41) is obtained as

$$\delta_1 = \frac{h^2}{2\pi^2 b^2} \int_o^{\infty} E_{1_o}(q)\, q^2\, dq \tag{5.52}$$

or as given in Ref. 3 as

$$\delta_1 = \frac{bh^2}{8\pi} \sum_{-\infty}^{\infty}\sum (-1)^m \frac{m^2 b^2 - 2n^2 h^2}{(m^2 b^2 + n^2 h^2)^{5/2}} \tag{5.53}$$

5.3.3 Slotted Wall Tunnel

The solution of Eq. (5.40) for the upwash at x = 0 in a tunnel with slotted walls is obtained by setting θ/R equal to zero. The coefficient $G_1(q)$ is then equal to zero and the upwash at the model position becomes

$$w = \frac{\Gamma s}{2\pi b} D_1 \tag{5.54}$$

The lift-interference factor is given as

$$\delta_o = \frac{h}{2\pi} D_1 \tag{5.55}$$

The variation of δ_o with the slot parameter P for uniformly distributed slots on the four tunnel walls ($P_v = P_h$) is shown in Fig. 5.8. This factor is also shown plotted versus P_h in Fig. 5.9 for various constant values of P_v. The combinations of P_h and P_v which produce zero lift interference at the model position in rectangular slotted tunnels of various height-to-width ratios are shown in Fig. 5.10. A common intersection of these curves occurs at $P_h = 0.39$ and $P_v = 0.64$.

The streamline-curvature factor at the model position can be obtained from Eq. (5.41) as

$$\delta_1 = \frac{h^2}{2\pi^2 b^2} \int_o^\infty E_{1_s}(q)\, q^2\, dq \tag{5.56}$$

As for the solid-blockage factor (see Section 5.1.3), Davis and Moore (Ref. 11) have obtained the lift-interference factor at the model position, δ_o, for the special case of a rectangular tunnel with solid vertical walls and slotted horizontal walls. The distribution of the lift interference along the longitudinal direction x for this special case can be derived by the image method in conjunction with Fourier transforms and is given by

$$\delta = \delta_o + \frac{h}{4\pi b} \sum_1^\infty \frac{x/\beta h}{n^2 \left[(x/\beta h)^2 + (2nb/h)^2\right]^{\frac{1}{2}}} - \frac{h^2}{\pi b^2} \sum_o^\infty j \int_o^\infty C_n(q) \sin\left(\frac{qx}{\beta h}\right) \alpha_n(q)\, dq \tag{5.57}$$

where $j = \begin{cases} 1 & n = 0 \\ 2 & n \neq 0 \end{cases}$

$$C_n(q) = \frac{(1 - F\alpha_n)}{q\left[(1 + F\alpha_n)e^{2\alpha_n} - (1 - F\alpha_n)\right]}$$

$$\alpha_n = \left[q^2 + (n\pi h/b)^2\right]^{\frac{1}{2}}$$

and δ_o is the factor at x = 0 as derived by Davis and Moore which is given by

$$\delta_o = \frac{\pi h}{24b} - \frac{1}{4(1+F)} - \frac{\pi h}{b} \sum_{1}^{\infty} \frac{n(b-n\pi hF)}{(b + n\pi hF)\, e^{2n\pi h/b} - (b-n\pi hF)} \tag{5.58}$$

The streamline-curvature factor as determined from Eq. (5.57) is given by

$$\delta_1 = \frac{h^2}{4\pi b^2} \sum_{1}^{\infty} \frac{1}{n^3} - \frac{2}{\pi} \frac{h^2}{b^2} \sum_{o}^{\infty} j \int_o^{\infty} C_n(q)\, q\, \alpha_n(q)\, dq \tag{5.59}$$

The distributions of the lift-interference factor along the axis of rectangular tunnels with solid vertical walls and slotted horizontal walls are shown in Figs. 5.11a through c for tunnel height-to-width ratios of 1.0, 0.8, and 0.5 respectively. The values of the lift-interference factor, δ_o, and the streamline curvature, δ_1, at x = 0 for these same tunnel configurations are shown plotted versus P_h in Figs. 5.12 and 5.13, respectively.

5.3.4 Perforated Wall Tunnel

For a tunnel with perforated walls, the upwash velocity is obtained by setting F = 0 in Eq. (5.40). The result is given by

$$w = \frac{\Gamma s}{2\pi b} \left[D_{1c} + \frac{\beta}{2\pi b} \int_o^{\infty} G_{1p}(q)\, q\, dq \right] \tag{5.60}$$

The corresponding interference factor is given by

$$\delta_o = \frac{h}{2\pi} \left[D_{1c} + \frac{\beta}{2\pi b} \int_o^{\infty} G_{1p}(q)\, q\, dq \right] \tag{5.61}$$

The flow curvature at the origin is obtained from Eq. (5.41) and is given by

$$\delta_1 = \frac{h^2}{2\pi^2 b^2} \int_o^{\infty} E_{1p}(q)\, q^2\, dq \tag{5.62}$$

Values of δ_o and δ_1 as given by Eqs. (5.61) and (5.62) for all walls perforated are being evaluated and will be presented in a separate report.

For the special case of a rectangular tunnel with solid vertical walls and perforated horizontal walls, the distribution of the lift interference along the longitudinal direction x can be derived by the image method in conjunction with Fourier transforms and is given by

$$\delta(x) = (\delta_o)_{closed} + \frac{h}{4\pi b} \sum_{1}^{\infty} \frac{x/\beta h}{n^2 \left[(x/\beta h)^2 + (2nb/h)^2 \right]^{\frac{1}{2}}}$$

$$- \frac{h^2}{2\pi b^2} \sum_{o}^{\infty} j \int_o^{\infty} \left[D_n(q) \cos\left(\frac{qx}{\beta h}\right) + E_n(q) \sin\left(\frac{qx}{\beta h}\right) \right] \alpha_n(q)\, dq \qquad (5.63)$$

where $j = \begin{cases} 1 & n = 0 \\ 2 & n \neq 0 \end{cases}$

$(\delta_o)_{closed}$ is the lift interference for closed tunnels, see Eq. (5.46).

$$D_n(q) = \frac{\alpha_n/qR}{q \left\{ (\sinh \alpha_n)^2 + \left[(\alpha_n/qR) \cosh \alpha_n \right]^2 \right\}}$$

$$E_n(q) = \frac{e^{-\alpha_n} \left[\sinh \alpha_n - (\alpha_n/qR) \cosh \alpha_n \right]}{q \left\{ (\sinh \alpha_n)^2 + \left[(\alpha_n/qR) \cosh \alpha_n \right]^2 \right\}}$$

$$\alpha_n(q) = \left[q^2 + (n\pi h/b)^2 \right]^{\frac{1}{2}}$$

The streamline-curvature factor as determined from Eq. (5.63) is given by

$$\delta_1 = \frac{h^2}{4\pi b^2} \sum_{1}^{\infty} \frac{1}{n^3} - \frac{h^2}{\pi b^2} \sum_{o}^{\infty} j \int_o^{\infty} E_n(q)\, q\, \alpha_n(q)\, dq \qquad (5.64)$$

The distributions of the lift-interference factor along the axis of rectangular tunnels with solid vertical walls and perforated horizontal walls are shown in Fig. 5.14a through c

for tunnel height-to-width ratios of 1.0, 0.8, and 0.5, respectively. The values of the lift-interference factor, δ_Q, and the streamline curvature, δ_1, at x = 0 for these same tunnel configurations are plotted versus Q_h in Figs. 5.15 and 5.16, respectively.

SECTION VI
APPLICATION OF THE INTERFERENCE FACTORS

In the previous sections interference factors to account for the presence of the tunnel walls have been enumerated for various types of ventilated wall tunnels. It now remains to illustrate how these factors are applied to correct the tunnel operating parameters as well as the model forces and moments. It is convenient to treat the blockage-interference factors which affect the longitudinal velocity and the lift-interference factors which affect the upwash velocity separately.

6.1 BLOCKAGE CORRECTIONS

The blockage factor $\epsilon_B = \epsilon_s + \epsilon_w$ determines the increment which must be added to the tunnel velocity to obtain a true or corrected velocity at the model. In equation form, the corrected velocity is

$$U_C = U + u_s + u_w \tag{6.1}$$

or in terms of the blockage factors

$$U_C = U(1 + \epsilon_s + \epsilon_w) \tag{6.2}$$

It is evident that a correction to the velocity in a compressible flow implies corrections to the other stream properties, such as density and pressure. These corrections are readily obtained on the basis of the usual assumption that the flow is adiabatic. It is assumed that the correction terms are small compared with unity, so that the squares and products of these terms may be neglected. The analysis procedure is presented in Ref. 15 where the following equations are obtained.

$$M_C = M\left[1 + \left(1 + \frac{\gamma-1}{2} M^2\right) \epsilon_B\right] \tag{6.3}$$

$$(Re)_C = Re\left[1 + \left(1 - \frac{\gamma}{2} M^2\right) \epsilon_B\right] \tag{6.4}$$

$$\rho_C = \rho \ (1 - M^2 \epsilon_B) \qquad (6.5)$$

$$(q_\infty)_C = q_\infty \left[1 + (2-M^2) \ \epsilon_B\right] \qquad (6.6)$$

The corrected dynamic pressure can be used directly to obtain the nondimensional coefficients from the measured model forces and moments. As an alternate procedure it is sometimes convenient to calculate these coefficients using the uncorrected value of the dynamic pressure and then apply a correction to the coefficient. In this case if C_F represents a typical nondimensional coefficient, the corrected coefficient is given by

$$(C_F)_C = C_F \left[1 - (2-M^2) \ \epsilon_B\right] \qquad (6.7)$$

6.2 BUOYANCY CORRECTION

The gradients in the longitudinal stream velocity due to the solid and wake blockage also produce an additional correction to the model drag coefficient as discussed previously. This additional correction referred to as a buoyancy correction is given by

$$\Delta C_D = (\Delta C_D)_{sg} + (\Delta C_D)_{wg} \qquad (6.8)$$

which must be subtracted from the drag coefficient measured in the tunnel.

6.3 UPWASH CORRECTIONS

The upwash at the model is equivalent to an upward inclination of the stream approaching the model. Thus the true angle of incidence of a model will be greater than the actual setting relative to the tunnel axis. As a further consequence, the lift force is inclined forward by the same angle causing a reduction of the drag force as compared to free air conditions. It follows that the corrections which must be applied to the wind tunnel measurements on a wing to allow for the lift interference at the model position are given by

$$\Delta\alpha = \frac{w}{U} = \lambda_o \delta_o \qquad (6.9)$$

and

$$\Delta C_D = C_L \lambda_o \delta_o \tag{6.10}$$

where $\lambda_o = cC_L/2h$ in a two-dimensional tunnel and SC_L/C in a three-dimensional tunnel.

6.4 STREAMLINE CURVATURE CORRECTIONS

The longitudinal variation in the upwash along the axis of a wing introduces a streamline curvature. As discussed in Chapter 6 of Ref. 16, the variation in upwash results in a correction to the angle of attack as well as the lift and pitching-moment coefficients. The correction to the angle of attack can be written as

$$\Delta\alpha = \left(\frac{1}{U}\frac{\partial w}{\partial x}\right) x_1 = \lambda_1 x_1 \delta_1 \tag{6.11}$$

where $\lambda_1 = cC_L/4\beta h^2$ for a two-dimensional tunnel, $SC_L/2\beta r_o C$ for a circular tunnel, and $SC_L/2\beta hC$ for a rectangular tunnel, and x_1 takes on the value of $\bar{c}/4$.

The corrections to the lift coefficient and the pitching moment about the quarter chord are given in turn by

$$\Delta C_L = -\frac{\Delta\alpha}{\beta}\frac{\partial C_L}{\partial\alpha} = -\frac{\lambda_1 x_1 \delta_1}{\beta}\frac{\partial C_L}{\partial\alpha} \tag{6.12}$$

and

$$\Delta C_m = -\frac{\Delta C_L}{4} = -\frac{\lambda_1 x_1 \delta_1}{4\beta}\frac{\partial C_L}{\partial\alpha} \tag{6.13}$$

6.5 CORRECTION FOR TAIL SURFACE

When testing a complete aircraft model with a tail surface, it is usually sufficient to apply a correction to the pitching-moment coefficient only. This correction is a result of the difference in downwash angle between the wing and the tail, $\Delta\alpha_t$, and results in the following correction

$$\Delta C_{m_t} = \Delta\alpha_t \frac{\partial C_{m_t}}{\partial\alpha_t} \tag{6.14}$$

The value of $\Delta\alpha_t$ can be obtained from Eq. (6.11) where $x_1 = \ell_t$ is the distance between the centroids of the wing and tail surfaces.

Equation (6.14) can be expressed in terms of the tail lift-curve slope (see Ref. 16) as

$$\Delta C_{m_t} = \frac{q_t \, S_t \, \ell_t}{q_\infty \, S \, c} \frac{\partial C_{L_t}}{\partial \alpha_t} \Delta\alpha_t \tag{6.15}$$

The appropriate equations and figures to be used to evaluate the interference factors in the above equations are listed in the tables of Appendix IV.

SECTION VII
CONCLUDING REMARKS

The material presented in this report is intended to introduce the reader to the steadily growing body of information on wall interference in ventilated wall wind tunnels. In concluding the discussion, a number of observations concerning the results presented will be noted. In addition, some of the areas in which further study is proceeding will be pointed out.

The following tabulations list the values of the slot and porosity parameters, P and Q, required to obtain zero interference for the various interference factors in slotted and perforated tunnels of the types considered in the body of the report.

For a two-dimensional tunnel, the values of P and Q are as follows:

Type of Interference	Slotted	Perforated
Ω_s	0.45	0.44
δ_o	0	0
δ_1	0.39	0.56

The solid-blockage interference is eliminated at almost the same values of P and Q in two-dimensional slotted and perforated tunnels respectively. The upwash correction in a

two-dimensional tunnel is eliminated completely only with completely closed walls. The open-area ratio in a two-dimensional tunnel to obtain a zero streamline-curvature correction is less in a slotted tunnel and greater in a perforated tunnel than that required for zero blockage.

As pointed out in the text the interference at the model position caused by the wake velocity gradient ($\partial\epsilon_w/\partial x$) is eliminated at the same value of either P for the slotted tunnel or Q for the perforated tunnel as that required to eliminate the solid-blockage interference. The ideal slotted tunnel has the added advantage that any value of $P > 0$ will eliminate both the velocity gradient due to solid blockage ($\partial\epsilon_s/\partial x$) and the wake blockage (ϵ_w). This advantage will be modified, however, if viscous effects of the flow in the slots are taken into account. In the perforated wall tunnels, the velocity gradient due to solid blockage is near its maximum value when the solid blockage is zero and the wake blockage gets smaller as the porosity is increased and is zero at $Q = 1$ (i.e., for an open tunnel) only.

For a circular tunnel, the values of P and Q required to obtain zero interference are as follows:

Type of Interference	Slotted	Perforated
Ω_s	0.64	0.45
δ_0	0.50	0.46
δ_1	0.62	0.68

In a circular slotted tunnel, the streamline-curvature correction is zero at about the same open area as that for zero solid blockage; however, to eliminate the upwash correction a lower open area is required. For the circular perforated tunnel, the upwash correction is eliminated at about the same porosity as that for zero blockage, but for zero streamline curvature a higher porosity is required.

For the types of rectangular tunnels for which numerical calculations are presently available, the following values of P and Q are required to obtain zero interference for the type of interference indicated:

Type of Interference	Slotted Vertical and Horizontal Walls, $P_h = P_v$		
	h/b = 1.0	h/b = 0.8	h/b = 0.5
Ω_s	0.61	0.58	0.56
δ_o	0.45	0.42	0.39
	Solid Vertical and Slotted Horizontal Walls		
Ω_s	0.85	0.72	0.58
δ_o	0.52	0.44	0.39
δ_1	0.64	0.58	0.54
	Solid Vertical and Perforated Horizontal Walls		
Ω_s	0.66	0.57	0.51
δ_o	0.52	0.45	0.40
δ_1	0.72	0.68	0.65

In all three types of rectangular tunnels considered, the values of P or Q at which zero interference occurs decreases as the tunnel height-to-width ratio decreases. As indicated by the results for the two slotted tunnels, the effects of the sidewalls diminish almost completely for the tunnel with a height-to-width ratio of 0.5.

An examination of Figs. 5.4 and 5.10 indicates that a wide range of combinations of P_v and P_h, including that for which $P_h = P_v$, exists which will eliminate either the solid-blockage or lift interference for a slotted rectangular tunnel with a particular height-to-width ratio. In addition, for each type of interference a common intersection of the interference-free curves occurs for all of the slotted rectangular tunnels with a height-to-width ratio between 0.5 and 1.0. For zero solid blockage the intersection occurs at $P_h = 0.56$ and $P_v = 0.63$, and for zero upwash interference at $P_h = 0.39$ and $P_v = 0.64$.

Since prior studies of rectangular tunnels were limited to those with only the horizontal walls slotted, a configuration of slots providing the simultaneous elimination of both solid-blockage and lift interference was not possible. However, by including the effects due to the presence of slotted vertical boundaries, a superposition of Figs. 5.4 and 5.10 indicates that a single slotted wall configuration will eliminate both blockage and lift interference with tunnels of height-to-width ratios above approximately 0.8.

The choice of slot parameters leading to this objective is $P_h = 0.30$ and $P_v = 0.79$ for a square tunnel and $P_h = 0.30$ and $P_v = 0.95$ for a tunnel with a height-to-width ratio of 0.8.

The solid blockage and upwash interference are eliminated at about the same value of Q in a three-dimensional perforated tunnel. It appears therefore that in this case the solid blockage and upwash velocity gradients could be reduced or possibly eliminated by a variation in the porosity distribution in the longitudinal direction along the position of the model while still maintaining zero solid blockage and zero upwash at the model position.

Since the interference calculations in rectangular tunnels with all walls ventilated have heretofore not been available, a common practice has been to apply the results from a circular tunnel to a rectangular tunnel. The validity of this procedure can be assessed by comparing the corresponding figures for the circular and rectangular tunnels. For example, Figs. 4.1 and 5.2 indicate that the indicated practice is fairly accurate for a square tunnel; however, the discrepancies become progressively larger as the height-to-width ratio of the rectangular tunnels decreases below 1.0.

As pointed out previously, the results in this report are applicable to a small model on the centerline of the tunnel. It is apparent from the results obtained in rectangular tunnels of various height-to-width ratios that as the model is positioned closer or further from a tunnel boundary, the interference effects will be changed. A number of papers dealing with an off-centerline position of the model in two-dimensional and circular ventilated tunnels are available. The results presented in this report for a rectangular tunnel can also be extended without difficulty to models off the tunnel centerline. With respect to wing span, the results presented refer to a wing with a span approaching zero tunnel breadth for the circular and rectangular tunnels. The effect of finite wing span on the interference factors has been determined for some configurations of circular and rectangular tunnels as shown for example in Ref. 14. Although the effects of wing span are shown to be significant, it would appear that validation of the basic theory accounting for the first-order effects should be substantiated more thoroughly before attempting to account for these second-order effects.

The results shown for slotted wall tunnels in the previous sections are applicable to an ideal slotted wall, i.e., a wall where the viscous effects of the flow through the slots have not been considered. As discussed by the authors of many of the referenced papers, the effects of viscosity on the flow through slotted walls can be taken into account by retaining

the "R" term in the general boundary condition (see Eq. (2.10)). The result is that for various values of the slot parameter, P, a particular value of the porosity parameter, Q, can be found for which the various interference factors can be made zero. The general equations for the solid-blockage and lift-interference factors have been solved for the simultaneous values of P and Q which provide zero interference and the results are shown in Figs. 7.1 through 7.3. As indicated, the inclusion of the viscosity term modifies the results for an ideal slotted tunnel significantly.

The results presented in this report are applicable to steady flow. In Ref. 17, however, it is shown that a relationship exists between the steady and oscillatory upwash fields because of wall interference in incompressible or low-frequency compressible flow. An additional parameter δ'_o is introduced which is related to the integral of the interference factor δ upstream of the model to infinity (see Figs. 3.6 and 3.8). Equations showing the corrections to the direct pitching derivatives and derivatives of lift due to pitching as obtained from oscillatory wind tunnel tests are presented in Ref. 17 in terms of the lift-interference factors δ_o and δ_1 given in this report and the additional parameter δ'_o. Further discussion of these results is beyond the scope of this paper and will be treated separately.

As a final comment, the authors would like to point out the widespread lack in the use of corrections for data from ventilated wall tunnels. This neglect is most probably due to the lack of fundamental experimental programs to check the validity of the theoretical analyses. These studies are especially lacking in the case of perforated wall tunnels. Attention has been drawn recently to this shortcoming as a result of discrepancies between uncorrected tunnel and flight data and some investigations of the problem have been conducted. However, much more basic experimental study on the order of that presented in Ref. 4 is required.

REFERENCES

1. Baldwin, B. S., Turner, J. B., and Knechtel, E. D. "Wall Interference in Wind Tunnels with Slotted and Porous Boundaries at Subsonic Speeds." NACA TN 3176, May 1954.

2. Wright, R. H. "The Effectiveness of the Transonic Wind Tunnel as a Device for Minimizing Tunnel-Boundary Interference for Model Tests at Transonic Speeds." AGARD Report 294, 1959.

3. Garner, H. C., Rogers, E. W. E., Acum, W. E. A., and Maskell, E. C. "Subsonic Wind Tunnel Wall Corrections." AGARDograph 109, October 1966.

4. Lo, C. F. and Binion, T. W. Jr. "A V/STOL Wind Tunnel Wall Interference Study." AIAA Paper No. 69-171.

5. Lo, C. F. "Method of Calculating the Wind Tunnel Interference for Steady and Oscillating Wings in Tunnels of Arbitrary Wall Configuration." AEDC-TR-68-42, March 1968.

6. Goodman, T. R. "The Porous Wall Wind Tunnel, Part II, Interference Effect on a Cylindrical Body in a Two-Dimensional Tunnel at Subsonic Speed." Cornell Aero. Lab. Report No. AD-594-A-3, 1950.

7. Pindzola, M. and Chew, W. L. "A Summary of Perforated Wall Wind Tunnel Studies at the Arnold Engineering Development Center." AEDC-TR-60-9, August 1960.

8. Kassner, R. R. "Subsonic Flow over a Body Between Porous Walls." WADC TR-52-9, 1952.

9. Brescia, R. "Wall Interference in a Perforated Wall Wind Tunnel." NACA TM 1429, May 1957.

10. Theodorsen, T. "The Theory of Wind-Tunnel Wall Interference." NACA Report 410, 1932.

11. Davis, D. D., Jr. and Moore, D. "Analytical Study of Blockage and Lift-Interference Corrections for Slotted Tunnels Obtained by the Substitution of an Equivalent Homogeneous Boundary for the Discrete Slots." NACA RM L53E07b, June 1953.

12. Acum, W. E. A. "Note on the Evaluation of Solid-Blockage Corrections for Rectangular Wind Tunnels with Slotted Walls." ARC R & M 3297, 1961.

13. Holder, D. R. "Upwash Interference in a Rectangular Wind Tunnel with Closed Side Walls and Porous Slotted Floor and Roof." ARC R & M No. 3322, 1963.

14. Holder, D. R. "Upwash Interference on Wings of Finite Span in a Rectangular Wind Tunnel with Closed Side Walls and Porous-Slotted Floor and Roof." ARC R & M No. 3395, 1965.

15. Allen, H. J. and Vincenti, W. G. "Wall Interference in a Two-Dimensional Wind Tunnel, with Consideration of the Effect of Compressibility." NACA Report No. 782, 1944.

16. Pope, A. and Harper, J. J. Low-Speed Wind Tunnel Testing. John Wiley & Sons, Inc., New York, 1966.

17. Garner, H. C., Moore, A. W., and Wight, K. C. "The Theory of Interference Effects on Dynamic Measurements in Slotted-Wall Tunnels at Subsonic Speeds and Comparisons with Experiment." NPL Aero Report 1211, ARC 28 339, September 1966.

APPENDIX I
LIST OF INTEGRANDS

The following is a listing of portions of the integrands of the various equations given in the text.

$$I_A = \left[\cosh q + Fq \sinh q\right]^2 + \left[(\beta/R) \sinh q\right]^2$$

$$I_B = \left[1 - (Fq)^2 - (\beta/R)^2\right] + \left[(1 - Fq)^2 + (\beta/R)^2\right] e^{-2q}$$

$$I_C = \left[(1 - Fq)(\cosh q + Fq \sinh q) - (\beta/R)^2 \sinh q\right] e^{-q}$$

$$I_D = \left[\sinh q + \cosh q + Fq \sinh q\right] e^{-q}$$

$$I_E = \left[\sinh q + Fq \cos q + (1 - Fq) \cosh q\right] e^{-q}$$

$$I_F = \left[\sinh q + Fq \cosh q\right]^2 + \left[(\beta/R) \cosh q\right]^2$$

$$I_G = \left[(1 - Fq)(\sinh q + Fq \cosh q) - (\beta/R)^2 \cosh q\right] e^{-q}$$

$$I_H = K_1(q)\, I_0(q) + K_0(q) I_1(q) = 1/q$$

$$I_K = K_0(q)\, I_0(q) - q\, F\, K_1(q)\, I_0(q) + qF\, K_0(q)\, I_1(q) - \left[q^2 F^2 + (\beta/R)^2\right] K_1(q)\, I_1(q)$$

$$I_M = \left[I_0(q) + qF\, I_1(q)\right]^2 + \left[(\beta/R)\, I_1(q)\right]^2$$

$$I_N = q^2 \left[(1 - F)\, I_1(q) + qF\, I_0(q)\right]^2 + (\beta/R)^2 \left[I_1(q) - q\, I_0(q)\right]^2$$

$$I_P = \left[q\, I_1(q)\right]^2 + (\beta/R)^2 \left[I_1(q) - q\, I_0(q)\right]^2$$

$$I_Q = q^2 \left[(1 - F)\, K_1(q) - q\, F\, K_0(q)\right] \left[(1 - F)\, I_1(q) + q\, F\, I_0(q)\right] + (\beta/R)^2 \left[K_1(q) + q\, K_0(q)\right] \left[I_1(q) - q\, I_0(q)\right]$$

$$I_R = q^2\, K_1(q)\, I_1(q) + (\beta/R)^2 \left[K_1(q) + q\, K_0(q)\right] \left[I_1'(q) - q\, I_0(q)\right]$$

APPENDIX II
EQUATIONS FOR EVALUATING THE SERIES COEFFICIENTS A_m AND B_m

The following sets of linear algebraic simultaneous equations are used to determine the constant coefficients given in Section V. The number of points, chosen uniformly distributed along the horizontal and vertical walls, must be more than the number of terms in the series.

1. General Boundary Condition

$$\sum_{0,2,4}^{M} (B_m + i A_m) \left\{ - i \cos m\theta \; I_m\left(\frac{qr}{b}\right) + \left(-i q \frac{h}{b} F_v + \frac{\beta}{R_v}\right) \left[\cos\theta \cos m\theta \; I_{m+1}\left(\frac{qr}{b}\right) + \frac{m}{qr/b} \cos(m-1)\theta \; I_m\left(\frac{qr}{b}\right)\right]\right\} = - \left[K_o\left(\frac{qr}{b}\right) - \left(q \frac{h}{b} F_v + i \frac{\beta}{R_v}\right) \cos\theta \; K_1\left(\frac{qr}{b}\right)\right] \Bigg|_{\substack{r = r_v \\ \theta = \theta_v}} \qquad \text{(II-1a)}$$

and

$$\sum_{0,2,4}^{M} (B_m + i A_m) \left\{ - i \cos m\theta \; I_m\left(\frac{qr}{b}\right) + \left(-i q \frac{h}{b} F_h + \frac{\beta}{R_h}\right) \left[\sin\theta \cos m\theta \; I_{m+1}\left(\frac{qr}{b}\right) - \frac{m}{qr/b} \sin(m-1)\theta \; I_m\left(\frac{qr}{b}\right)\right]\right\} = - \left[K_o\left(\frac{qr}{b}\right) - \left(q \frac{h}{b} F_h + i \frac{\beta}{R_h}\right) \sin\theta \; K_1\left(\frac{qr}{b}\right)\right] \Bigg|_{\substack{r = r_h \\ \theta = \theta_h}} \qquad \text{(II-1b)}$$

2. Closed Tunnel ($F \to \infty$ or $\frac{\beta}{R} \to \infty$)

$$\sum_{o,2,4}^{M} A_{m_c} \left[\cos\theta \cos m\theta \; I_{m+1}\left(\frac{qr}{b}\right) + \frac{m}{qr/b} \cos(m-1)\theta \; I_m\left(\frac{qr}{b}\right) \right]$$

$$= \cos\theta \; K_1\left(\frac{qr}{b}\right) \Bigg|_{\substack{r = r_v \\ \theta = \theta_v}} \qquad \text{(II-2a)}$$

and

$$\sum_{o,2,4}^{M} A_{m_c} \left[\sin\theta \cos m\theta \; I_{m+1}\left(\frac{qr}{b}\right) - \frac{m}{qr/b} \sin(m-1)\theta \; I_m\left(\frac{qr}{b}\right) \right]$$

$$= \sin\theta \; K_1\left(\frac{qr}{b}\right) \Bigg|_{\substack{r = r_h \\ \theta = \theta_h}} \qquad \text{(II-2b)}$$

3. Open Jet ($F = 0$ and $\beta/R = 0$)

$$\sum_{o,2,4}^{M} A_{m_o} \cos m\theta \; I_m\left(\frac{qr}{b}\right) = - K_o\left(\frac{qr}{b}\right) \Bigg|_{\substack{r = r_v \text{ or } r_h \\ \theta = \theta_v \text{ or } \theta_h}} \qquad \text{(II-3)}$$

4. Slotted Wall Tunnel ($\beta/R = 0$)

$$\sum_{o,2,4}^{M} A_{m_s} \left\{ \cos m\theta \; I_m\left(\frac{qr}{b}\right) + q\frac{h}{b} F_v \left[\cos\theta \cos m\theta \; I_{m+1}\left(\frac{qr}{b}\right) + \frac{m}{qr/b} \cos(m-1)\theta \; I_m\left(\frac{qr}{b}\right) \right] \right\}$$

$$= - \left[K_o\left(\frac{qr}{b}\right) - q\frac{h}{b} F_v \cos\theta \; K_1\left(\frac{qr}{b}\right) \right] \Bigg|_{\substack{r = r_v \\ \theta = \theta_v}} \qquad \text{(II-4a)}$$

and

$$\sum_{o,2,4}^{M} A_{m_s} \left\{ \cos m\theta \; I_m\left(\frac{qr}{b}\right) + q\frac{h}{b} F_h \left[\sin\theta \cos m\theta \; I_{m+1}\left(\frac{qr}{b}\right) - \frac{m}{qr/b} \sin(m-1)\theta \; I_m\left(\frac{qr}{b}\right)\right]\right\}$$

$$= -\left[K_o\left(\frac{qr}{b}\right) - q\frac{h}{b} F_h \sin\theta \; K_1\left(\frac{qr}{b}\right)\right]\Bigg|_{\substack{r = r_h \\ \theta = \theta_h}} \qquad \text{(II-4b)}$$

5. Perforated Wall Tunnel (F = 0)

$$\sum_{o,2,4}^{M} (B_{m_p} + i A_{m_p}) \left\{ -i \cos m\theta \; I_m\left(\frac{qr}{b}\right) + \frac{\beta}{R_v}\left[\cos\theta \cos m\theta \; I_{m+1}\left(\frac{qr}{b}\right) + \frac{m}{qr/b}\cos(m-1)\theta \; I_m\left(\frac{qr}{b}\right)\right]\right\}$$

$$= -\left[K_o\left(\frac{qr}{b}\right) - i\frac{\beta}{R_v}\cos\theta \; K_1\left(\frac{qr}{b}\right)\right]\Bigg|_{\substack{r = r_v \\ \theta = \theta_v}} \qquad \text{(II-5a)}$$

and

$$\sum_{o,2,4}^{M} (B_{m_p} + i A_{m_p}) \left\{ -i \cos m\theta \; I_m\left(\frac{qr}{b}\right) + \frac{\beta}{R_h}\left[\sin\theta \cos m\theta \; I_{m+1}\left(\frac{qr}{b}\right) - \frac{m}{qr/b}\sin(m-1)\theta \; I_m\left(\frac{qr}{b}\right)\right]\right\}$$

$$= -\left[K_o\left(\frac{qr}{b}\right) - i\frac{\beta}{R_h}\sin\theta \; K_1\left(\frac{qr}{b}\right)\right]\Bigg|_{\substack{r = r_h \\ \theta = \theta_h}} \qquad \text{(II-5b)}$$

APPENDIX III
EQUATIONS FOR EVALUATING THE SERIES COEFFICIENTS D_m, E_m, AND G_m

The following sets of equations are used to calculate the series coefficients required to evaluate the lift interference in Section V. The coefficients are determined in a similar manner to that outlined in Appendix II.

1. General Boundary Condition

$$\sum_{1,3,5}^{M} D_m r^m \left[\sin m\theta + F_v \frac{mh}{b} \cos\theta \sin(m-1)\theta\right] = - \sin\theta \cos\theta \left(1 - F_v 2 \frac{h}{b} \cos^2\theta\right)\Bigg|_{\substack{r = r_v \\ \theta = \theta_v}} \tag{III-1a}$$

and

$$\sum_{1,3,5}^{M} D_m r^m \left[\sin m\theta + F_h \frac{mh}{b} \sin\theta \cos(m-1)\theta\right] = - \frac{\sin^2\theta}{h/b} \left[1 + F_h \frac{h}{b} \cos 2\theta\right]\Bigg|_{\substack{r = r_h \\ \theta = \theta_h}} \tag{III-1b}$$

$$\sum_{1,3,5}^{M} (G_m + i E_m) \left\{- i \sin m\theta \, I_m\left(\frac{qr}{b}\right) + \left(-iq \frac{h}{b} F_v + \frac{\beta}{R_v}\right)\left[\cos\theta \sin m\theta \, I_{m+1}\left(\frac{qr}{b}\right) + \frac{m}{qr/b} \sin(m-1)\theta \, I_m\left(\frac{qr}{b}\right)\right]\right\} = - \left[\sin\theta \, K_1\left(\frac{qr}{b}\right) + \left(q \frac{h}{b} F_v + i \frac{\beta}{R_v}\right) \sin\theta \cos\theta \, K_2\left(\frac{qr}{b}\right)\right]\Bigg|_{\substack{r = r_v \\ \theta = \theta_v}} \tag{III-2a}$$

and

$$\sum_{1,3,5}^{M} (G_m + i\,E_m) \left\{ - i \sin m\theta\; I_m\left(\frac{qr}{b}\right) + \left(- i\,q\,\frac{h}{b}\,F_h + \frac{\beta}{R_h} \right) \left[\sin\theta \sin m\theta\; I_{m+1}\left(\frac{qr}{b}\right) + \frac{m}{qr/b} \cos(m-1)\theta\; I_m\left(\frac{qr}{b}\right) \right] \right\}$$

$$= - \left\{ \sin\theta\; K_1\left(\frac{qr}{b}\right) + \left(q\,\frac{h}{b}\,F_h + i\,\frac{\beta}{R_h} \right) \left[\frac{K_1\,(qr/b)}{qr/b} - \sin^2\theta\; K_2\left(\frac{qr}{b}\right) \right] \right\} \Bigg|_{\substack{r = r_h \\ \theta = \theta_h}} \qquad \text{(III-2b)}$$

2. Closed Tunnel ($F \to \infty$ or $\frac{\beta}{R} \to \infty$)

$$\sum_{1,3,5}^{M} D_{m_c}\, r^m\, m \sin(m-1)\theta = 2 \sin\theta \cos^2\theta \Big|_{\substack{r = r_v \\ \theta = \theta_v}} \qquad \text{(III-3a)}$$

and

$$\sum_{1,3,5}^{M} D_{m_c}\, r^m\, m \cos(m-1)\theta = - \frac{\sin\theta \cos 2\theta}{h/b} \Bigg|_{\substack{r = r_h \\ \theta = \theta_h}} \qquad \text{(III-3b)}$$

$$\sum_{1,3,5}^{M} E_{m_c} \left[\cos\theta \sin m\theta\; I_{m+1}\left(\frac{qr}{b}\right) + \frac{m}{qr/b} \sin(m-1)\theta\; I_m\left(\frac{qr}{b}\right) \right]$$

$$= - \sin\theta \cos\theta\; K_2\left(\frac{qr}{b}\right) \Bigg|_{\substack{r = r_v \\ \theta = \theta_v}} \qquad \text{(III-4a)}$$

and

$$\sum_{1,3,5}^{M} E_{m_c} \left[\sin\theta \sin m\theta \, I_{m+1}\left(\frac{qr}{b}\right) + \frac{m}{qr/b} \cos(m-1)\theta \, I_m\left(\frac{qr}{b}\right) \right]$$

$$= - \left[\frac{K_1 (qr/b)}{qr/b} - \sin^2\theta \, K_2\left(\frac{qr}{b}\right) \right] \Bigg|_{\substack{r = r_v \\ \theta = \theta_v}} \qquad \text{(III-4b)}$$

3. Open Jet (F = 0 and $\beta/R = 0$)

$$\sum_{1,3,5}^{M} D_{m_o} r^m \sin m\theta = - \sin\theta \, \frac{b}{r} \Bigg|_{\substack{r = r_v \text{ or } r_h \\ \theta = \theta_v \quad \theta_h}} \qquad \text{(III-5)}$$

and

$$\sum_{1,3,5}^{M} E_{m_o} \sin m\theta \, I_m\left(\frac{qr}{b}\right) = - \sin\theta \, K_1\left(\frac{qr}{b}\right) \Bigg|_{\substack{r = r_v \text{ or } r_h \\ \theta = \theta_v \quad \theta_h}} \qquad \text{(III-6)}$$

4. Slotted Wall Tunnel ($\beta/R = 0$)

$$\sum_{1,3,5}^{M} E_{m_s} \left\{ \sin m\theta \, I_m\left(\frac{qr}{b}\right) + q \frac{h}{b} F_v \left[\cos\theta \sin m\theta \, I_{m+1}\left(\frac{qr}{b}\right) + \frac{m}{qr/b} \sin(m-1)\theta \, I_m\left(\frac{qr}{b}\right) \right] \right\}$$

$$= - \left[\sin\theta \, K_1\left(\frac{qr}{b}\right) + q \frac{h}{b} F_v \sin\theta \cos\theta \, K_2\left(\frac{qr}{b}\right) \right] \Bigg|_{\substack{r = r_v \\ \theta = \theta_v}}$$

(III-7a)

and

$$\sum_{1,3,5}^{M} E_{m_s} \left\{ \sin m\theta \; I_m\left(\frac{qr}{b}\right) + q\,\frac{h}{b}\,F_h \left[\sin\theta \sin m\theta \; I_{m+1}\left(\frac{qr}{b}\right) + \frac{m}{qr/b}\cos(m-1)\theta \; I_m\left(\frac{qr}{b}\right)\right]\right\} = -\left\{ \sin\theta \; K_1\left(\frac{qr}{b}\right) + q\,\frac{h}{b}\,F_h \left[\frac{K_1(qr/b)}{qr/b} - \sin^2\theta \; K_2\left(\frac{qr}{b}\right)\right]\right\}\Bigg|_{\substack{r = r_h \\ \theta = \theta_h}} \qquad \text{(III-7b)}$$

5. Perforated Wall Tunnel (F = 0)

$$\sum_{1,3,5}^{M} (G_{m_p} + i\,E_{m_p}) \left\{ -i \sin m\theta \; I_m\left(\frac{qr}{b}\right) + \frac{\beta}{R_v}\left[\cos\theta \sin m\theta \; I_{m+1}\left(\frac{qr}{b}\right) + \frac{m}{qr/b}\sin(m-1)\theta \; I_m\left(\frac{qr}{b}\right)\right]\right\} = -\left[\sin\theta \; K_1\left(\frac{qr}{b}\right) + i\,\frac{\beta}{R_v}\sin\theta\cos\theta \; K_2\left(\frac{qr}{b}\right)\right]\Bigg|_{\substack{r = r_v \\ \theta = \theta_v}} \qquad \text{(III-8a)}$$

and

$$\sum_{1,3,5}^{M} (G_{m_p} + i\,E_{m_p}) \left\{ -i \sin m\theta \; I_m\left(\frac{qr}{b}\right) + \frac{\beta}{R_h}\left[\sin\theta \sin m\theta \; I_{m+1}\left(\frac{qr}{b}\right) + \frac{m}{qr/b}\cos(m-1)\theta \; I_m\left(\frac{qr}{b}\right)\right]\right\} = -\left\{ \sin\theta \; K_1\left(\frac{qr}{b}\right) + i\,\frac{\beta}{R_v}\left[\frac{K_1(qr/b)}{qr/b} - \sin^2\theta K_2\left(\frac{qr}{b}\right)\right]\right\}\Bigg|_{\substack{r = r_h \\ \theta = \theta_h}} \qquad \text{(III-8b)}$$

APPENDIX IV
TABLES

TABLE I
INTERFERENCE FACTORS IN A TWO-DIMENSIONAL TUNNEL

KIND OF INTERFERENCE	CLOSED	OPEN	SLOTTED	PERFORATED
Solid blockage, ϵ_s	(3.8)	(3.10)	(3.13) 3.2	*(3.16) ** 3.4
Velocity gradient due to solid blockage, $\partial\epsilon_s/\partial x$	zero	zero	zero	(3.18) 3.5
Wake blockage, ϵ_w	(3.30)	zero	zero	(3.39) 3.4
Velocity gradient due to wake blockage, $\partial\epsilon_w/\partial x$	(3.31)	(3.33)	(3.36)	(3.42)
Upwash factor at model, δ_o	zero	(3.58)	(3.62) 3.7	(3.66) 3.9
Streamline curvature factor, δ_1	(3.56)	(3.60)	(3.64) 3.7	(3.68) 3.9

*Equation number
**Figure number

TABLE II
INTERFERENCE FACTORS IN A CIRCULAR TUNNEL

KIND OF INTERFERENCE	CLOSED	OPEN	SLOTTED	PERFORATED
Solid blockage, ϵ_s	(4.8)	(4.10)	(4.12) 4.1	*(4.14) ** 4.2
Velocity gradient due to solid blockage, $\partial\epsilon_s/\partial x$	zero	zero	zero	(4.15 4.3
Wake blockage, ϵ_w	(4.24)	zero	zero	(4.31) 4.2
Velocity gradient due to wake blockage, $\partial\epsilon_w/\partial x$	(4.25)	(4.27)	(4.29)	(4.33)
Upwash factor at model δ_o	(4.44)	(4.46)	(4.49) 4.5	(4.52) 4.7
Streamline curvature factor, δ_1	(4.45)	(4.47)	(4.50) 4.5	(4.53) 4.7

*Equation number
**Figure number

TABLE III
INTERFERENCE FACTORS IN A RECTANGULAR TUNNEL

KIND OF INTERFERENCE	CLOSED	OPEN	SLOTTED	PERFORATED
Solid blockage, ϵ_s	*(5.7) ** 5.1	(5.10) 5.1	(5.12) 5.2	(5.14)
Velocity gradient due to solid blockage $\partial\epsilon_s/\partial x$	zero	zero	zero	(5.15)
Wake blockage, ϵ_w	(5.24)	zero	zero	(5.33)
Velocity gradient due to wake blockage, $\partial\epsilon_w/\partial x$	(5.26)	(5.29)	(5.31)	(5.35)
Upwash factor at model, δ_o	(5.46)	(5.51)	(5.55) 5.7	(5.61)
Streamline curvature factor δ_1	(5.48)	(5.53)	(5.56)	(5.62)

*Equation number
**Figure number

APPENDIX V
ILLUSTRATIONS

$$F = \frac{K}{h} = \frac{\ell}{\pi h} \ln\left(\csc \frac{\pi a}{2\ell}\right)$$

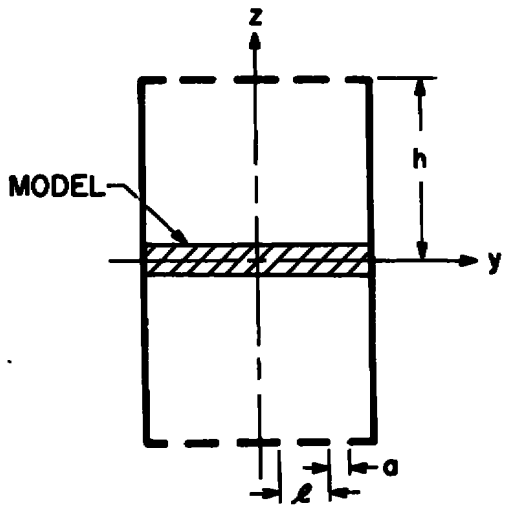

a. TWO-DIMENSIONAL TUNNEL

$$F = \frac{K}{r_o} = \frac{\ell}{\pi r_o} \ln\left(\csc \frac{\pi a}{2\ell}\right)$$

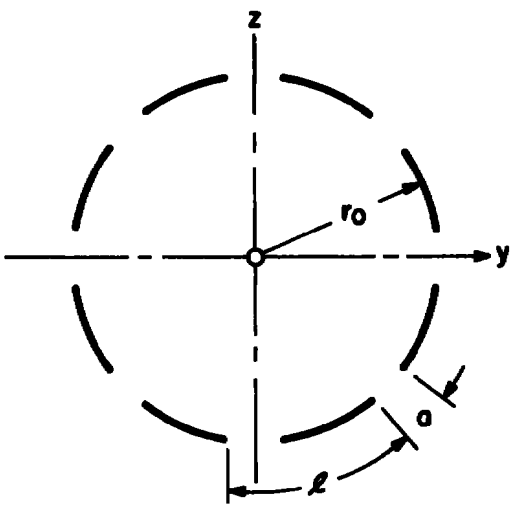

b. CIRCULAR TUNNEL

$$F = \frac{K}{h} = \frac{\ell}{\pi h} \ln\left(\csc \frac{\pi a}{2\ell}\right)$$

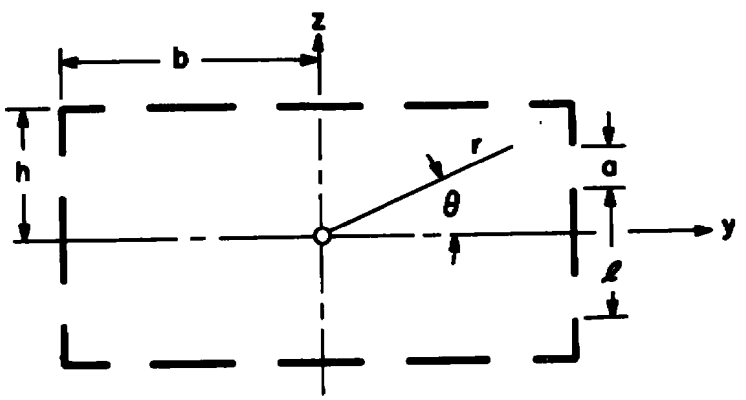

c. RECTANGULAR TUNNEL

Fig. 2.1 Coordinate System and Geometry of Wind Tunnel Cross Sections

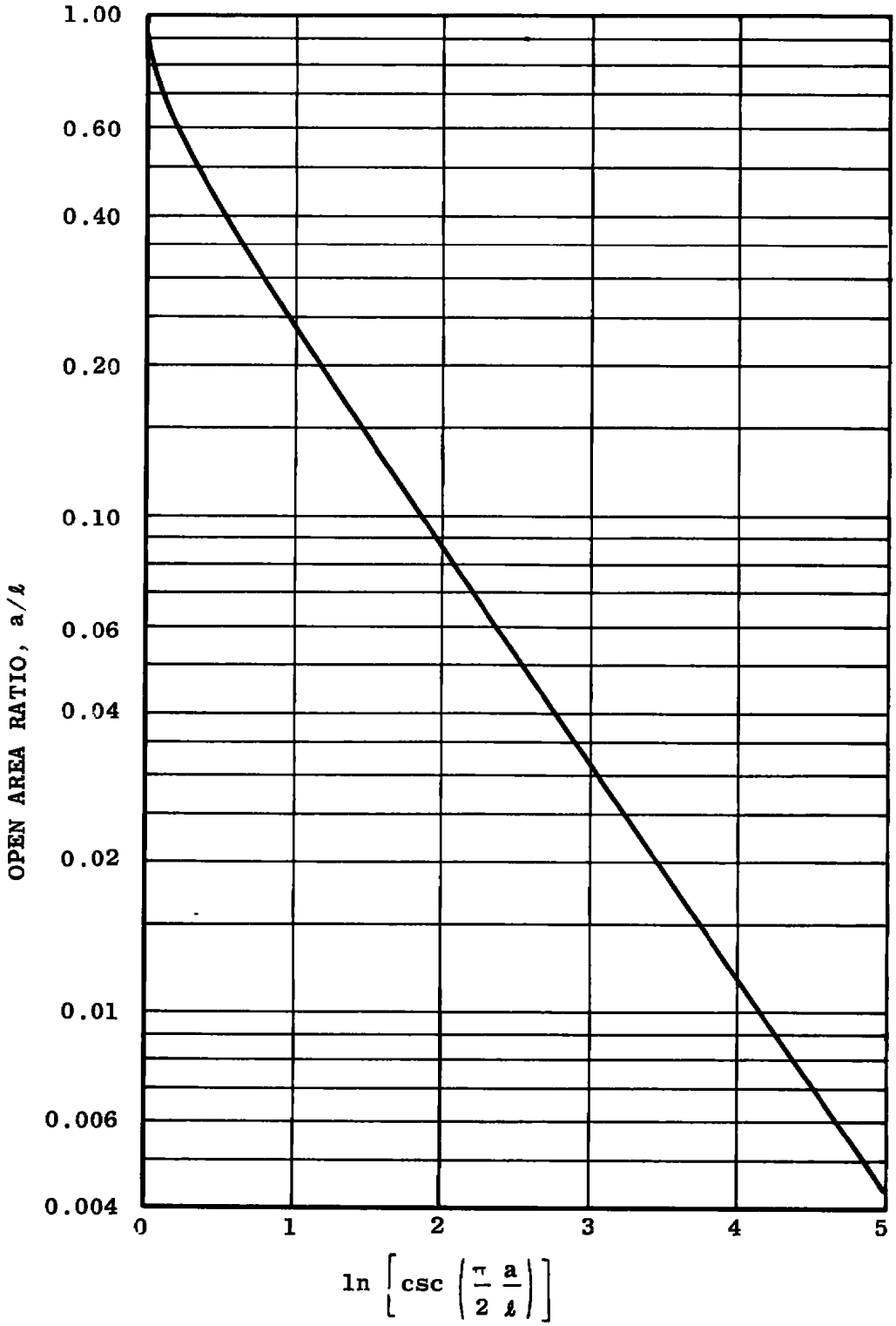

Fig. 2.2 Slot-Parameter Function for Various Open Area Ratios

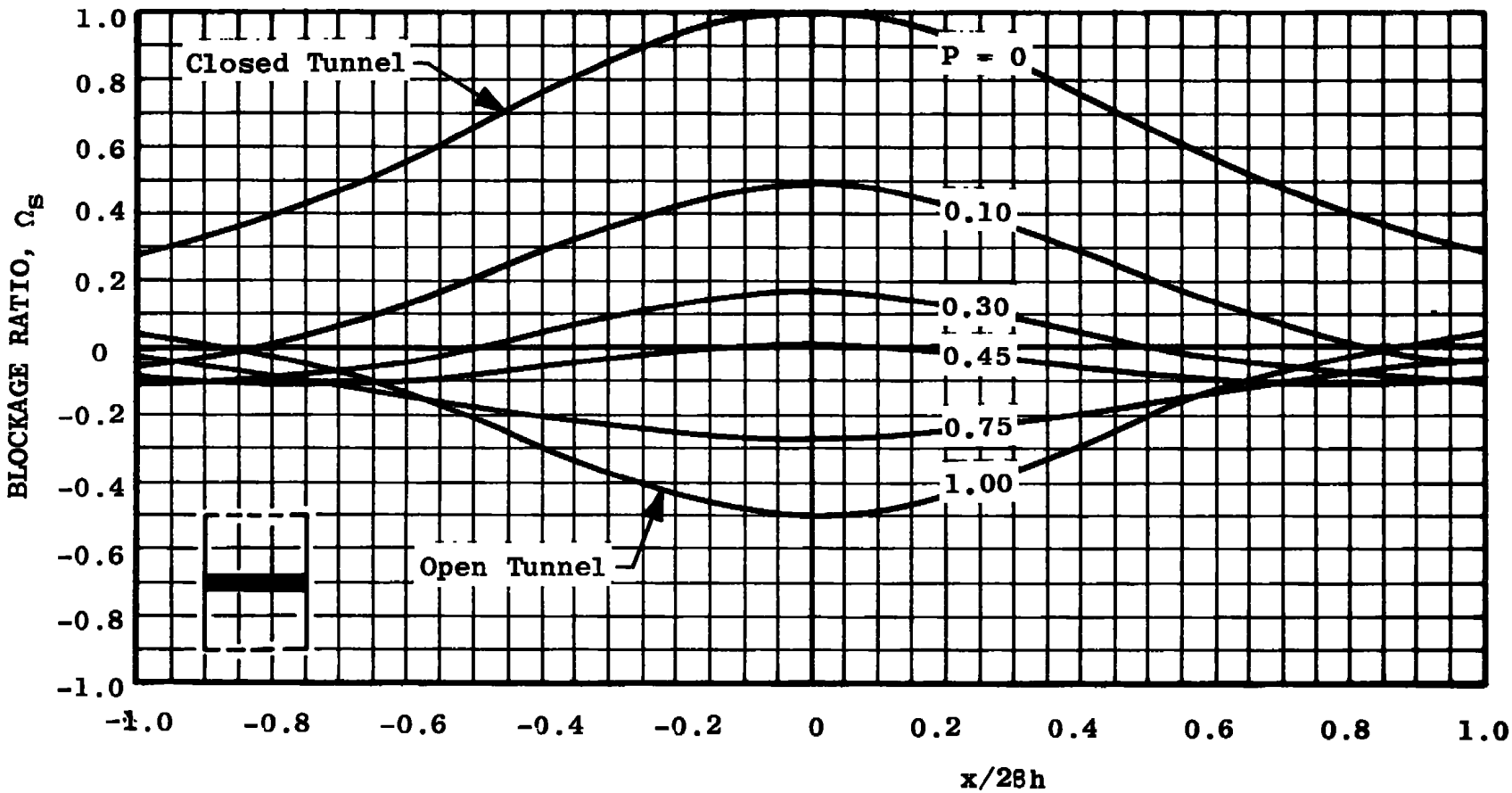

Fig. 3.1 Distribution of the Solid-Blockage Factor Ratio along a Two-Dimensional Slotted Tunnel

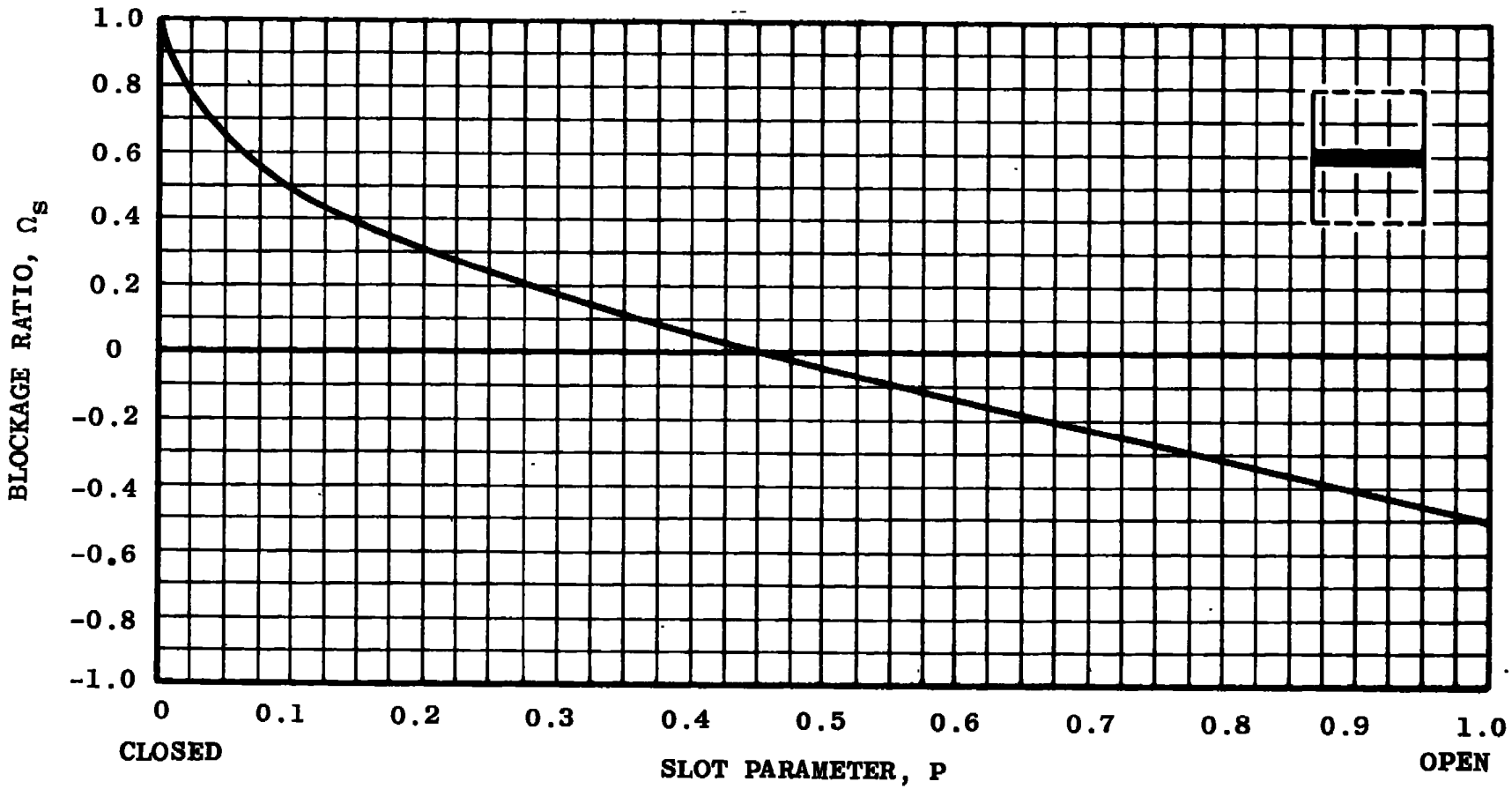

Fig. 3.2 Solid-Blockage Factor Ratio at x = 0 in a Two-Dimensional Slotted Tunnel

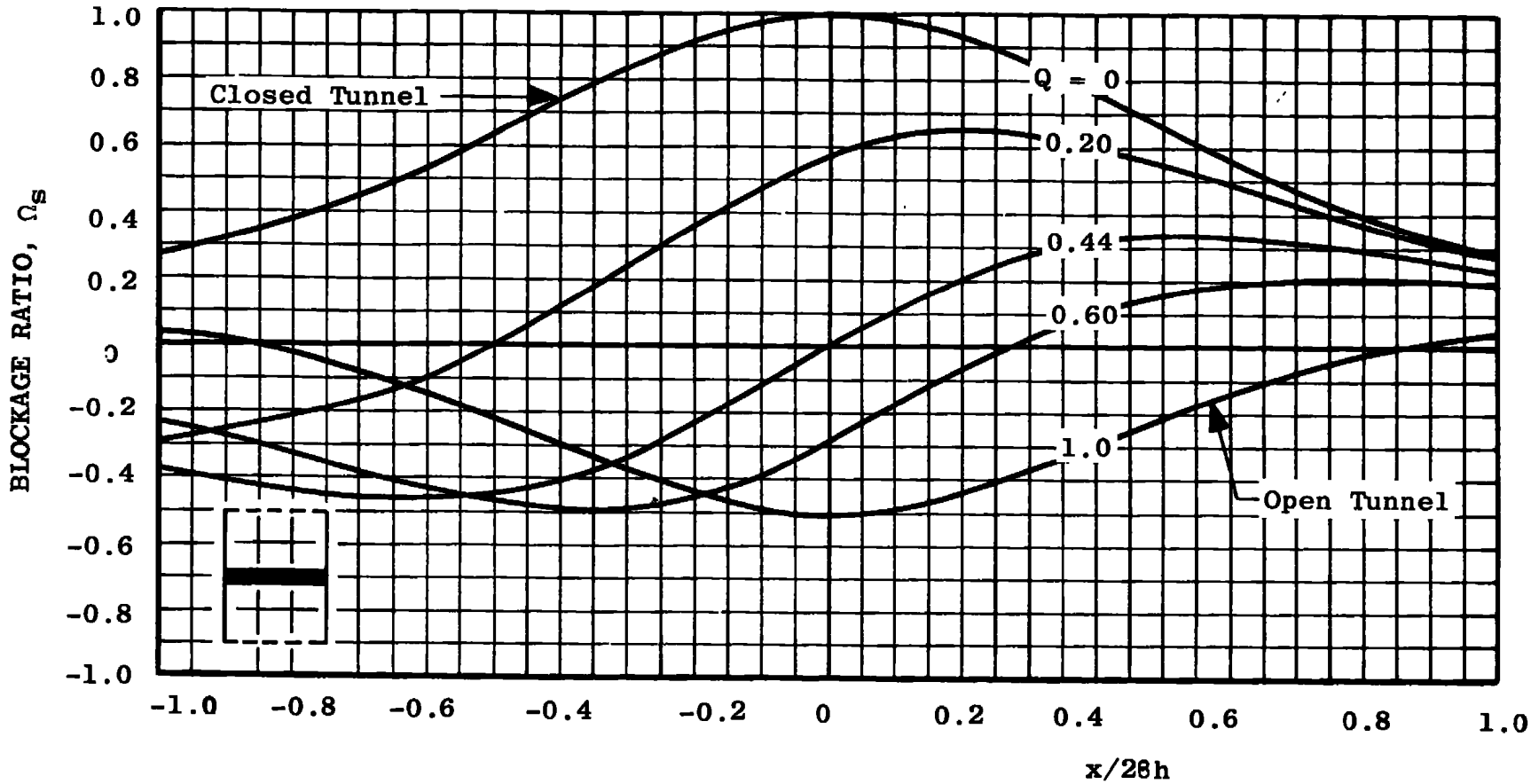

Fig. 3.3 Distribution of the Solid-Blockage Factor Ratio along a Two-Dimensional Perforated Tunnel

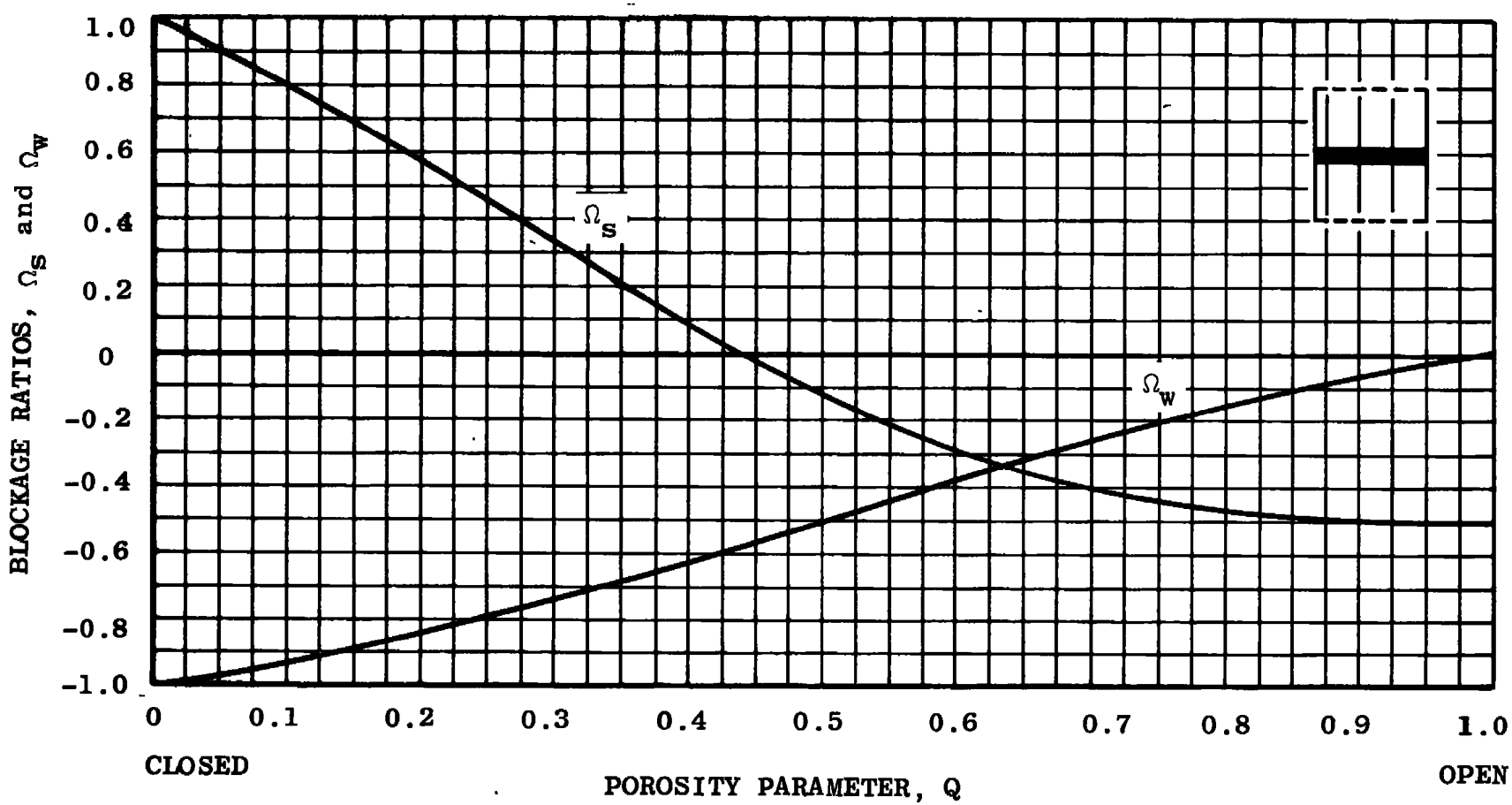

Fig. 3.4 Blockage Factor Ratios at x = 0 in a Two-Dimensional Perforated Tunnel

AEDC-TR-69-47

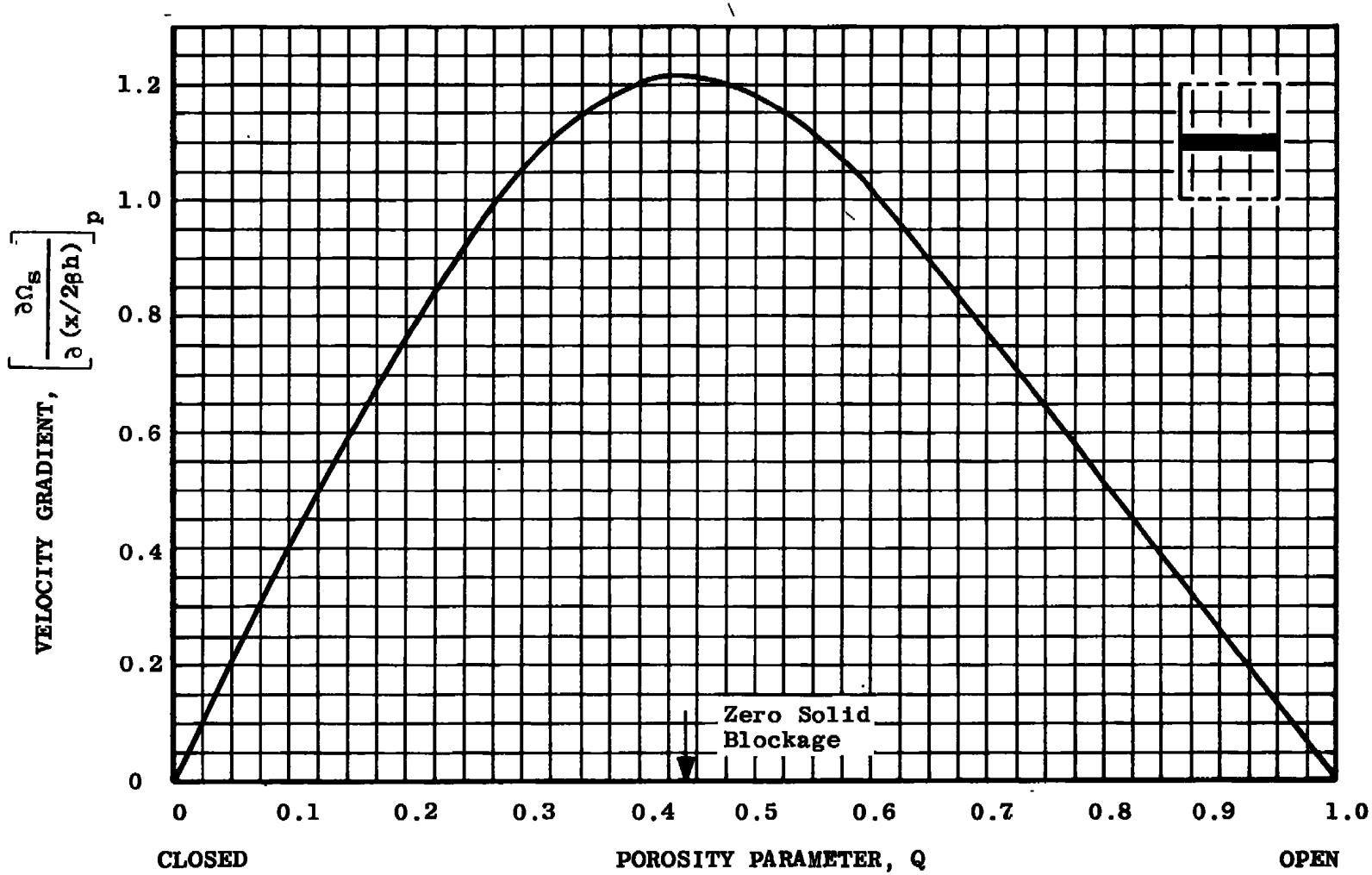

Fig. 3.5 Velocity Gradient due to Solid Blockage at x = 0 in a Two-Dimensional Perforated Tunnel

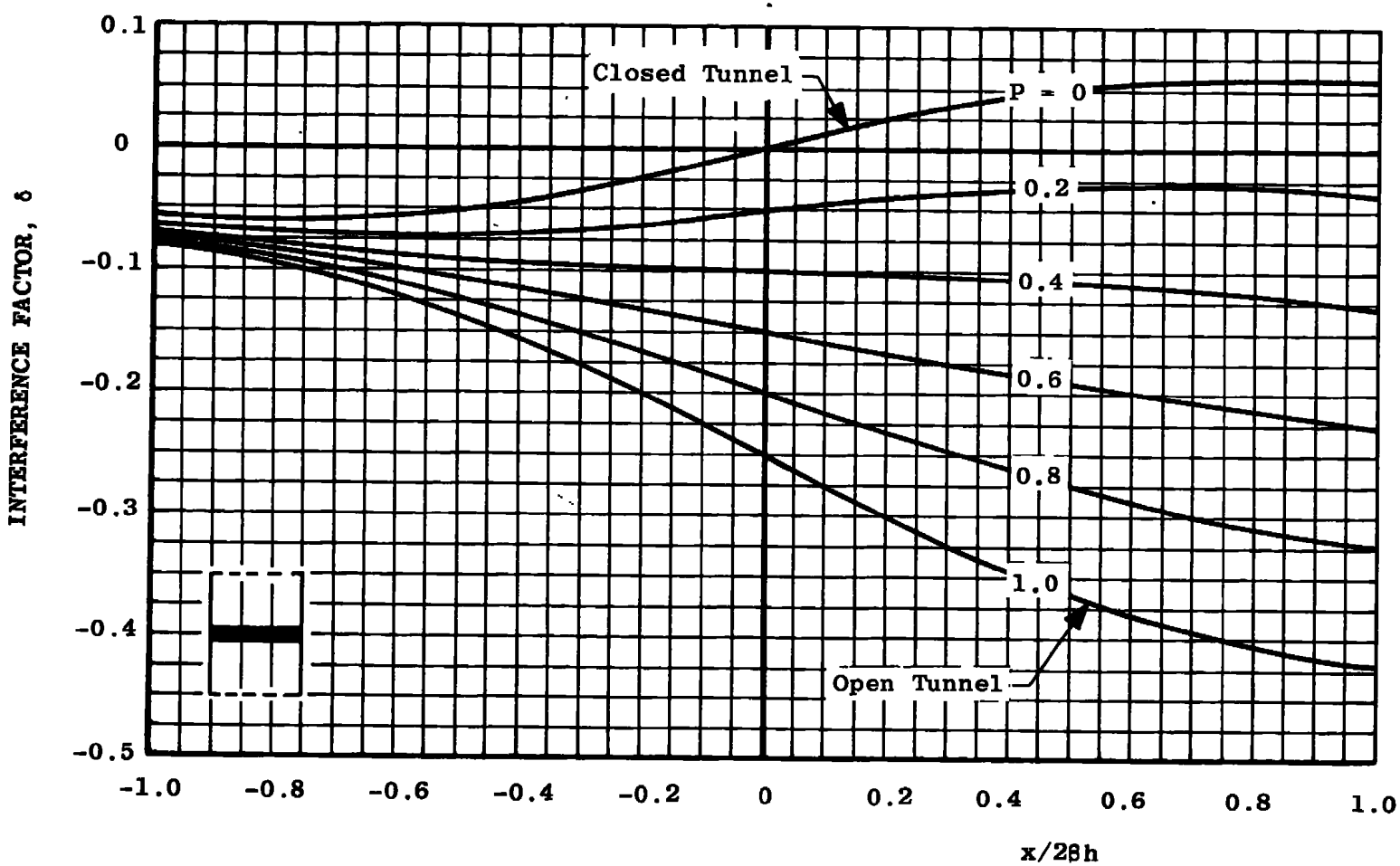

Fig. 3.6 Distribution of the Lift-Interference Factor along a Two-Dimensional Slotted Tunnel

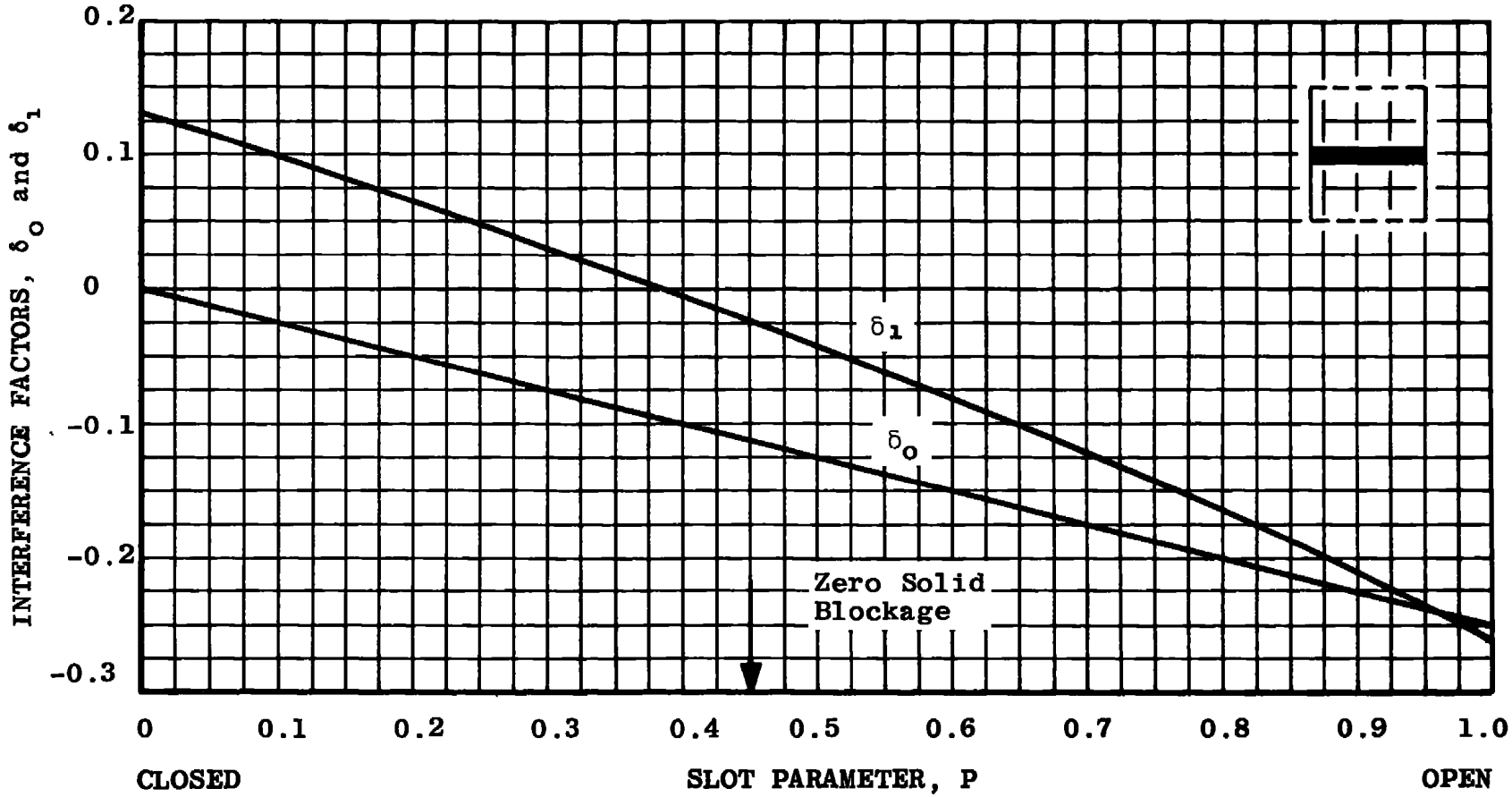

Fig. 3.7 Lift-Interference Factors at x = 0 in a Two-Dimensional Slotted Tunnel

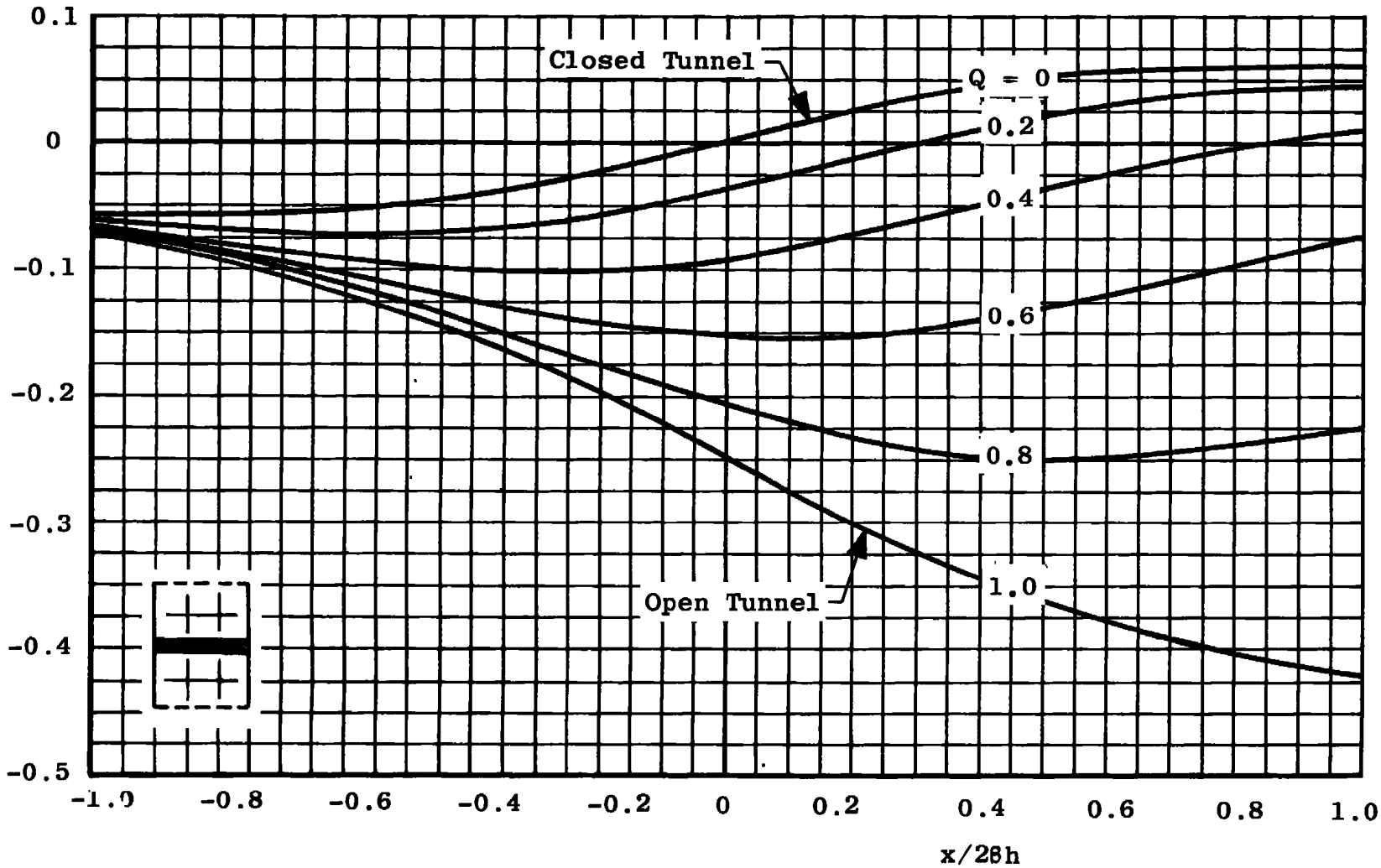

Fig. 3.8 Distribution of the Lift-Interference Factor along a Two-Dimensional Perforated Tunnel

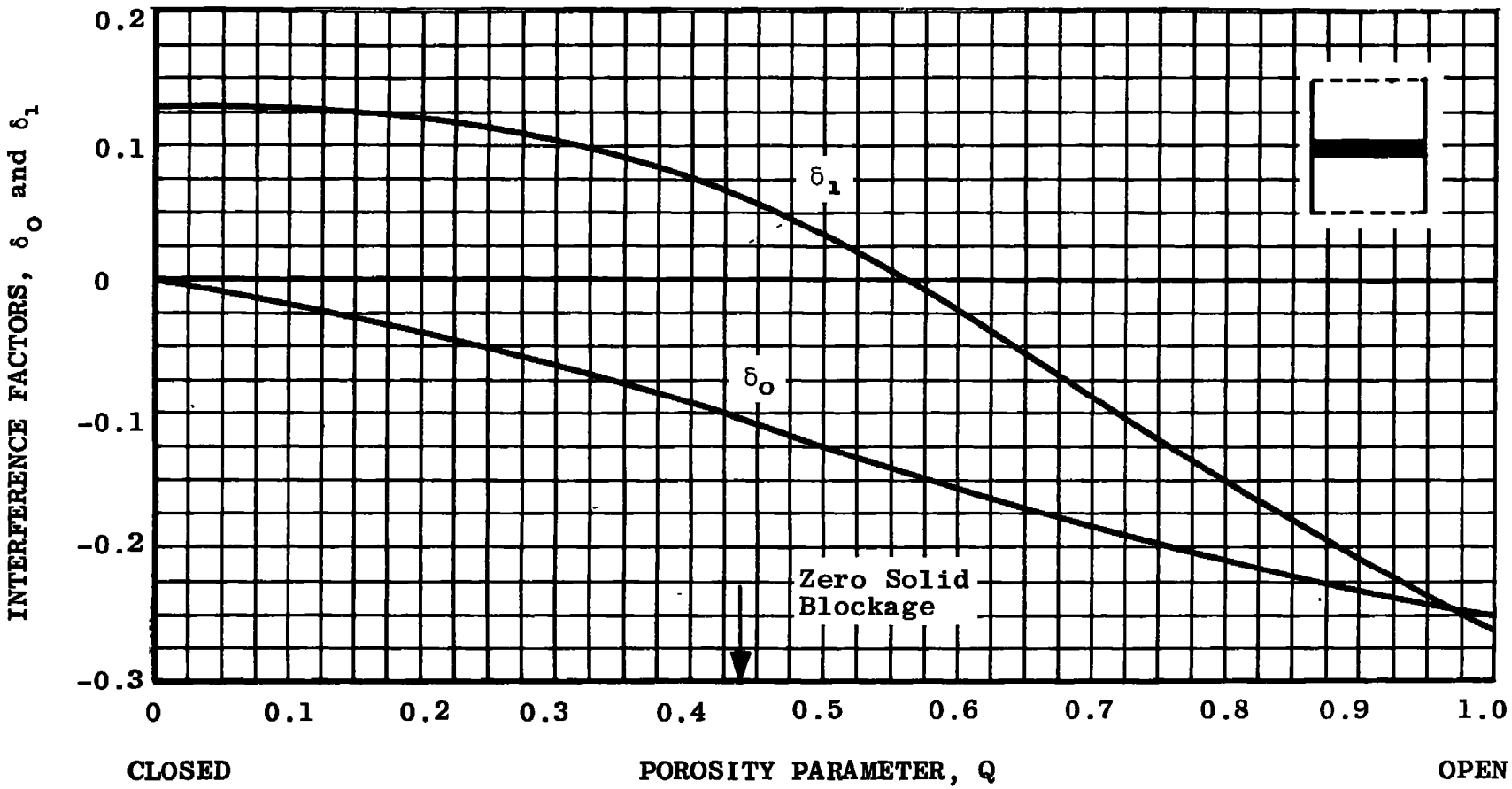

Fig. 3.9 Lift-Interference Factors at x = 0 in a Two-Dimensional Perforated Tunnel

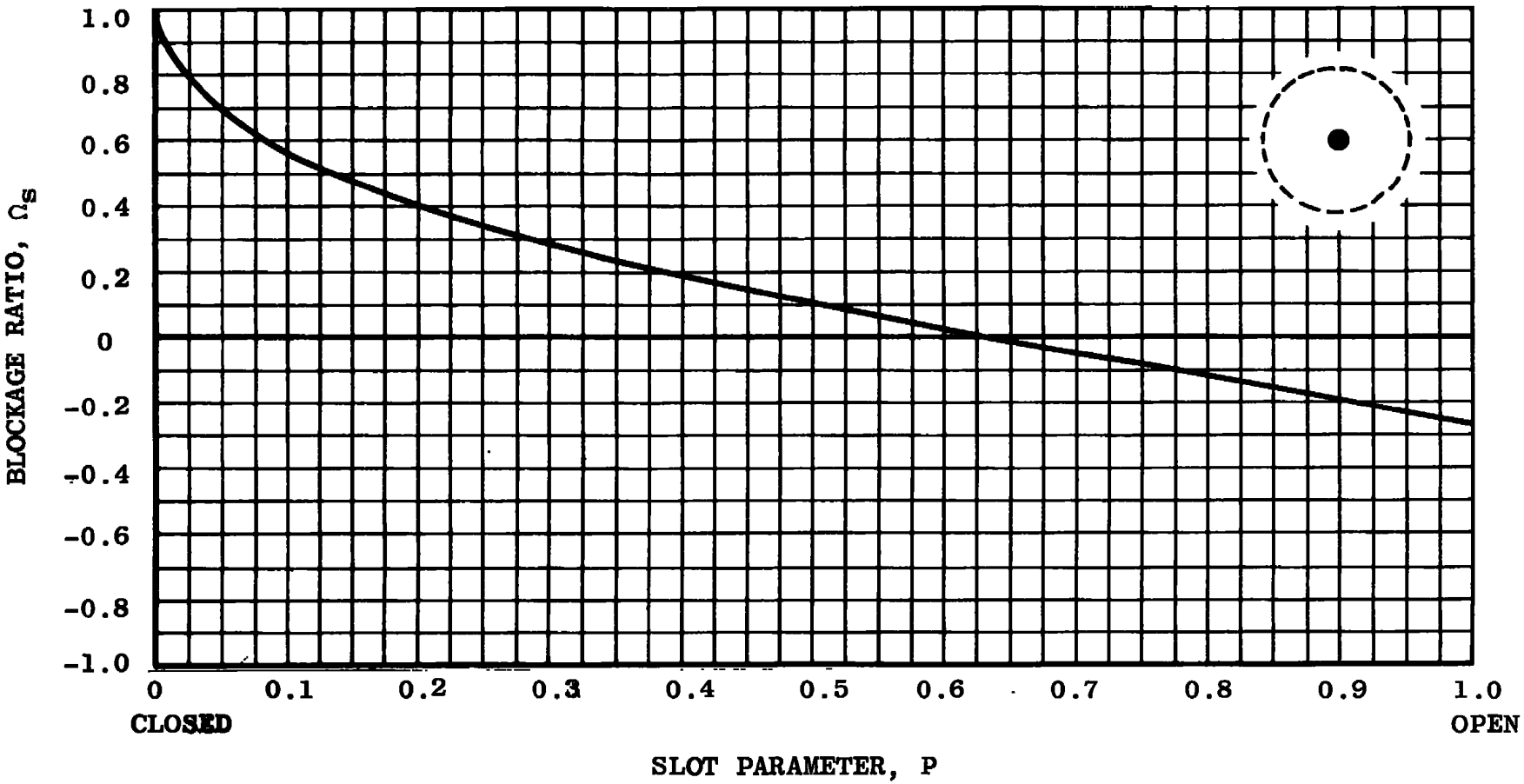

Fig. 4.1 Solid Blockage Factor Ratio at x = 0 in a Circular Slotted Tunnel

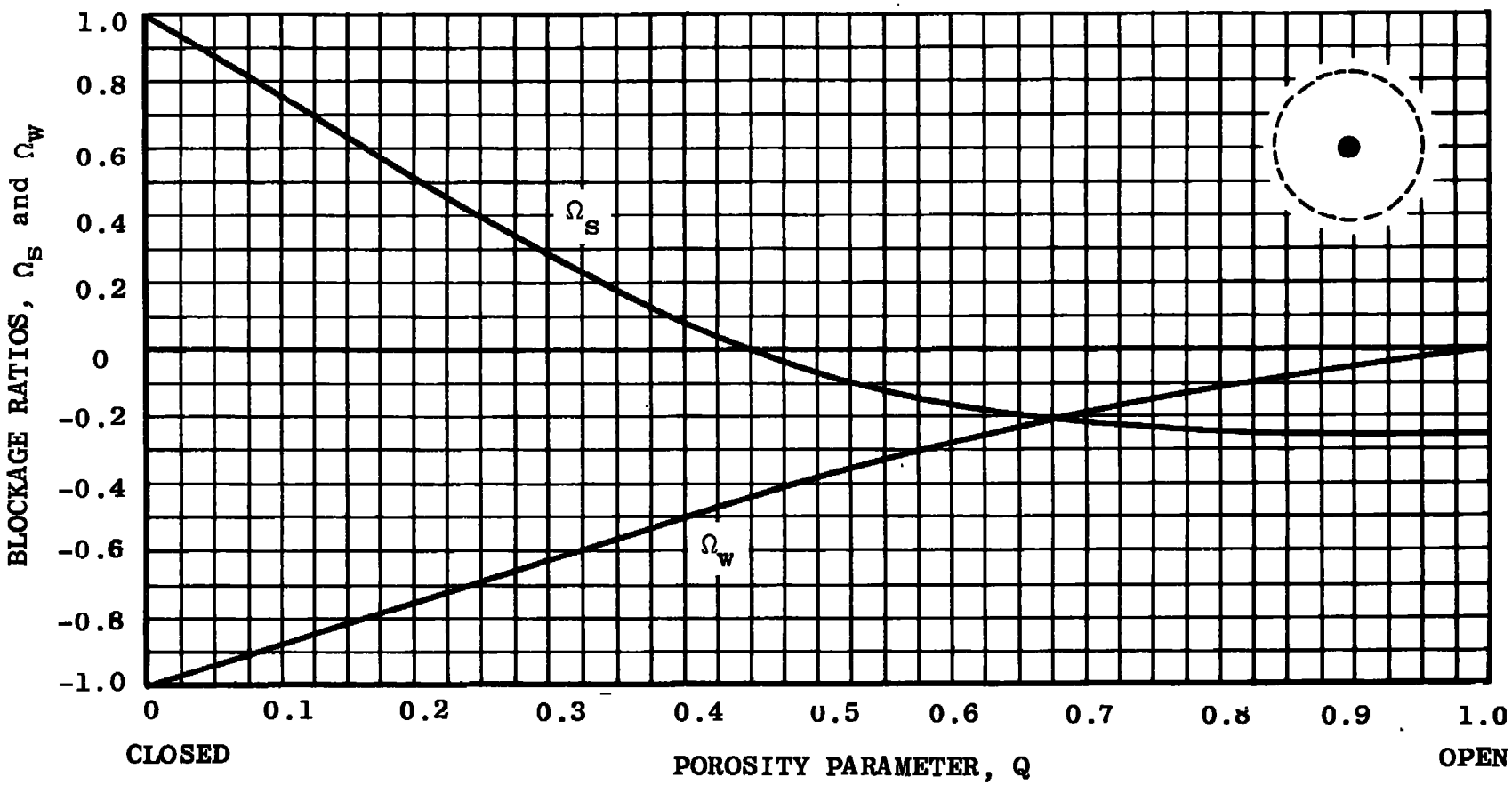

Fig. 4.2 Blockage Factor Ratios at x = 0 in a Circular Perforated Tunnel

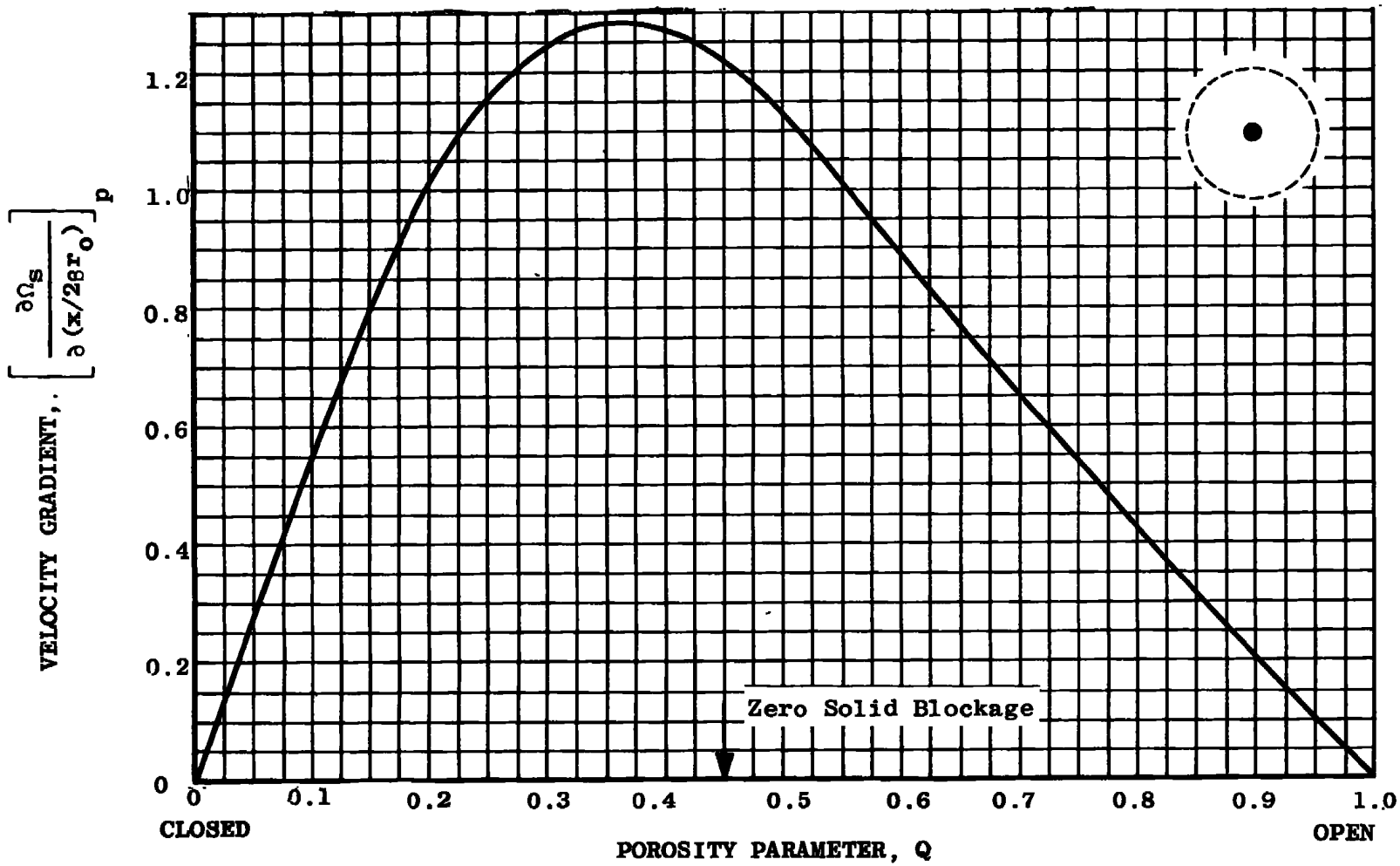

Fig. 4.3 Velocity Gradient due to Solid Blockage at x = 0 in a Circular Perforated Tunnel

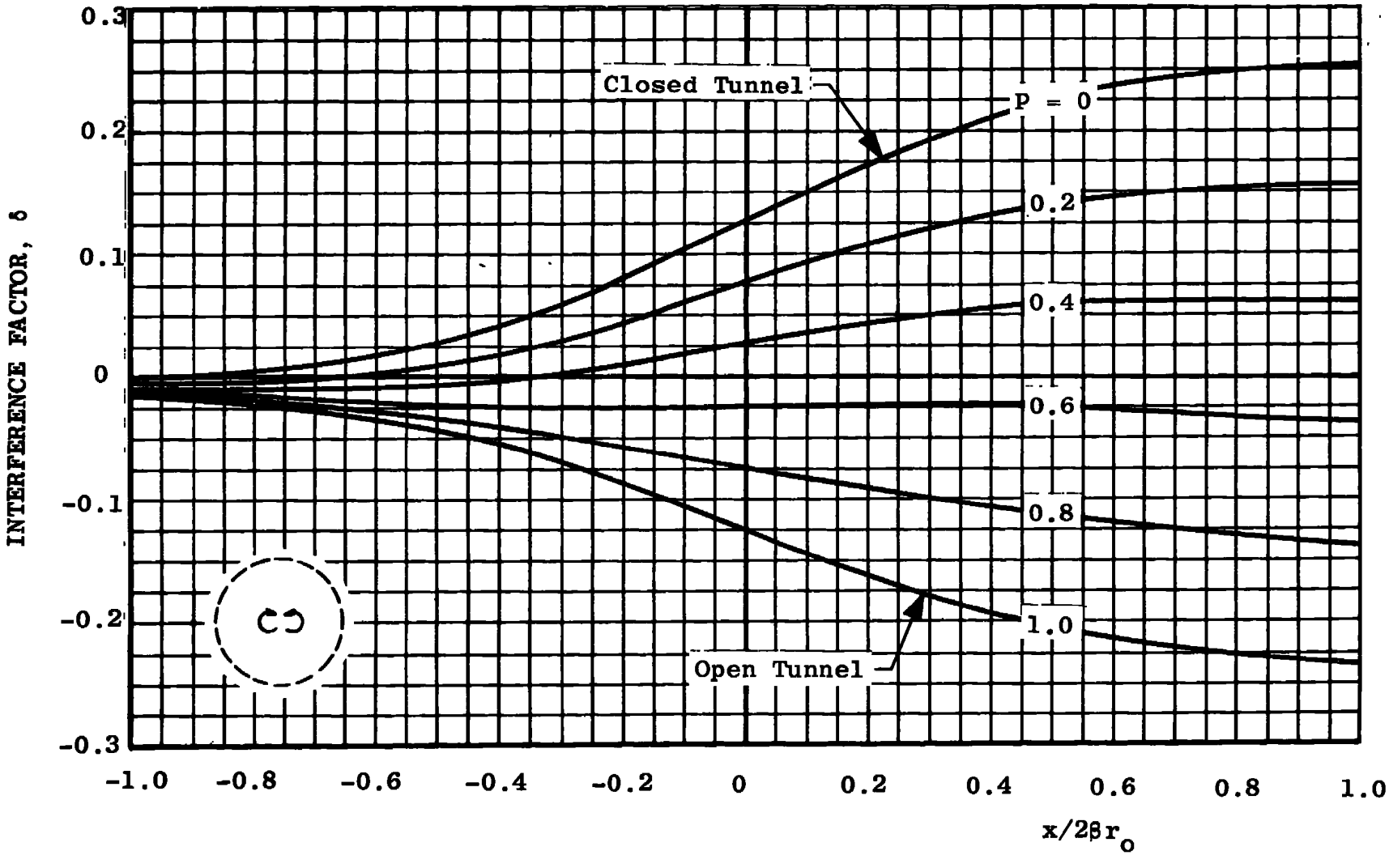

Fig. 4.4 Distribution of the Lift-Interference Factor along a Circular Slotted Tunnel

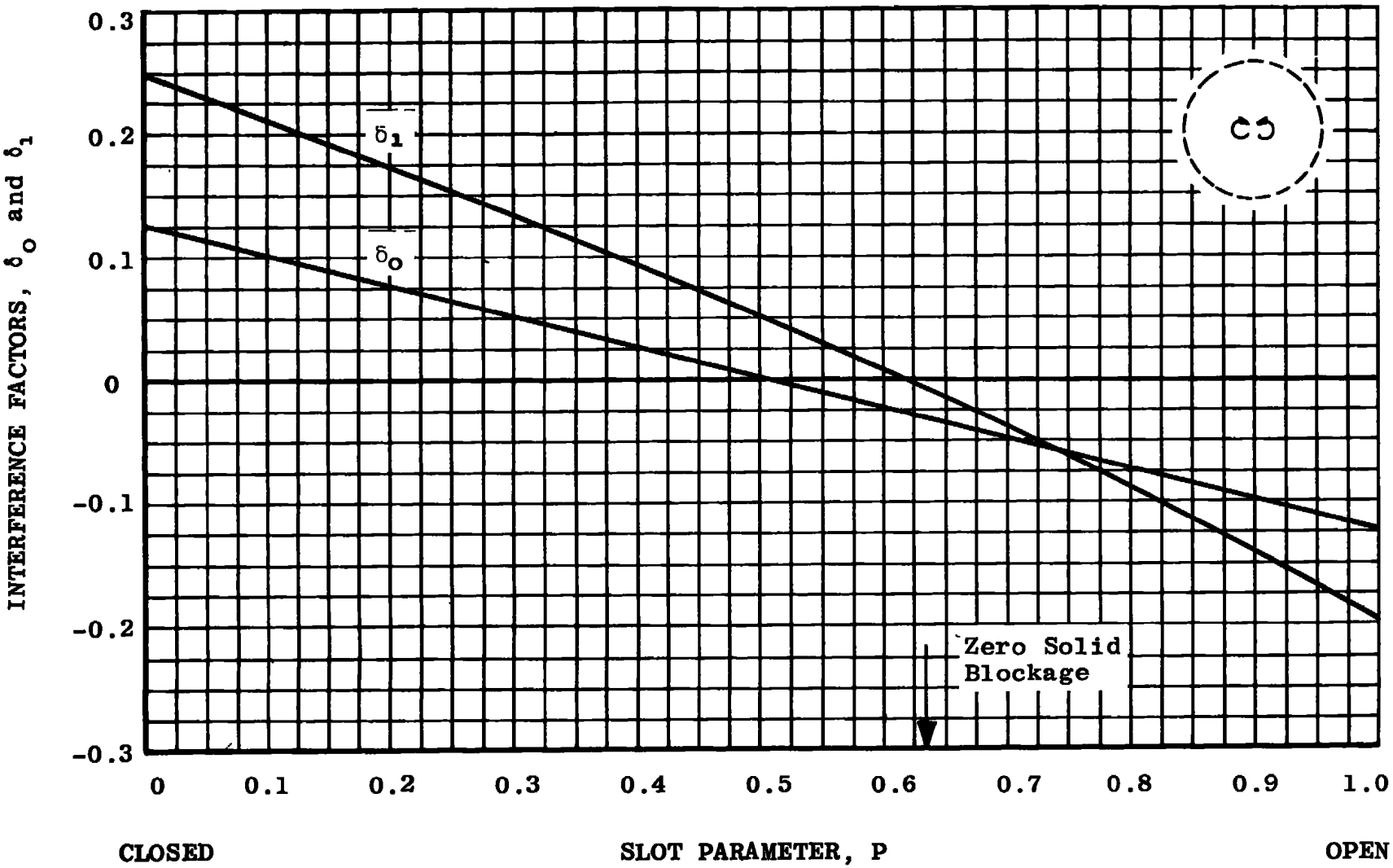

Fig. 4.5 Lift-Interference Factors at x = 0 in a Circular Slotted Tunnel

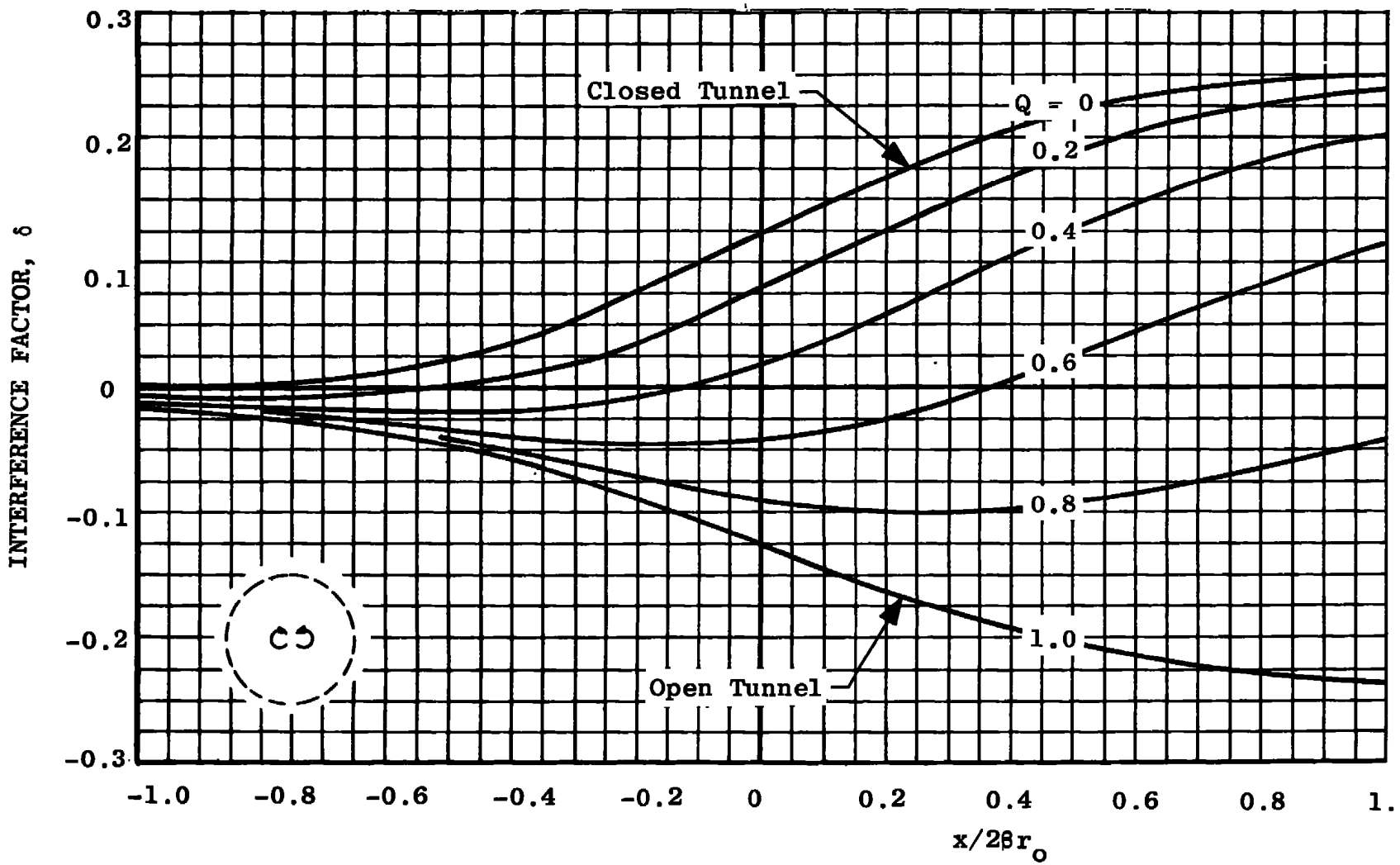

Fig. 4.6 Distribution of the Lift-Interference Factor along a Circular Perforated Tunnel

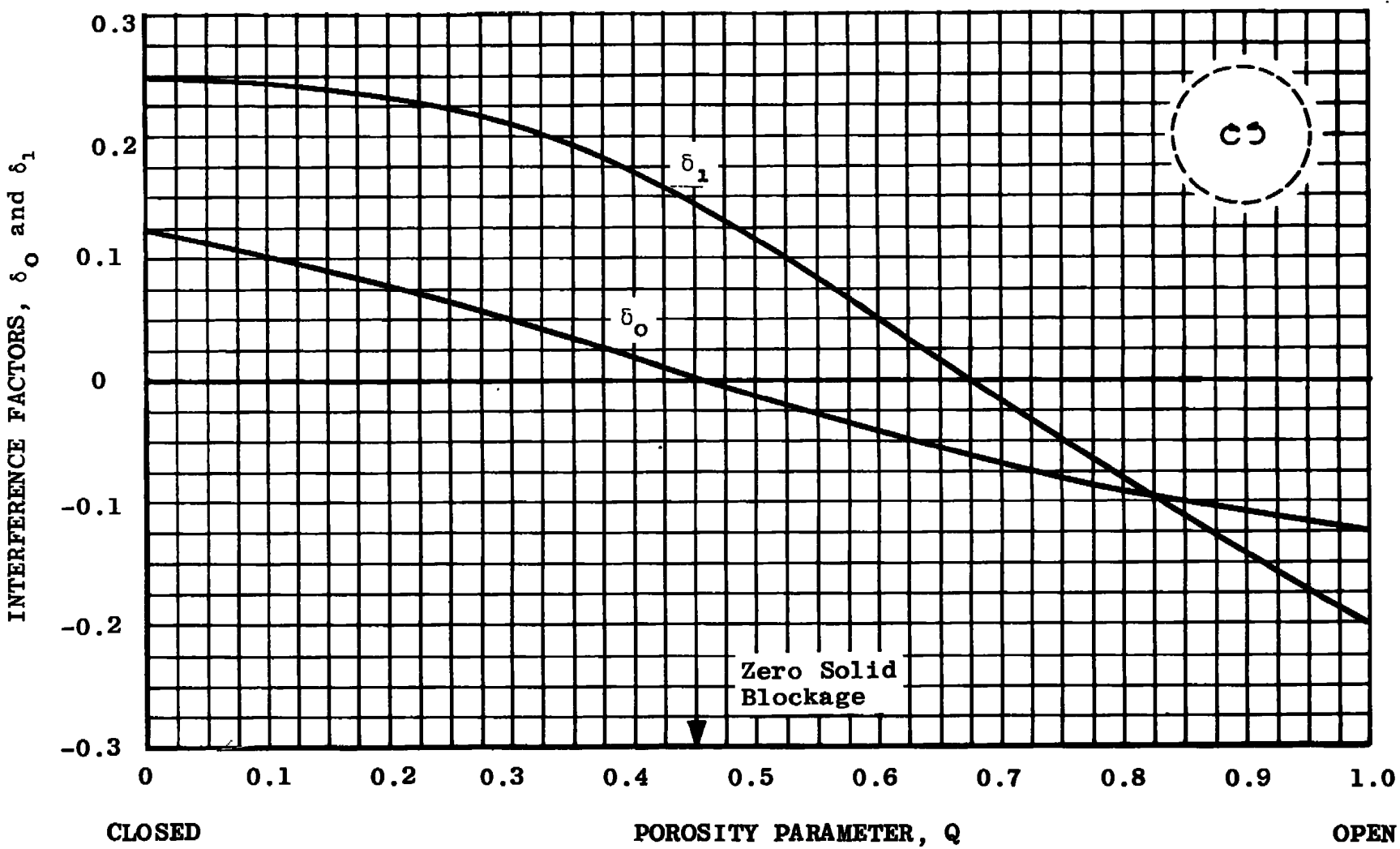

Fig. 4.7 Lift-Interference Factors at x = 0 in a Circular Perforated Tunnel

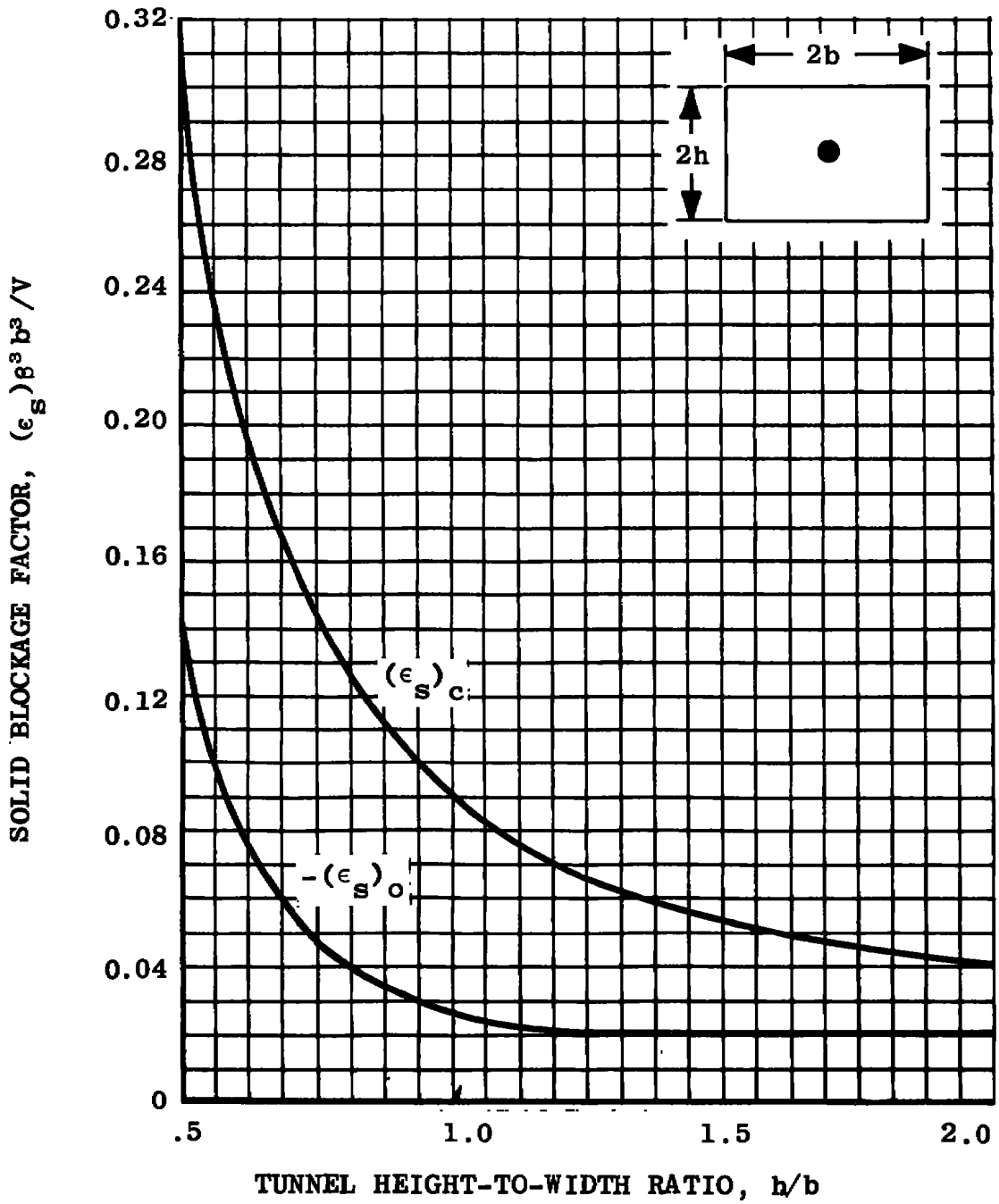

Fig. 5.1 Solid-Blockage Factor at x = 0 in Rectangular Closed and Open Tunnels

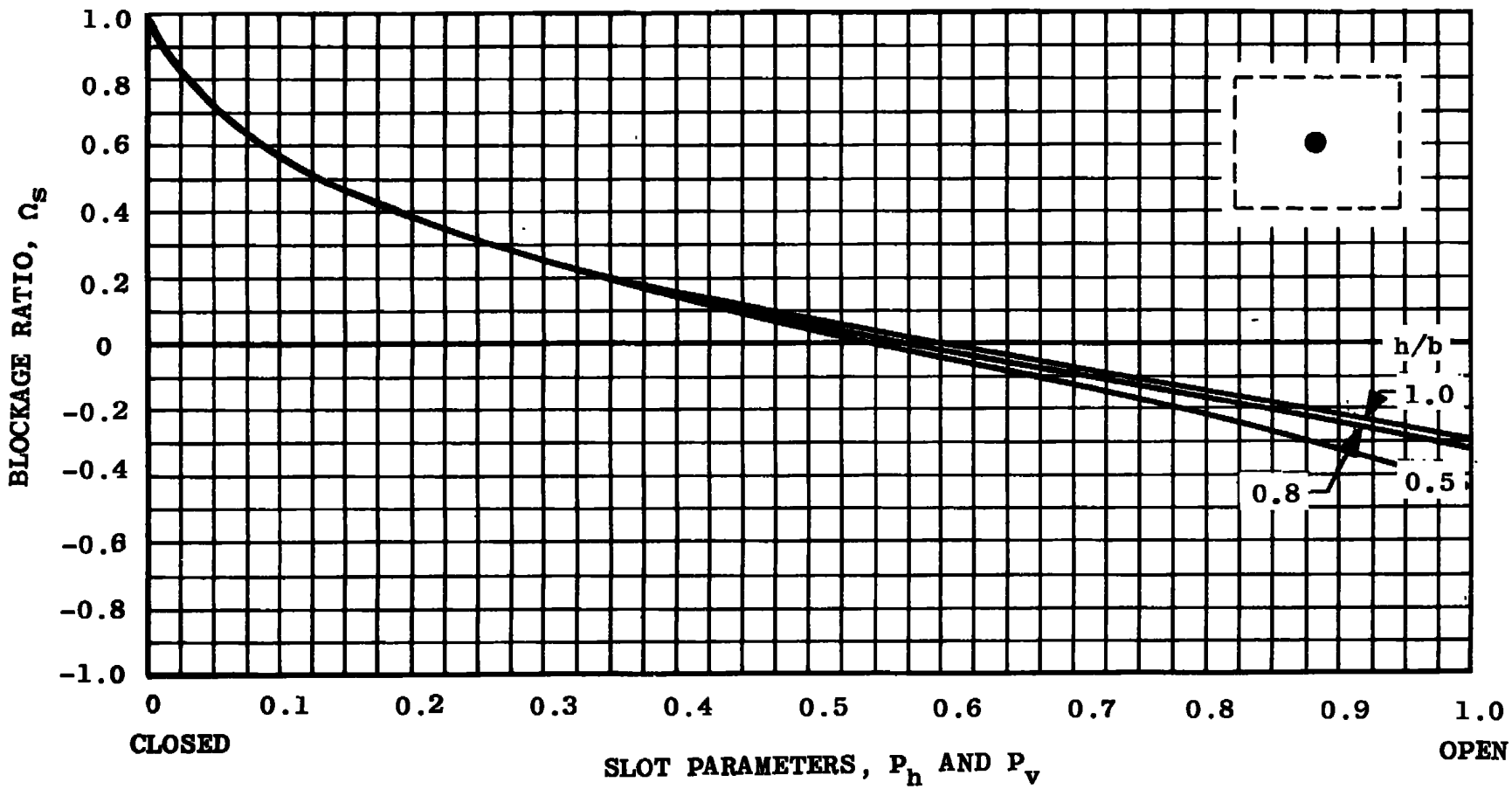

Fig. 5.2 Solid Blockage Factor Ratio at x = 0 in Rectangular Slotted Tunnels

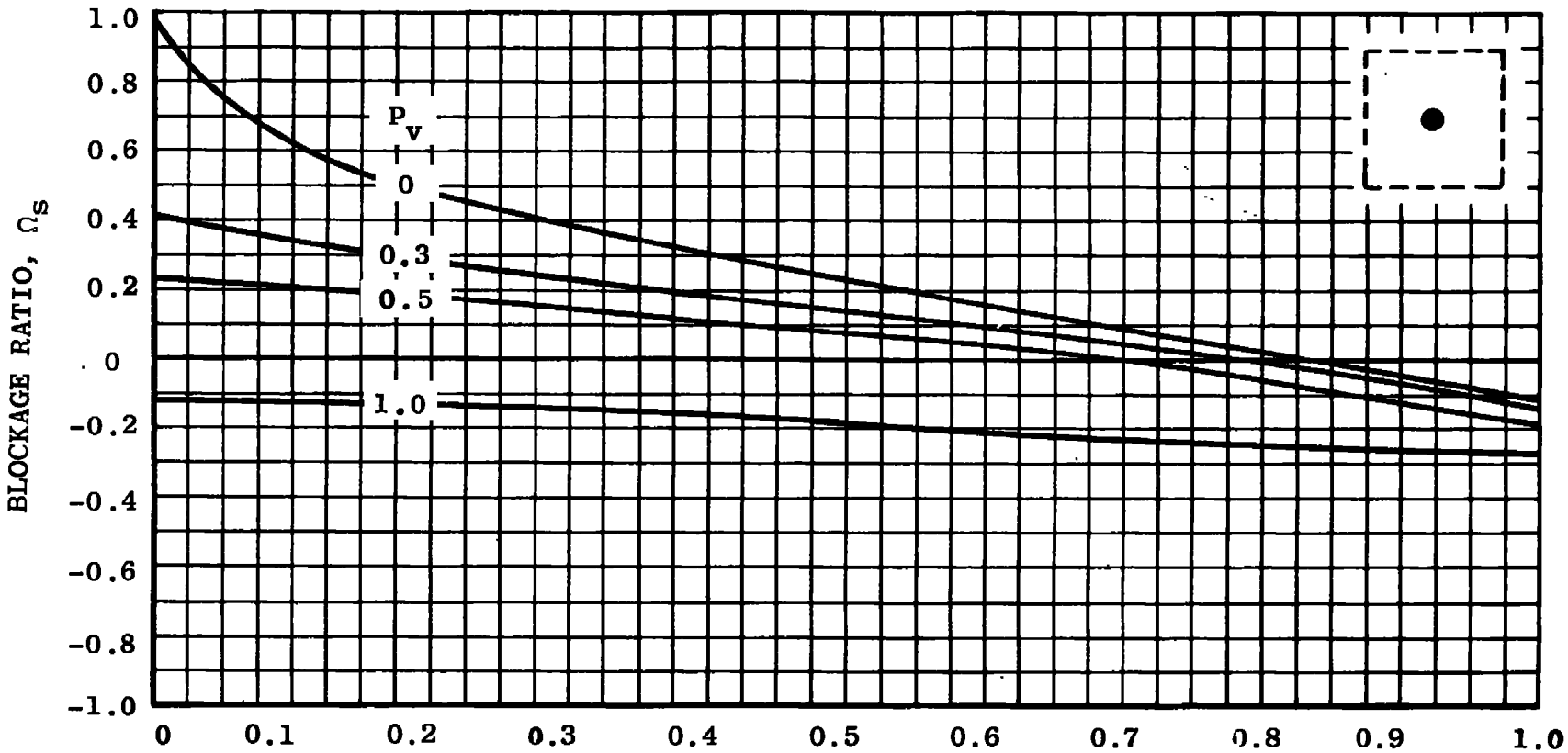

a. h/b = 1.0

Fig. 5.3 Solid Blockage Factor Ratio at x = 0 versus P_h for Various Values of P_v in a Rectangular Slotted Tunnel

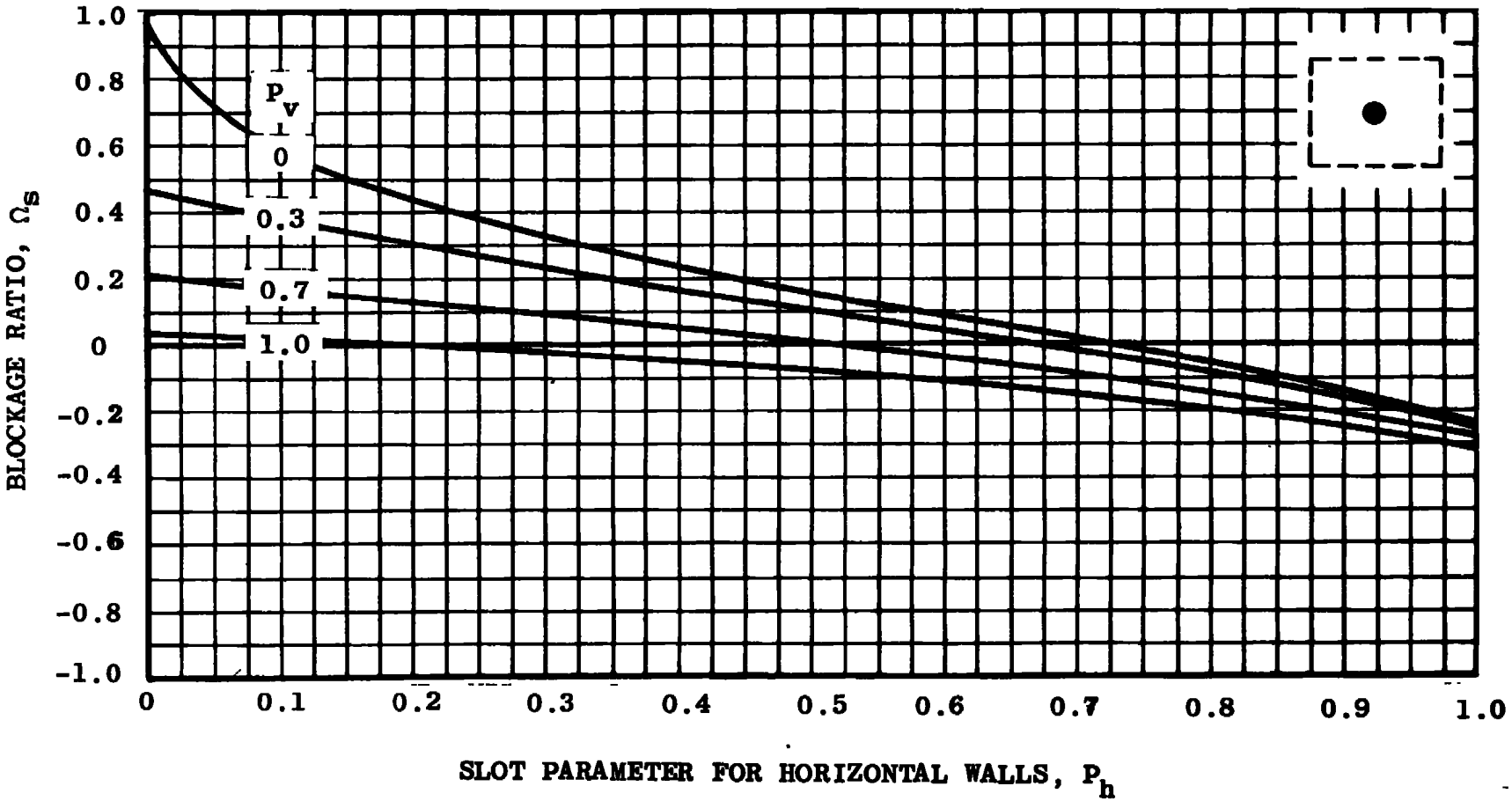

b. h/b = 0.8

Fig. 5.3 Continued

c. h/b = 0.5

Fig. 5.3 Concluded

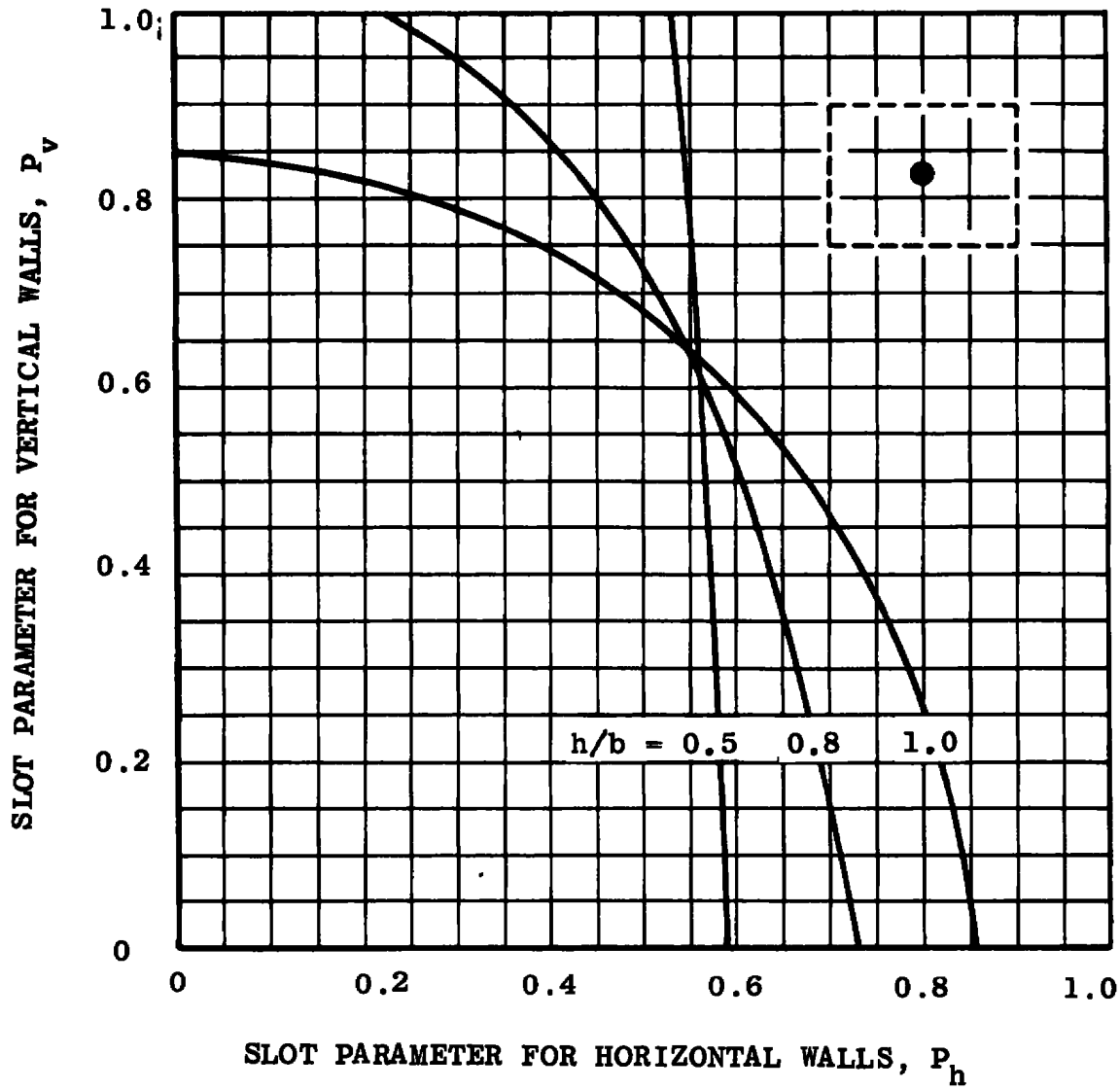

Fig. 5.4 Zero Solid-Blockage Interference Curves In Rectangular Slotted Tunnels

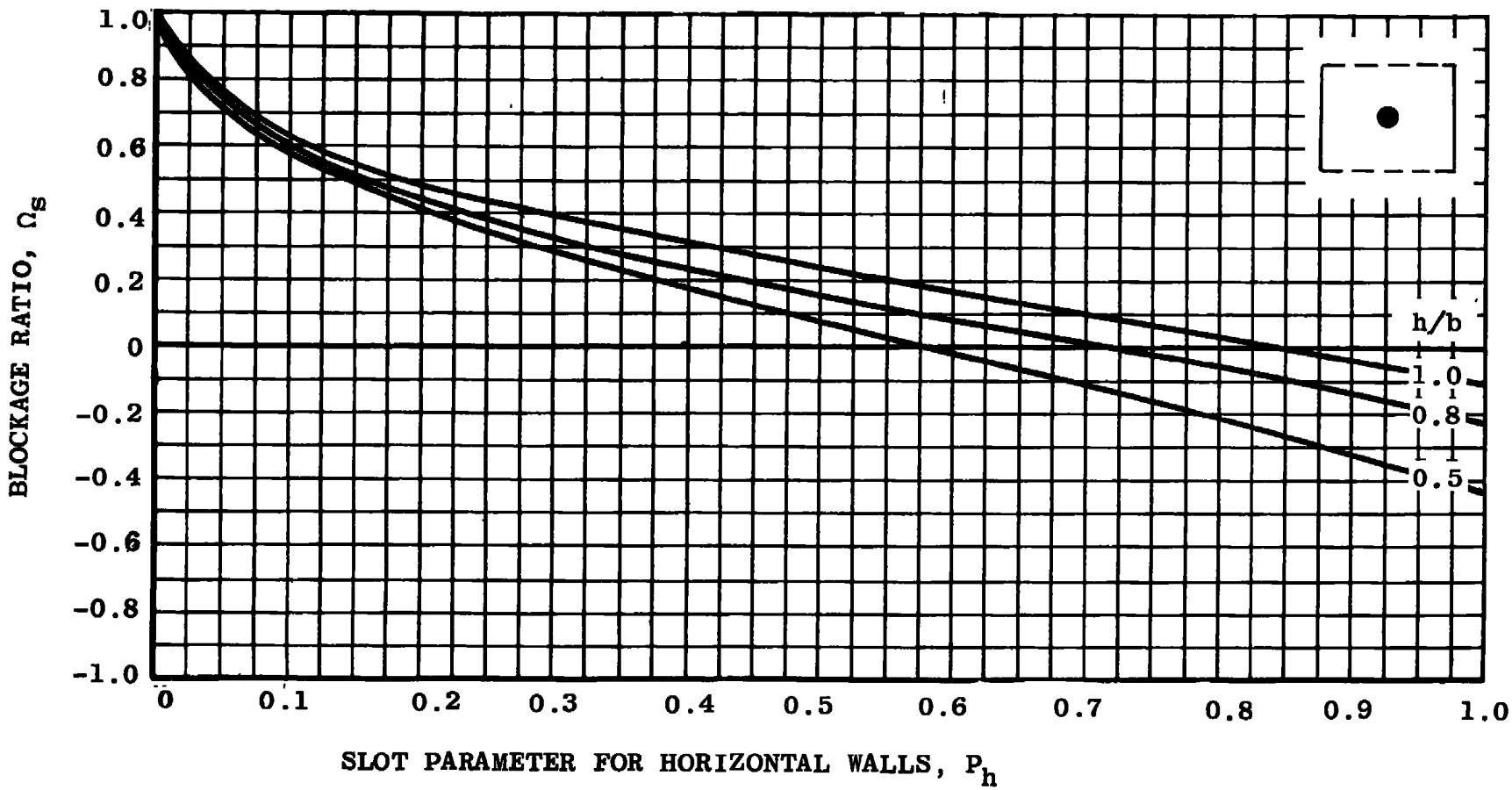

Fig. 5.5 Solid-Blockage Factor Ratio at x = 0 in Rectangular Tunnels with Solid Vertical Walls and Slotted Horizontal Walls

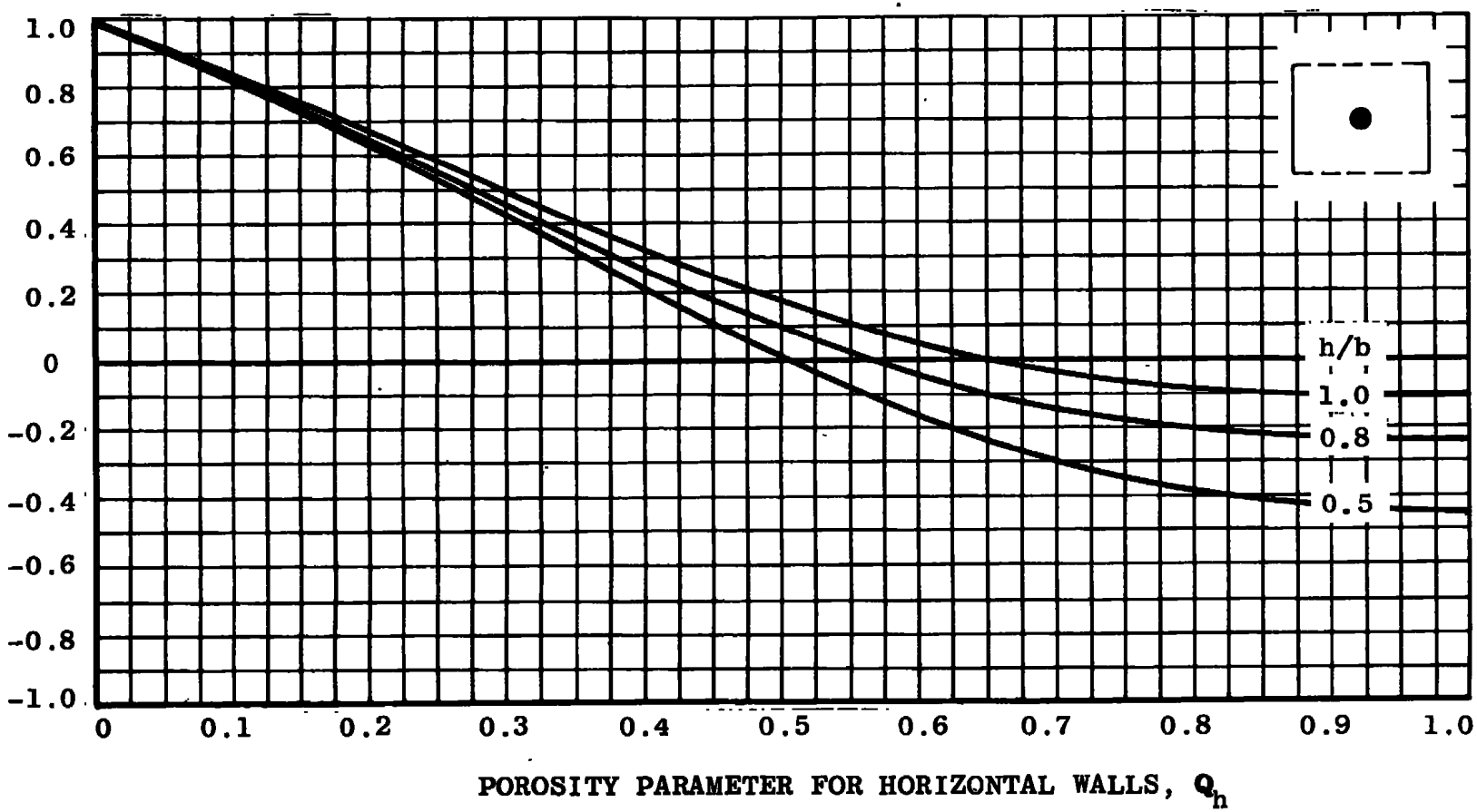

Fig. 5.6 Solid-Blockage Factor Ratio at x = 0 in Rectangular Tunnels with Solid Vertical Walls and Perforated Horizontal Walls

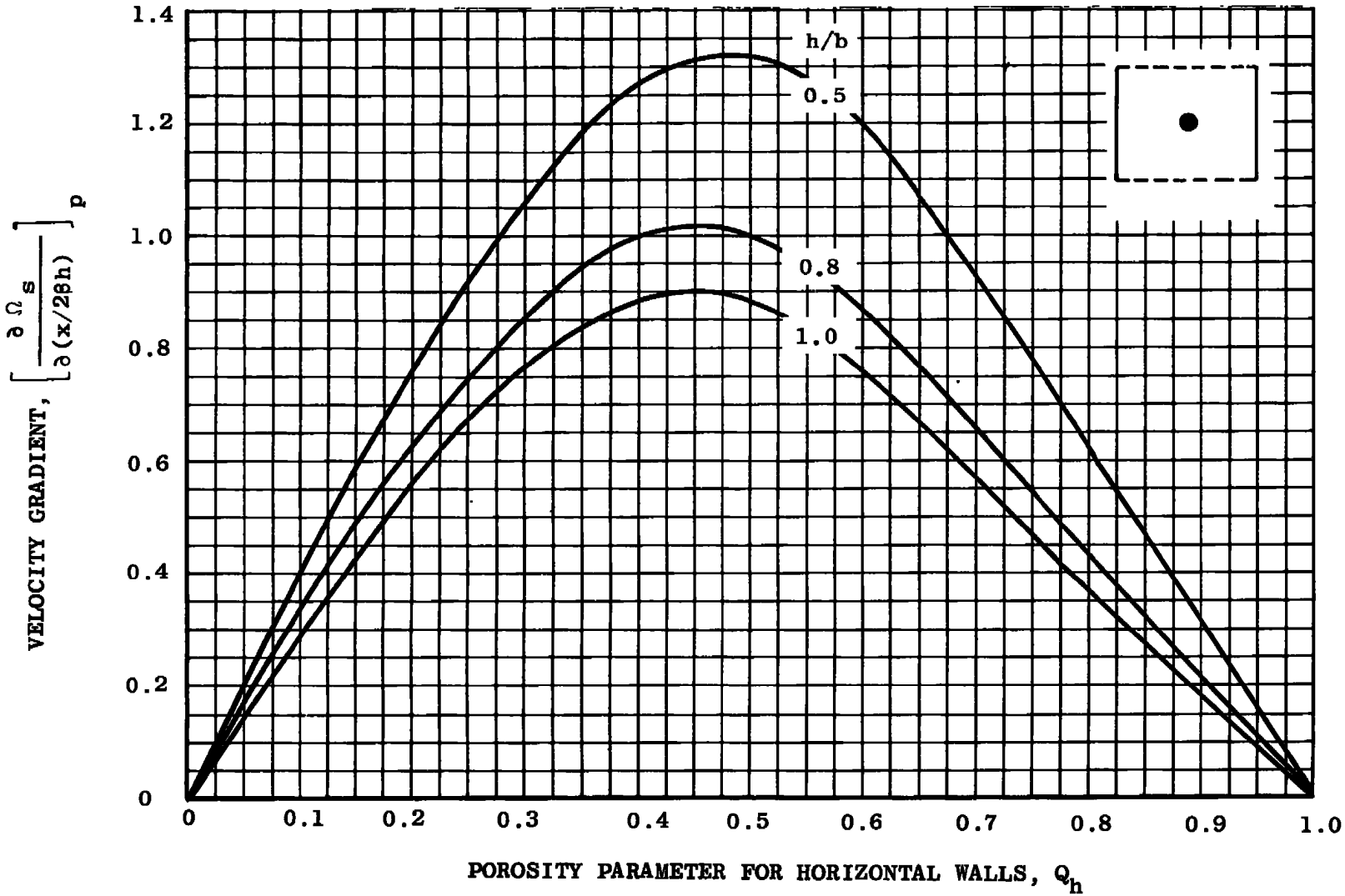

Fig. 5.7 Velocity Gradient due to Solid Blockage at x = 0 in Rectangular Tunnels with Solid Vertical Walls and Perforated Horizontal Walls

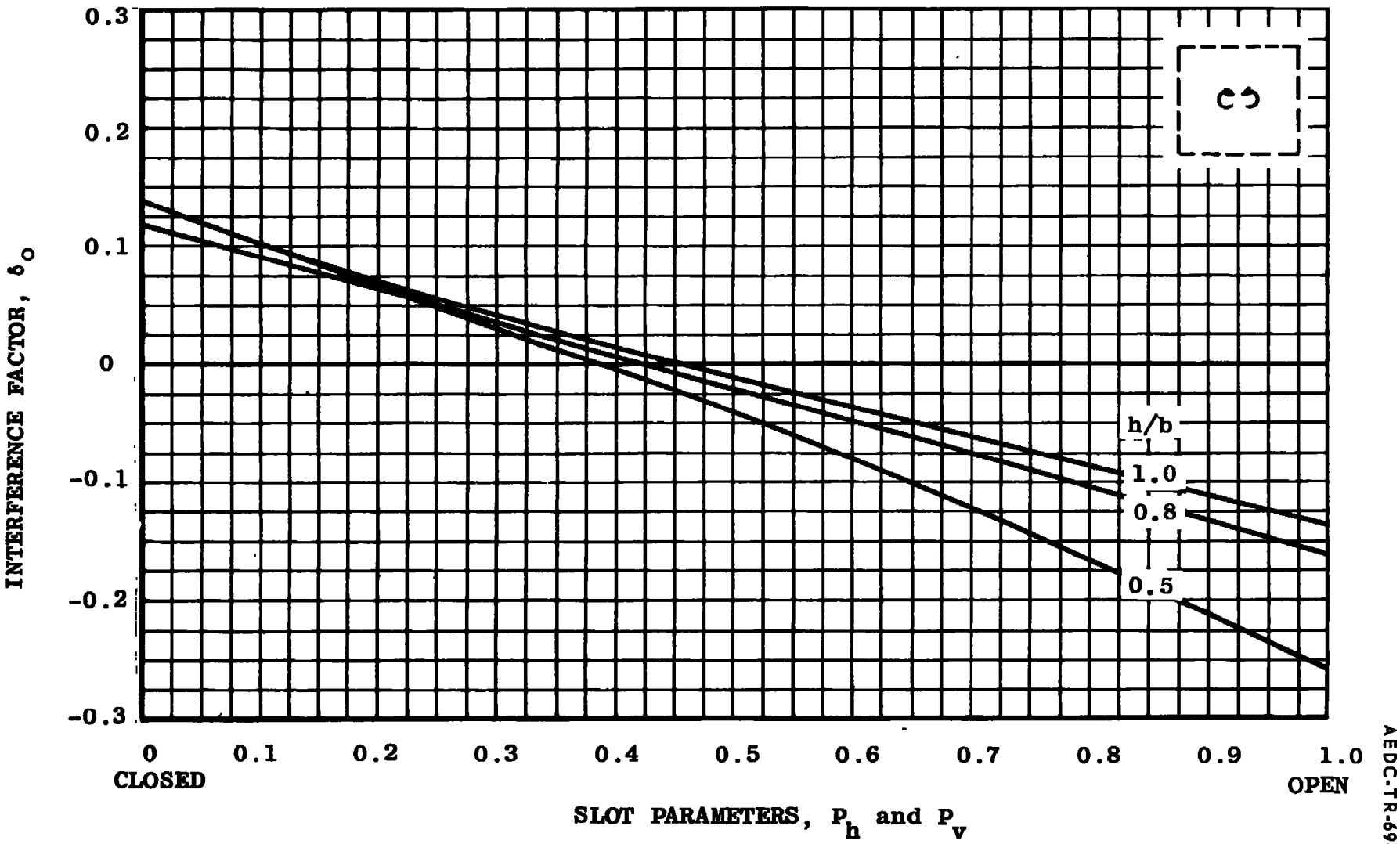

Fig. 5.8 Lift-Interference Factor at x = 0 in Rectangular Slotted Tunnels

AEDC-TR-69-47

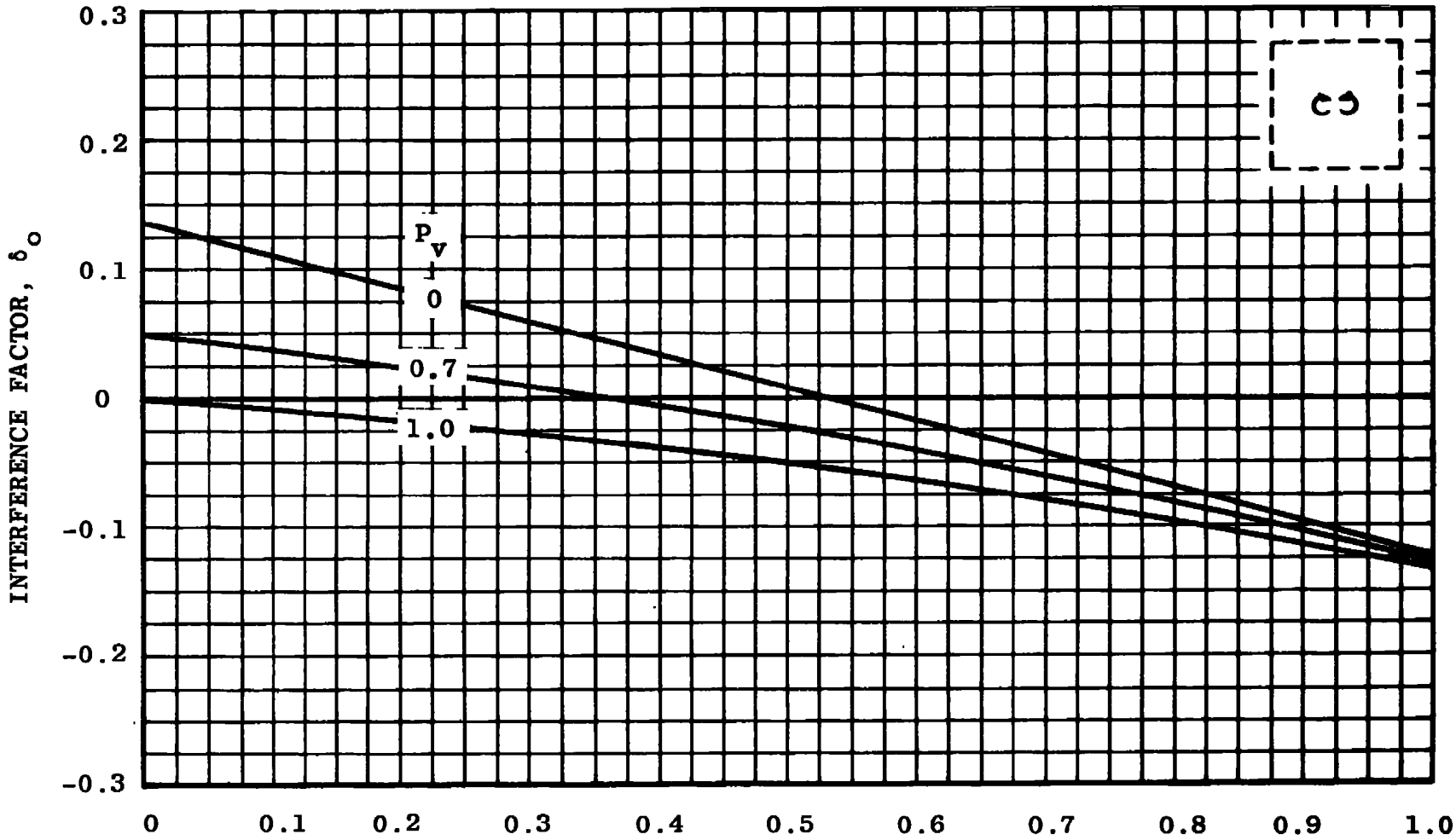

a. h/b = 1.0

Fig. 5.9 Lift-Interference Factor at x = 0 versus P_h for Various Values of P_v in a Rectangular Slotted Tunnel

b. h/b = 0.8

Fig. 5.9 Continued

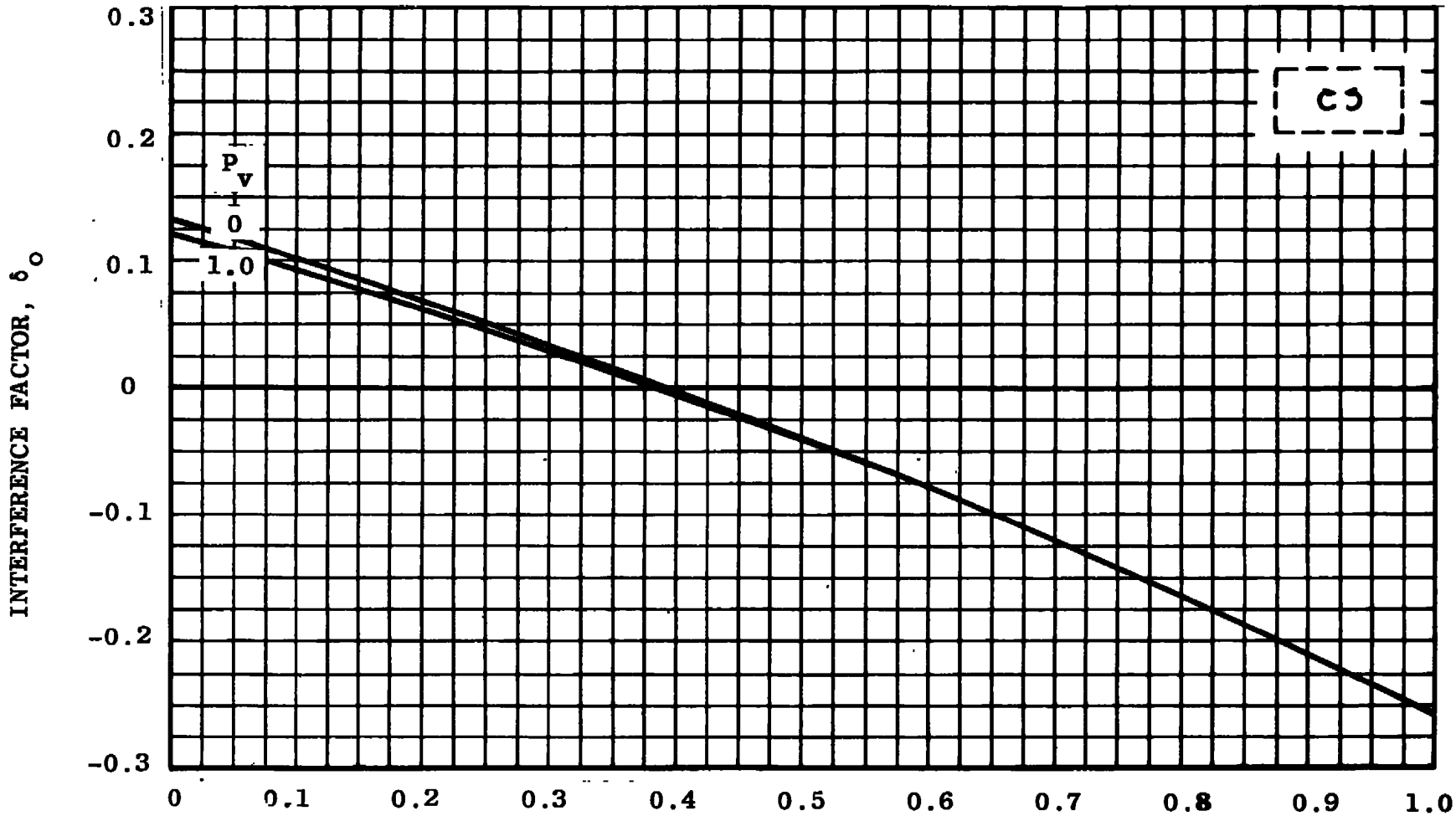

c. h/b = 0.5

Fig. 5.9 Concluded

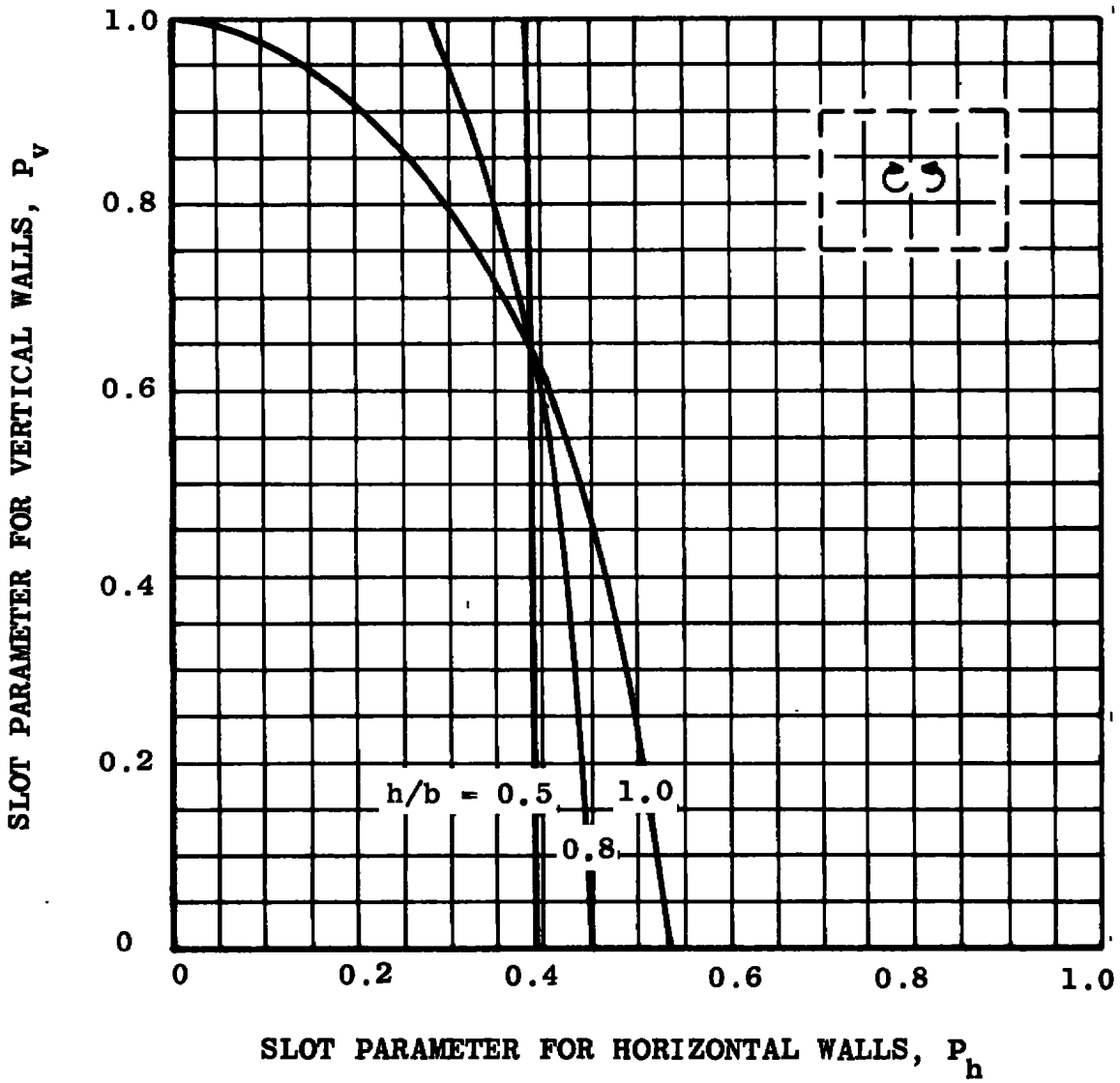

Fig. 5.10 Zero Lift-Interference Curves in Rectangular Slotted Tunnels

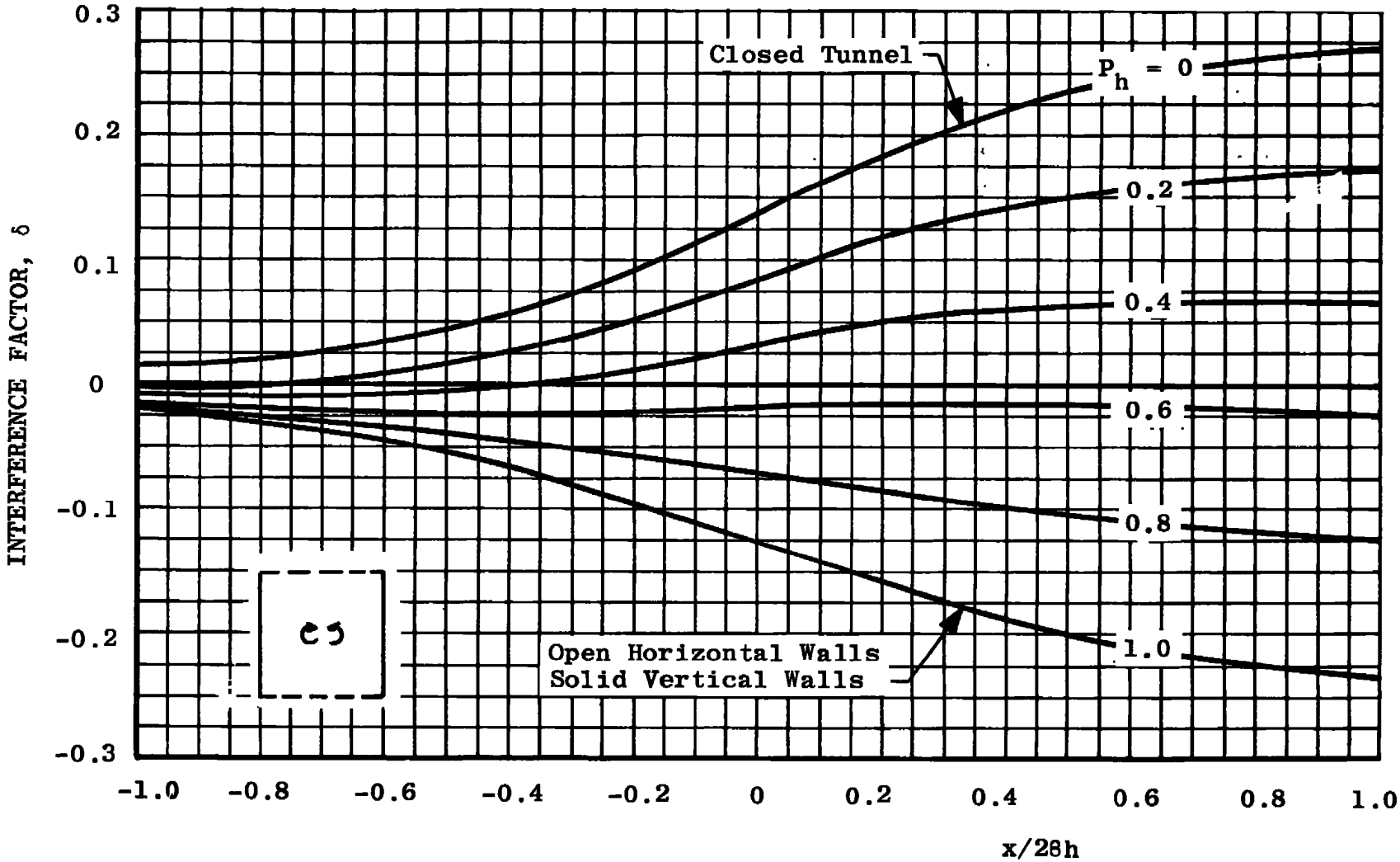

a. h/b = 1.0

Fig. 5.11 Distribution of the Lift-Interference Factor along a Rectangular Tunnel with Solid Vertical Walls and Slotted Horizontal Walls

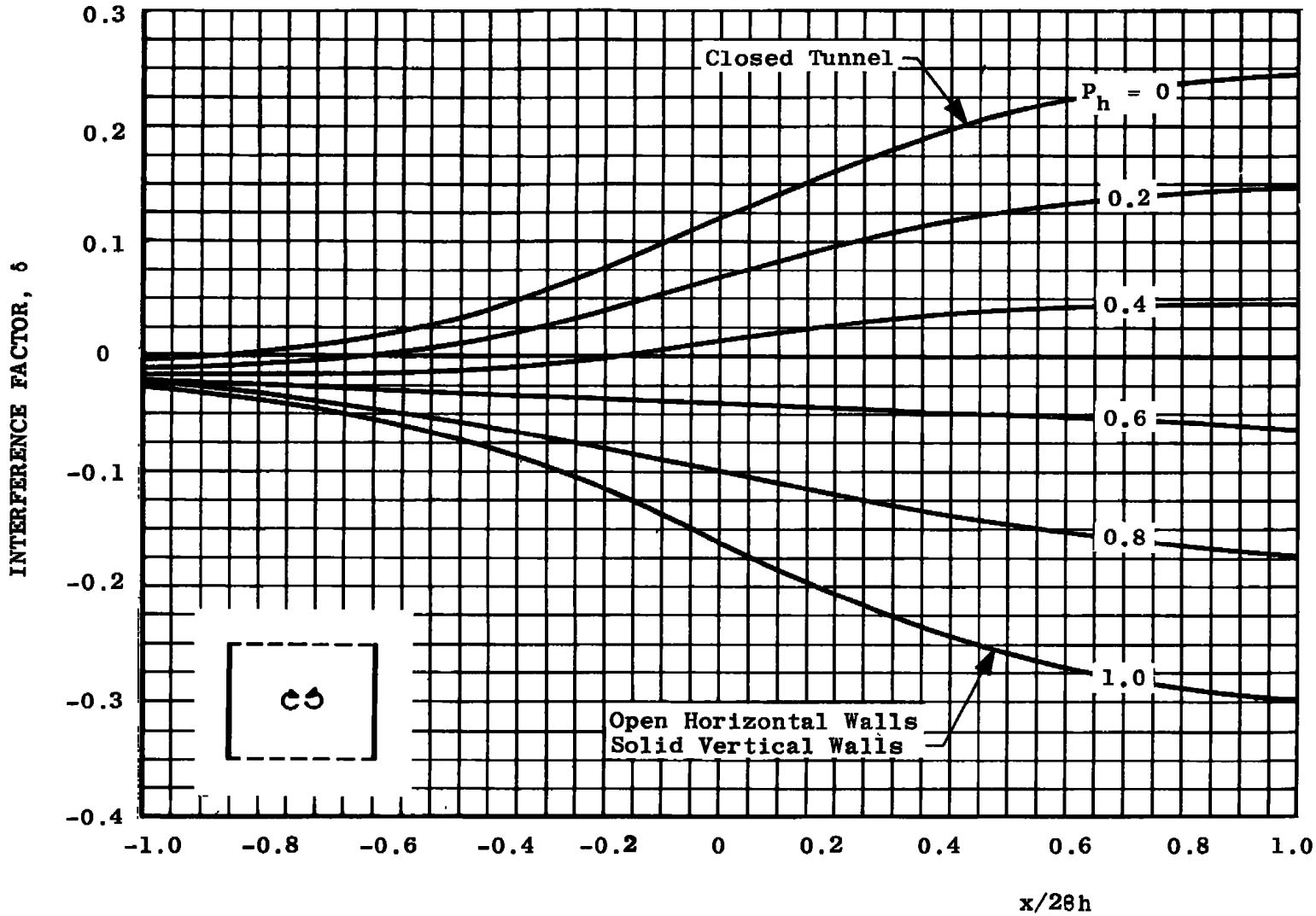

b. h/b = 0.8

Fig. 5.11 Continued

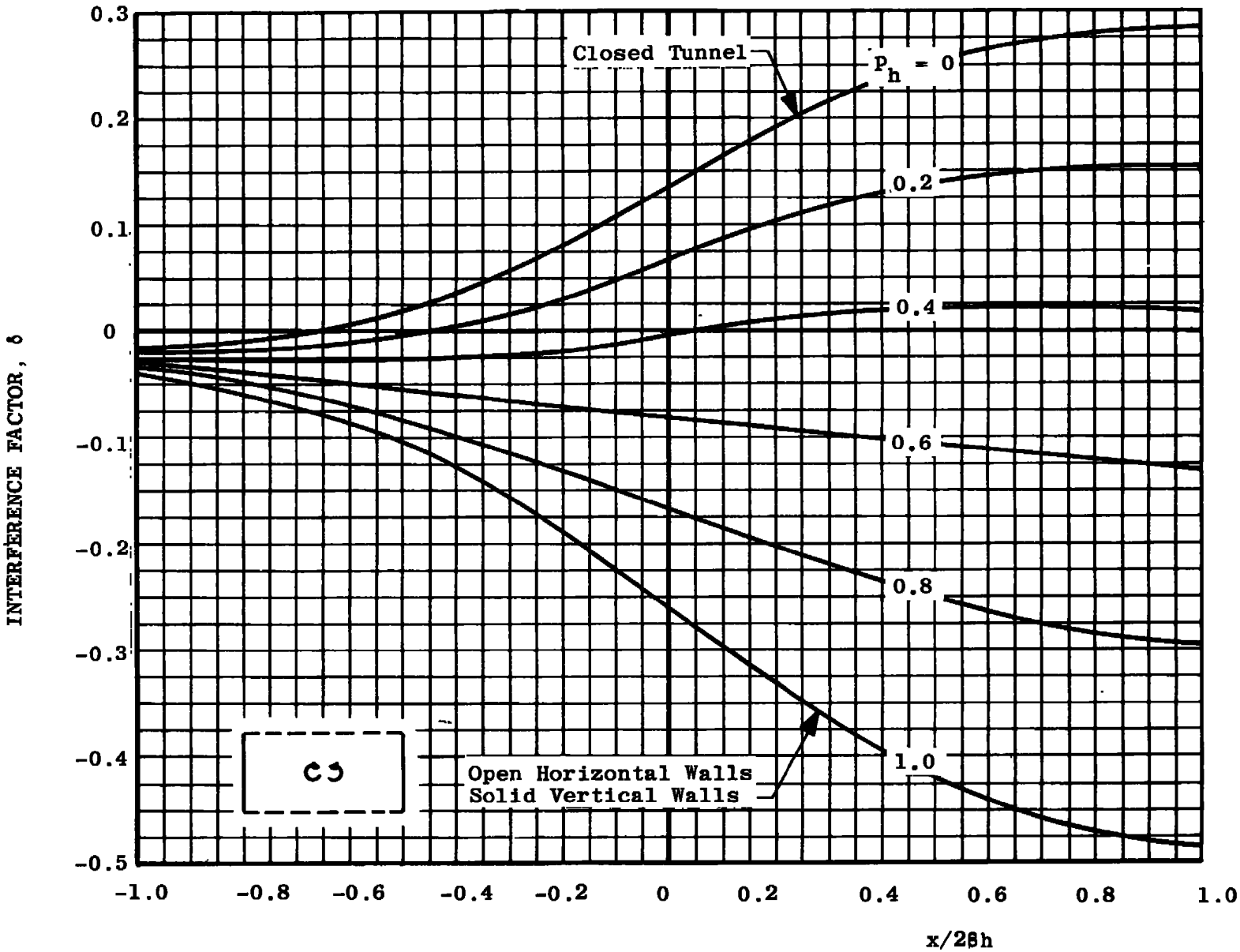

c. h/b = 0.5

Fig. 5.11 Concluded

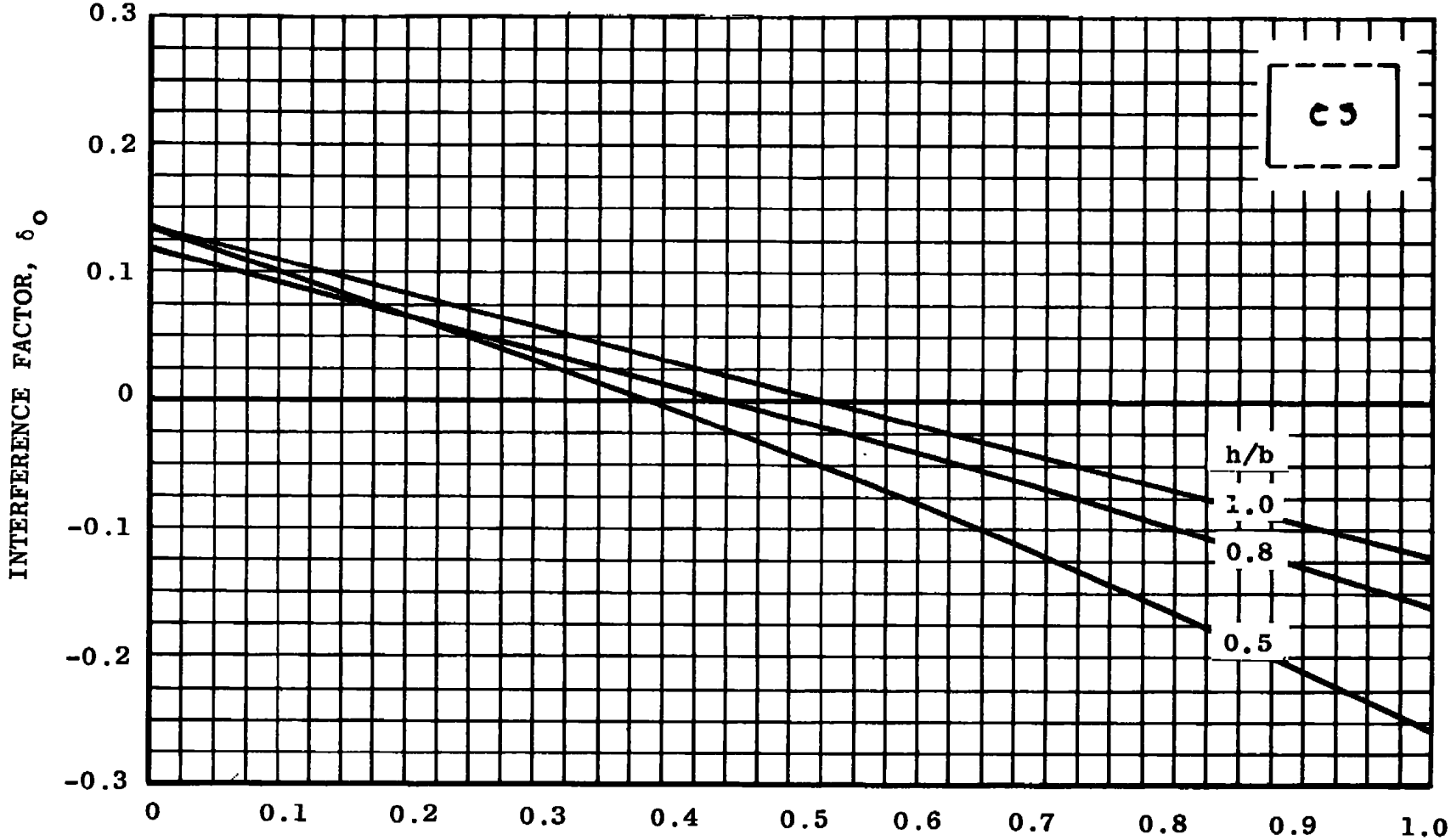

Fig. 5.12 Lift-Interference Factor at x = 0 in Rectangular Tunnels with Solid Vertical Walls and Slotted Horizontal Walls

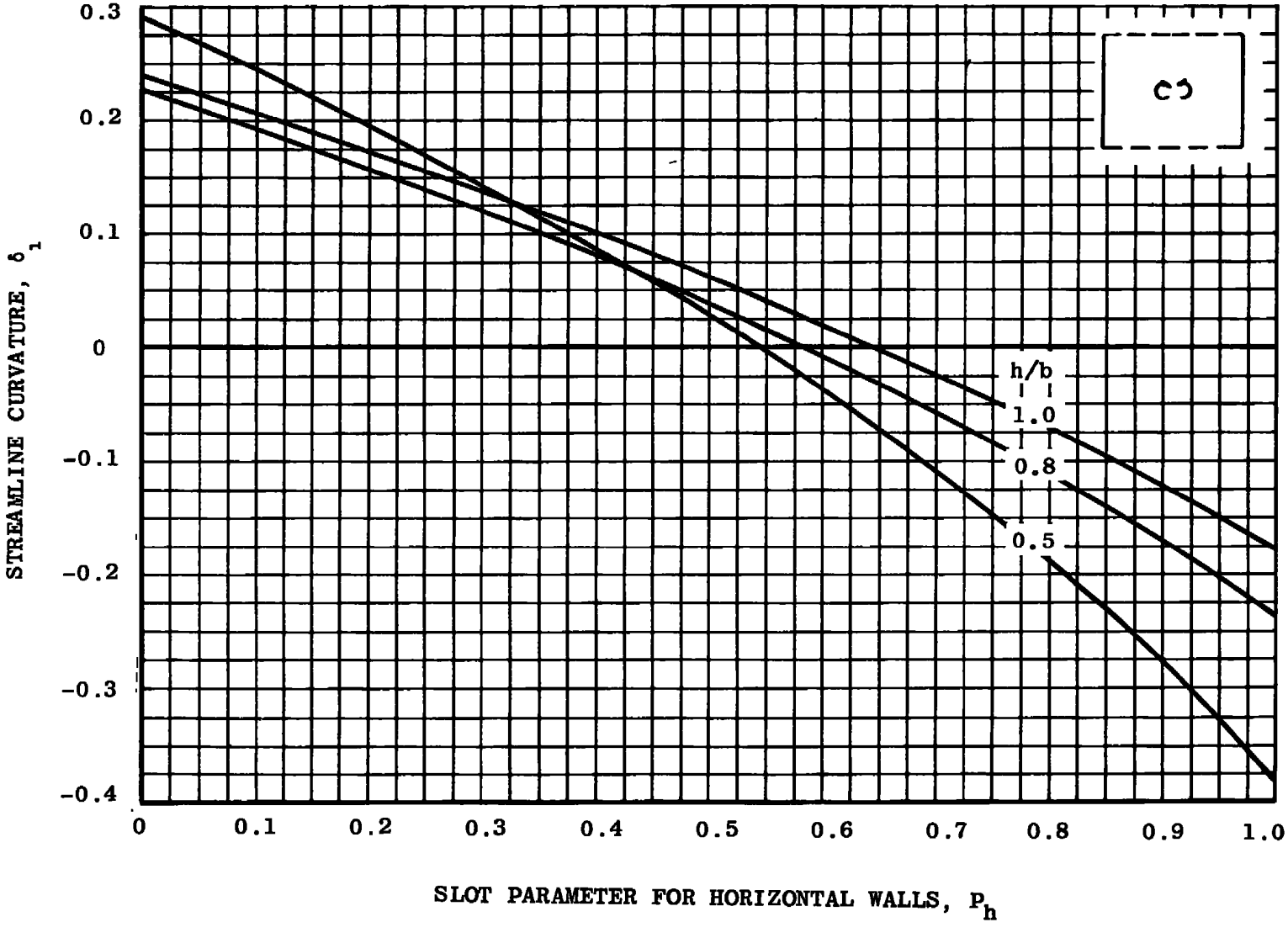

Fig. 5.13 Streamline-Curvature Factor at x = 0 in Rectangular Tunnels with Solid Vertical Walls and Slotted Horizontal Walls

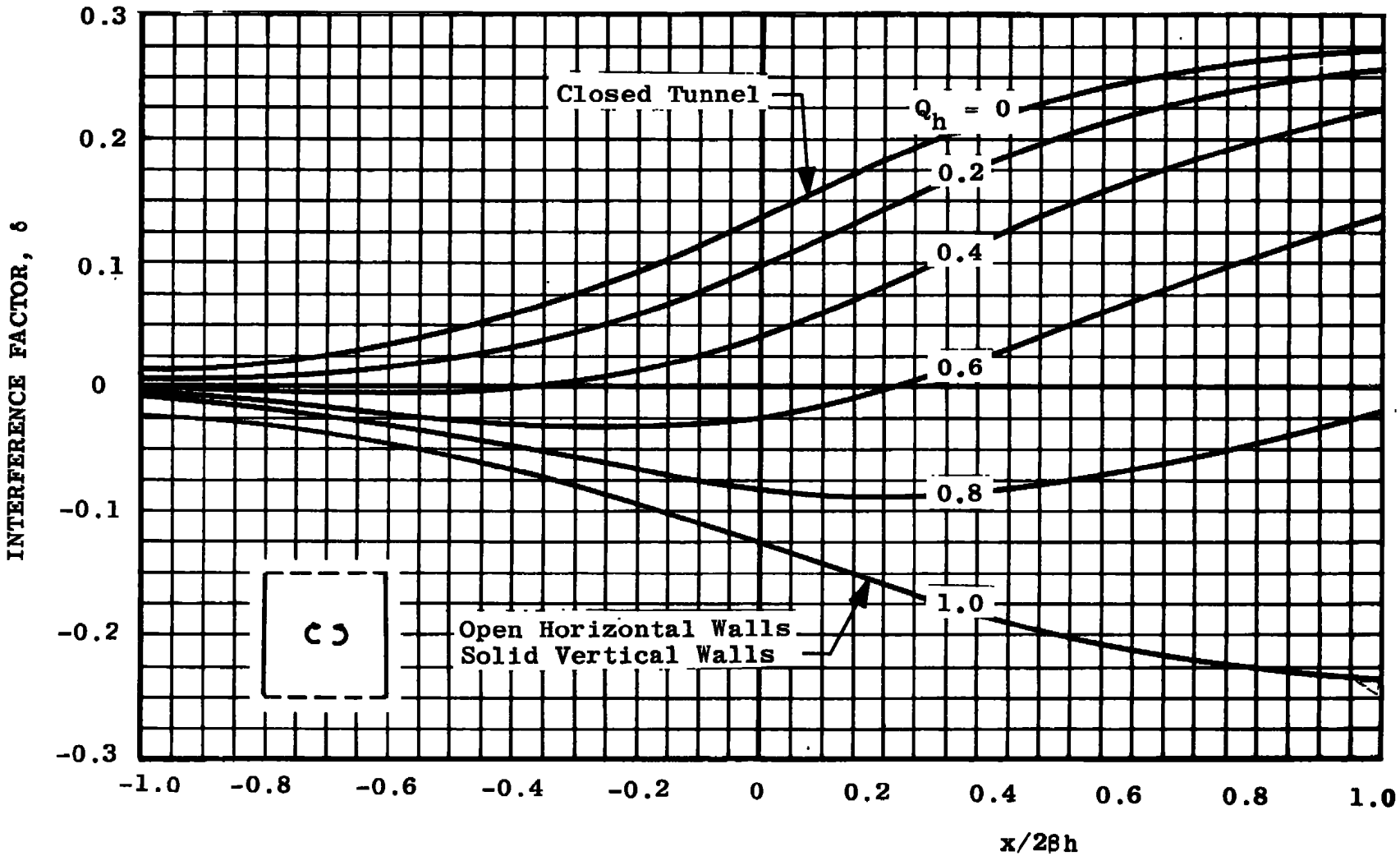

a. h/b = 1.0

Fig. 5.14 Distribution of the Lift-Interference Factor along a Rectangular Tunnel with Solid Vertical Walls and Perforated Horizontal Walls

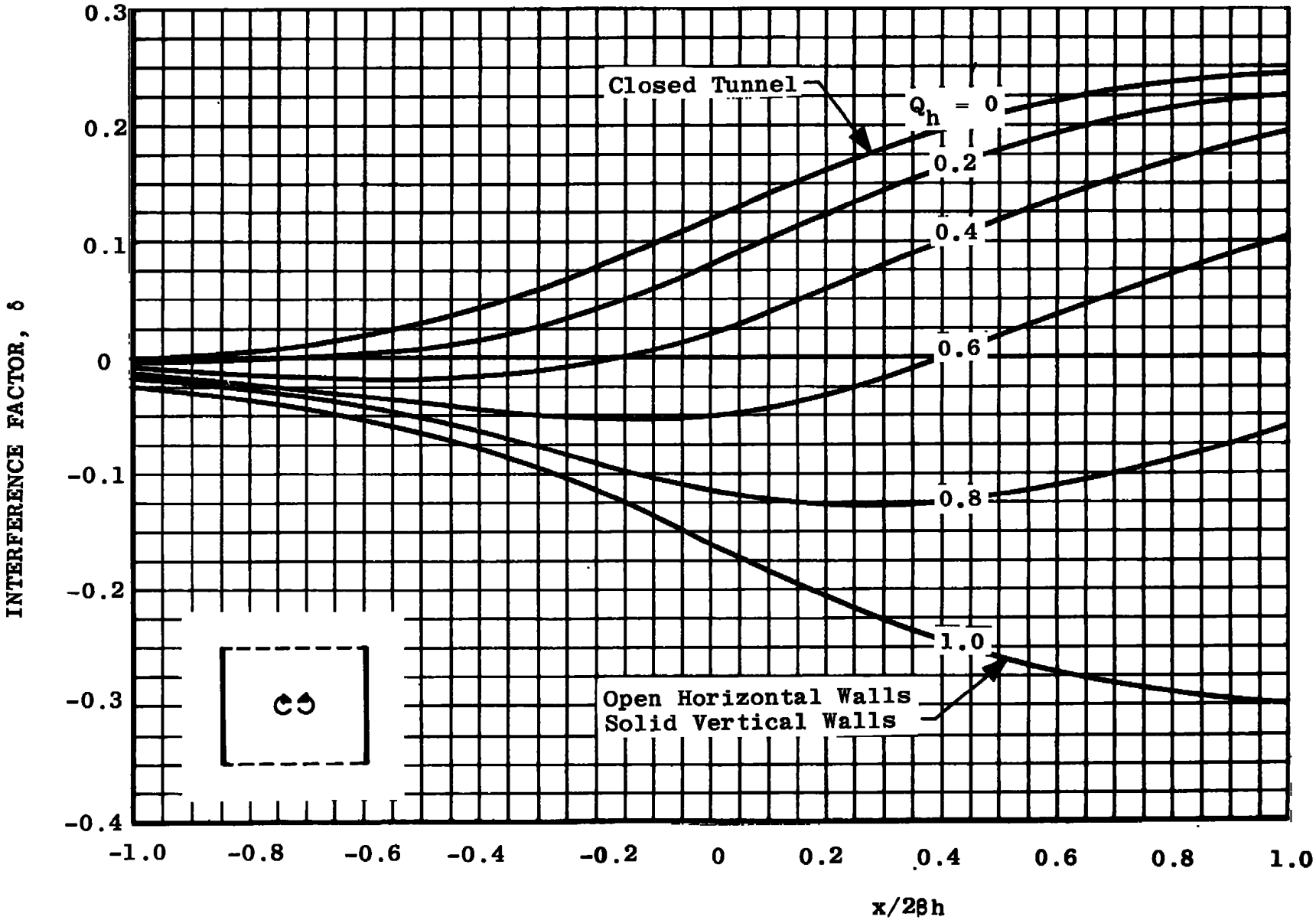

b. h/b = 0.8

Fig. 5.14 Continued

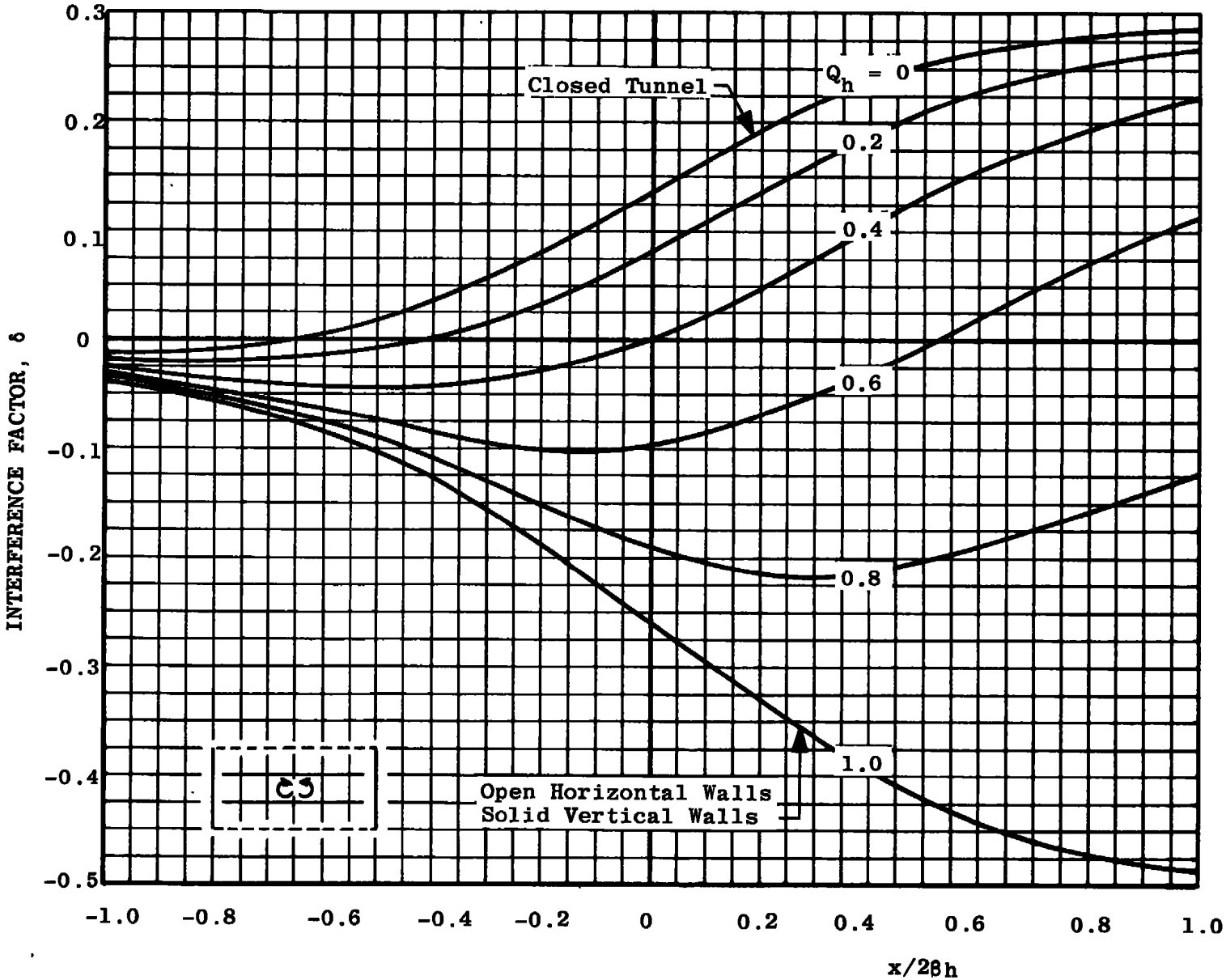

c. h/b = 0.5

Fig. 5.14 Concluded

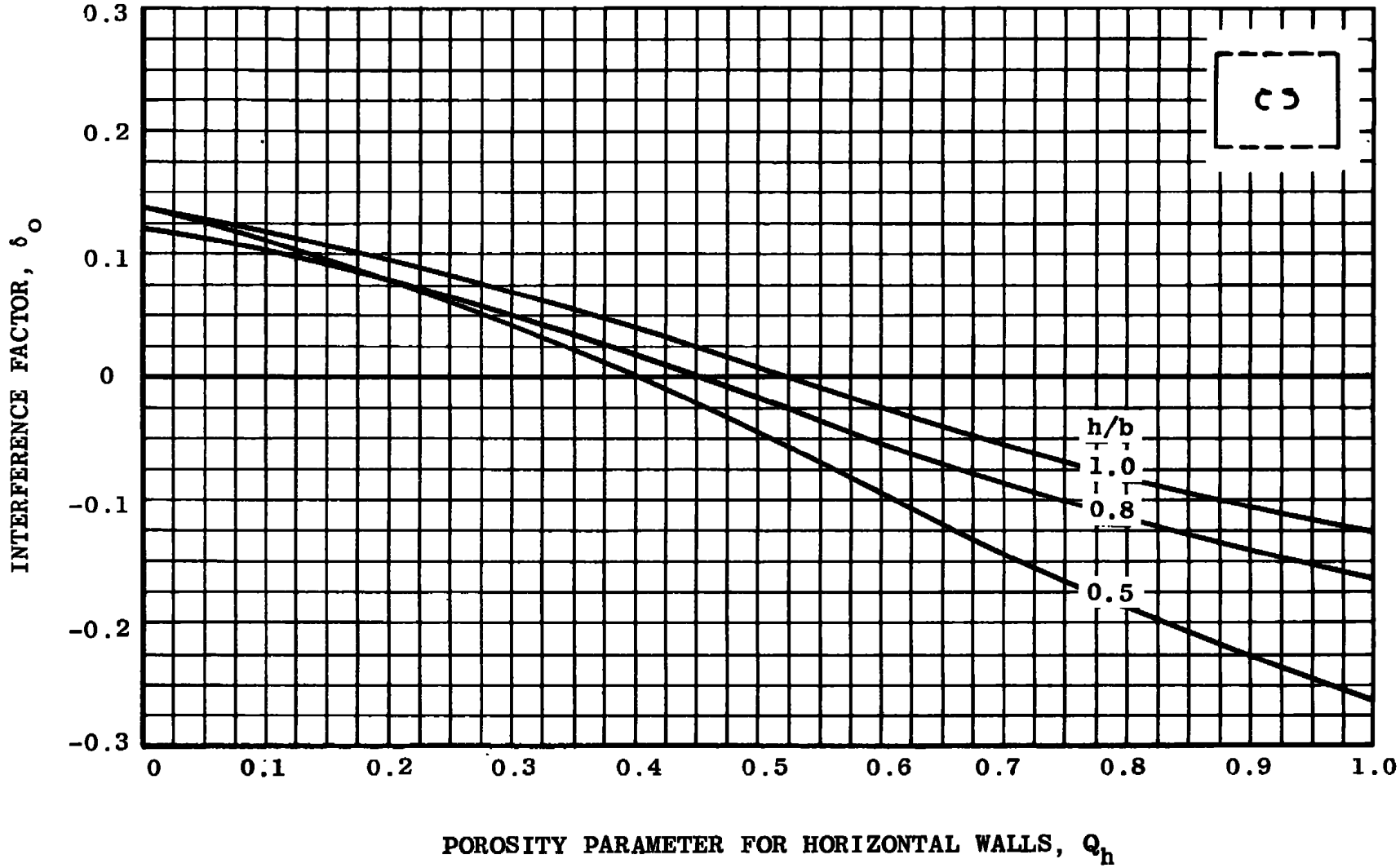

Fig. 5.15 Lift-Interference Factor at x = 0 in Rectangular Tunnels with Solid Vertical Walls and Perforated Horizontal Walls

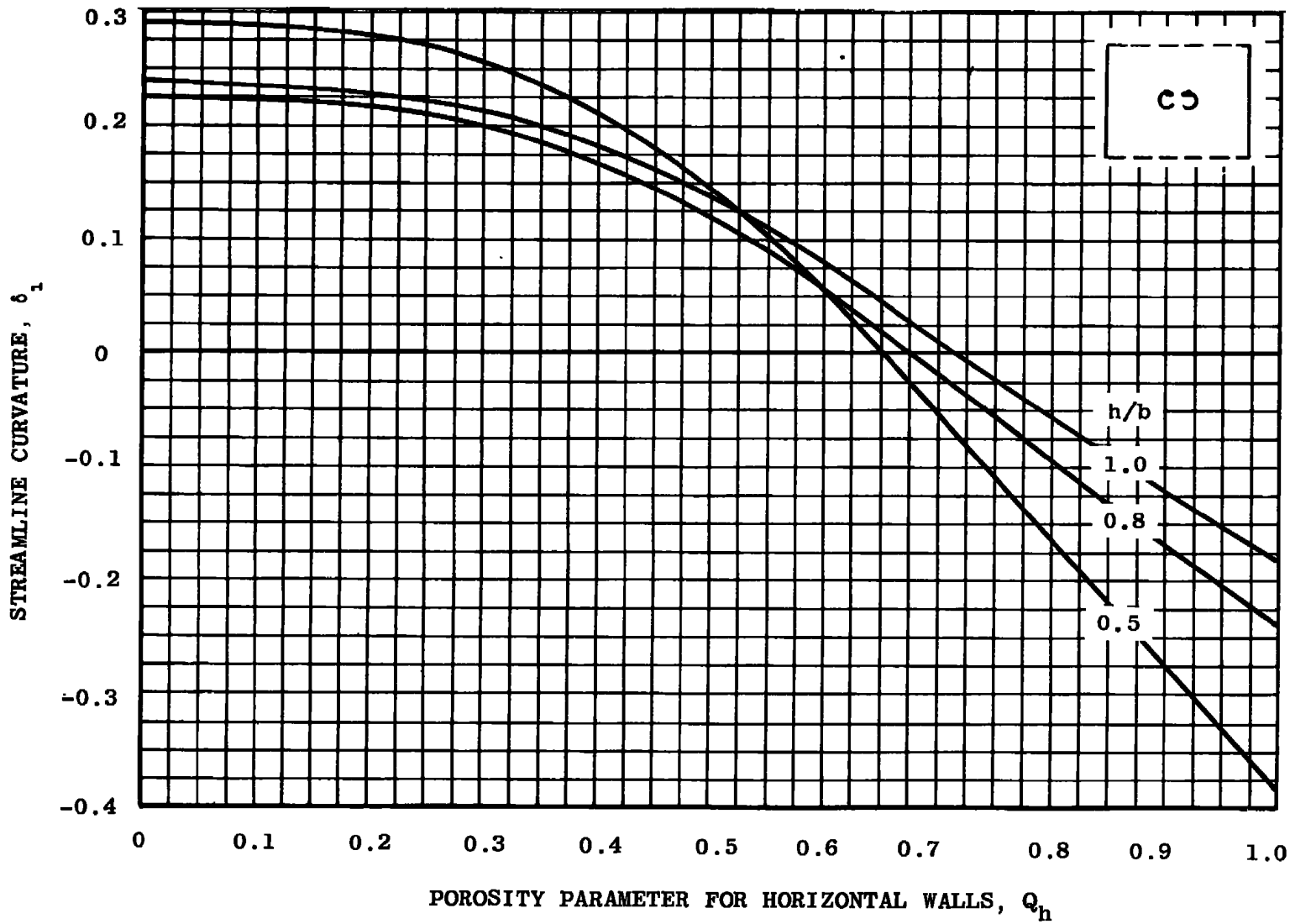

Fig. 5.16 Streamline-Curvature Factor at x = 0 in Rectangular Tunnels with Solid Vertical Walls and Perforated Horizontal Walls

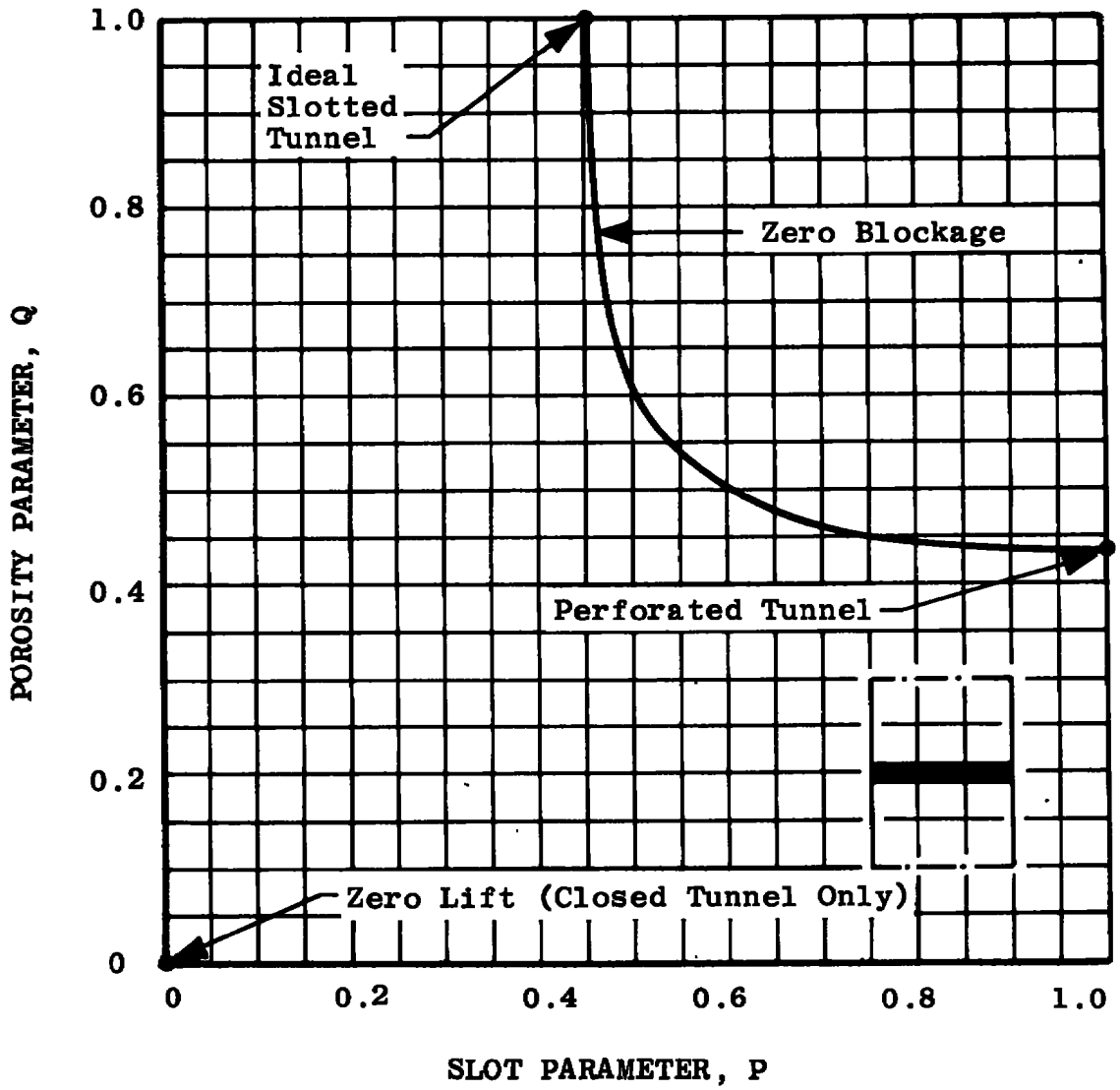

Fig. 7.1 Values of Slot and Porosity Parameters Required to Give Zero Interference in a Two-Dimensional Tunnel

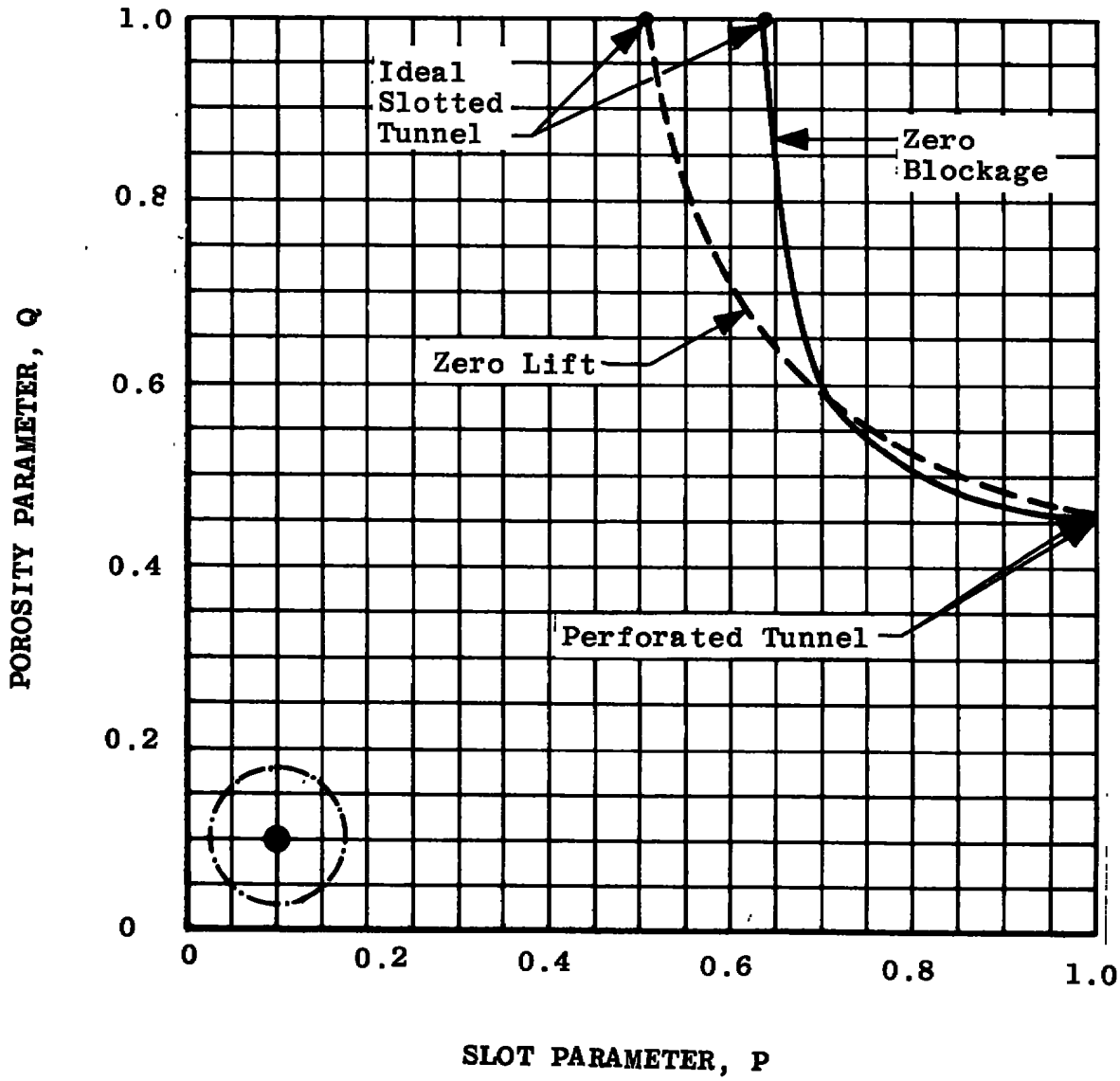

Fig. 7.2 Values of Slot and Porosity Parameters Required to Give Zero Interference in a Circular Tunnel

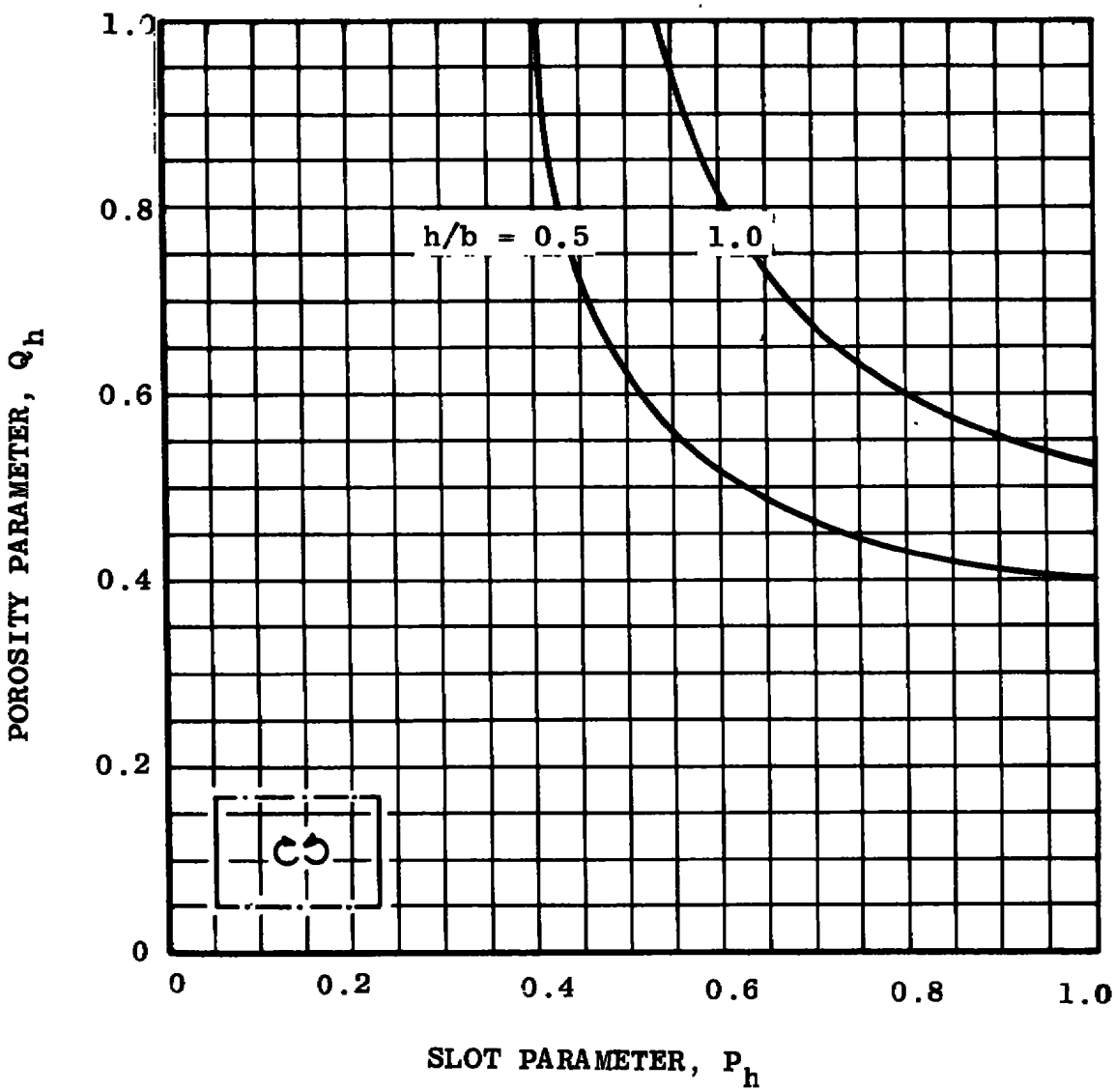

Fig. 7.3 Values of Slot and Porosity Parameters Required to Give Zero Lift Interference in Rectangular Tunnels with Solid Vertical Walls

UNCLASSIFIED

Security Classification

DOCUMENT CONTROL DATA - R & D

(Security classification of title, body of abstract and indexing annotation must be entered when the overall report is classified)

1. ORIGINATING ACTIVITY *(Corporate author)*
Arnold Engineering Development Center
ARO, Inc., Operating Contractor
Arnold Air Force Station, Tennessee 37389

2a. REPORT SECURITY CLASSIFICATION
UNCLASSIFIED

2b. GROUP
N/A

3. REPORT TITLE
BOUNDARY INTERFERENCE AT SUBSONIC SPEEDS IN WIND TUNNELS WITH VENTILATED WALLS

4. DESCRIPTIVE NOTES *(Type of report and inclusive dates)*
Final Report October 1968 to January 1969

5. AUTHOR(S) *(First name, middle initial, last name)*
M. Pindzola and C. F. Lo, ARO, Inc.

6. REPORT DATE	7a. TOTAL NO. OF PAGES	7b. NO. OF REFS
May 1969	127	17

8a. CONTRACT OR GRANT NO.	9a. ORIGINATOR'S REPORT NUMBER(S)
F40600-69-C-0001	
b. PROJECT NO. A016	AEDC-TR-69-47
c. Program Element 63101F	9b. OTHER REPORT NO(S) *(Any other numbers that may be assigned this report)*
d.	N/A

10. DISTRIBUTION STATEMENT
This document has been approved for public release and sale; its distribution is unlimited.

11. SUPPLEMENTARY NOTES	12. SPONSORING MILITARY ACTIVITY
Available in DDC.	Arnold Engineering Development Center, Air Force Systems Command, Arnold AF Station, Tenn. 37389

13. ABSTRACT

Equations and charts as obtained by theoretical analyses are presented for the evaluation of corrections which must be applied to test data as obtained from wind tunnels because of the presence of the test section boundaries. Results are presented for two-dimensional, circular, and rectangular tunnels with boundaries of the completely closed, completely open, slotted, or perforated variety. Interference factors accounting for the direct effects of model and wake blockage on the longitudinal velocity and of model lift on the upwash velocity are enumerated. In addition, consideration is given to the variation of the longitudinal and vertical velocity components along the tunnel axis leading to buoyancy and streamline-curvature corrections.

DD FORM 1 NOV 65 1473

UNCLASSIFIED

Security Classification

14. KEY WORDS	LINK A		LINK B		LINK C	
	ROLE	WT	ROLE	WT	ROLE	WT
subsonic flow						
wind tunnels						
facility design						
interference						
walls, ventilated						

AFSC
Arnold AFS Tenn